GBT MEMO 165

GBT Coordinates And Coordinate Transformations

M.A. Goldman

February 15, 1997

Abstract

Coordinate systems and frames used to describe the Green Bank Telescope, and transformations relating them are reviewed. Effects of gravity loading elastic deformations on coordinate frames and fiducial reference point locations are discussed. Laser rangefinder aiming corrections are calculated. Application of laser rangefinder metrology to telescope pointing determination is discussed.

1. INTRODUCTION.

This memo is intended to define certain control points, fiducial reference points, coordinate frames, and coordinate systems in those frames, which can be used to describe the geometry of the Green Bank Telescope. It is hoped that the memo will be a practical control document useful in defining and determining the dynamic location and orientation of laser ranging stations, receivers, and other objects mounted on the telescope feed arm.

The GBT may be considered a structural assembly composed of linked substructures. Individual substructures have limited degrees of freedom to move with respect to one another, and may flex elastically and dynamically, under the influence of weight loadings. To measure the dynamic geometry of the telescope by means of laser ranging we require mathematical local reference frames and local coordinates to describe the position and orientation in-the-large of each major substructure. We need to create physically measurable fiducial points on the substructures in order to allow measurements to be made of sufficient sample points to determine substructure location and orientation for the physical telescope. We also need to define structural and geometric frame control points to extend the geometric description of the ideal telescope to include change of shape of substructures when the GBT finite element model is used to predict the altered geometry of the telescope caused by gravity-induced elastic deformation.

The description of the telescope's geometry has several levels. These levels are: the reference optical telescope, the design telescope, the ideal tilted geometric telescope, the ideal tilted deformed telescope, the as-built telescope, and the as-measured telescope. We discuss these descriptions in the sections to follow.

2. The Reference Optical Telescope.

The reference optical telescope is just an optical design for a gregorian reflecting telescope with offset optics. Its first optical element is an off-axis surface patch on a paraboloid of revolution. This reflecting patch is designated as the "main reflecting surface" of the telescope. A near-parallel source beam of radiation is focused by this surface patch onto the focus point of the paraboloid, which is designated as the prime focus point of the telescope. The second optical element is an off-axis surface patch on an ellipsoid of revolution. This ellipsoidal patch is designated as the "subreflector surface" of the telescope. The physical structures embodying these surface elements are called the main reflector and secondary reflector of the telescope. (Fig. 1).

One of the two foci of the ellipsoid of revolution is located at the prime focus point, F_0. Radiation leaving the prime focus is reflected by the subreflector surface to the other ellipsoid focus, F_1, the gregorian focus of the telescope (also called the M1 focus). The line through the two foci is the major axis of the ellipsoid.

The paraboloid and ellipsoid axe intersect at the prime focus point, which is a common focus of those two quadric surfaces. These axes intersect at an angle β ($0 < \beta << 90°$). The plane passing though them defines the "tangential optical plane". Each surface patch is defined furthermore to be generated by the intersection of a plane perpendicular to the tangential plane with its defining quadric; such a plane cuts off a surface patch which is symmetric with respect to the tangential optical plane. The tangential optical plane is then a plane of symmetry of each reflecting surface and bisects it, and is also a unique plane of symmetry of the telescope. Let I_1 be the point in the tangential optical plane which defines the mid ray of the tangential fan of rays from the gregorian focus to the subreflector surface.

The gregorian focal plane of the optical telescope passes through the focus F_1

and is perpendicular to the ray I_1F_1. The rays I_1F_1 and F_0I_1 can be considered to define a (folded) optical axis of the telescope.

In a physical embodiment of the telescope the gregorian focal plane will coincide with flat machined surfaces of flanges attached to the receiver room turret's platter structure. The platter axis will be aligned perpendicular to the flanges and the focal plane. The flanges mate to flanges on the individual receiver support mounts. The platter flange centers, ideally, lie on a 56 inch radius circle centered on the turret axis, offset 56 inches from the gregorian focus. The receivers are rotated as required to the gregorian focus.

The turret platter is provided with eight receptacles on its perimeter, one for each receiver assembly. Each receptacle has three feed positioning slots (for the cardinal feed position, and three degrees on either side of the cardinal position). An index pin and motorized actuator is mounted on the ceiling of the feed room diametrically opposite the active feed. The receiver feed is locked into position by driving the index pin radially inward towards the turret axis, and engaging a slot on the appropriate receptacle.

The telescope's optical design is defined by the following parameters:

1. The focal length, f_p, of the paraboloid.
2. The angle, β , between the ellipsoid and paraboloid axes.
3. The eccentricity, e , of the ellipsoid.
4. The spacing, $2f_e$, between foci of the ellipsoid.
5. The offset angle, α , from the ellipsoid major axis, of the mid ray of the tangential plane ray fan from the gregorian focus to the subreflector..
6. The half-angle, Θ_H , of the tangential plane ray fan from the gregorian focus to the subreflector surface.
7. The half-angle, Θ^* , of the tangential plane ray fan from the prime focus to the intersection of the main reflector surface with the tangential plane.
8. The offset angle, Θ_0 , from the paraboloid axis, of the mid ray of the tangential plane ray fan from the prime focus to the parabolic arc intersection of the main reflector surface.

The reference optical design has been specified by Norrod and Srikanth in GBT Memo 155 [Nor-1]. The exact parameters of the optical telescope specified in this memo are:

f_p	6000 cm
β	5.570°
e	0.528
$2f_e$	1100 cm
α	17.899°
Θ_H	14.99°
Θ^*	42.825°
Θ_0	39.005° .

When referring to the optical telescope we use the following notation. Let:

V_0 denote the paraboloid vertex.

F_0 denote the prime focus point, the common focus of the ellipsoid and paraboloid.

F_1 denote the gregorian focus point, which is the other focus of the ellipsoid.

I_1 denote the intersection point of the tangential plane mid ray from the gregorian focus, with the subreflector surface.

a be the length of the major semi axis of the ellipsoid.

b be the length of the minor semi axis of the ellipsoid.

r_1 be the length of the ray F_1I_1 .

r_2 be the length of the ray F_0I_1 .

d_{sp} be the perpendicular distance of point I_1 to the paraboloid axis.

h_{sp} be the projected length of ray F_0I_1 along the paraboloid axis.

d_{mp} be the perpendicular distance of point F_1 to the paraboloid axis.

h_{mp} be the projected length of ray F_0F_1 along the paraboloid axis.

γ be the angle $F_0I_1F_1$.

The following geometric relations hold:

(2.1) $\quad a = \dfrac{f_e}{e}$,

(2.2) $\quad b = a\sqrt{1-e^2}$,

(2.3) $\quad r_1 + r_2 = 2a$.

Applying the law of cosines to triangle $F_0F_1I_1$ and using (2.3) one gets

(2.4) $\quad r_1 = \dfrac{f_e\,(\dfrac{1}{e} - e)}{1 - e\cos\alpha}$, $\quad r_2 = 2a - r_1$.

Applying the law of sines to the same triangle one gets

(2.5) $\quad \gamma = \sin^{-1}\left[(\dfrac{2f_e}{r_2})\,(\sin\alpha)\right]$.

By simple trigonometry,

(2.6) $\quad d_{sp} = r_2\ \sin(\alpha+\gamma-\beta)$, $\quad h_{sp} = r_2\ \cos(\alpha+\gamma-\beta)$.

(2.7) $\quad d_{mp} = 2\,f_e\,\sin(\beta)$, $\quad h_{mp} = 2\,f_e\,\cos(\beta)$.

The unit outward normal vector to the ellipsoidal surface patch at I_1 makes an angle $(\frac{\gamma}{2})+\alpha$ with the ellipsoid's major axis and makes an angle $(\frac{\gamma}{2})+\alpha-\beta$ with the paraboloid's axis.

The derived parameters of the reference optical design are:

Derived Parameter	Stated Value In GBT Document	Computed From (2.1)-(2.7)
a	410.106" (*)	1041.6667 cm (410.1050")
b	348.280" (*)	884.6296 cm (348.2794")
r_1	1510 cm (†)	1509.9158 cm (594.4550")
r_2	573 cm (†)	573.41748 cm (225.7549")
γ		36.127028°
d_{sp}	429.200 cm (‡)	429.1726 cm (168.9656")
h_{sp}	380.300 cm (‡)	380.2874 cm (149.7194")
$(\frac{\gamma}{2}) + \alpha$		35.962514°
$(\frac{\gamma}{2}) + \alpha - \beta$		30.392514°
d_{mp}	106.800 cm (‡)	106.7680 cm (42.0346")
h_{mp}	1094.800 cm (‡)	1094.8062 cm (431.0261") .

The optical geometry of the subreflector is illustrated in Fig. 1.

* RSI Contractor's Drawing 120730 .
† GBT Memo 155
‡ GBT Drawing C35102M081-Rev. B-Sheet 1. Design values on this drawing are optical design values, rounded to the nearest millimeter.

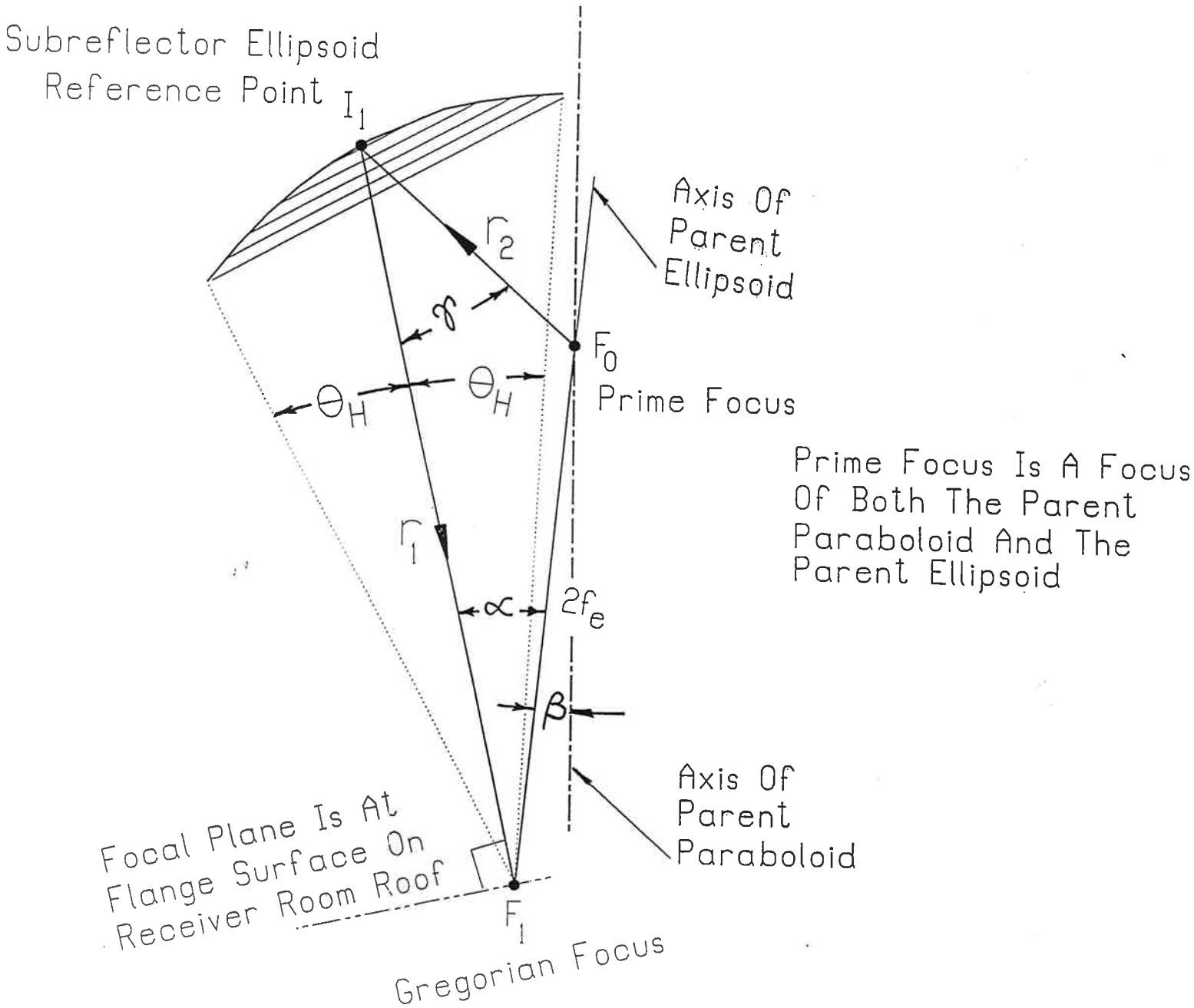

Figure 1. The Subreflector Ellipsoid Reference Geometry

3. The Design Telescope.

At the next level, the "design level", geometric reference control for the telescope is described by a set of design drawings, "Foci Arrangement And Coordinate Systems For The GBT", NRAO drawing C35102M081, [King-1].

These drawings describe the telescope as an assembly of individual rigid subassemblies: the alidade, feed arm together with the main reflector, prime focus receiver mount, subreflector. The alidade rests on a rigid horizontal plane, which represents the top of the alidade track.. The spatial relationship between the subassemblies is defined for an ideal configuration of the telescope, which we call the "design configuration". The design configuration describes the telescope as an ideal elevation-azimuth antenna at an elevation angle $\mathrm{EL}_{ant} = 90°$ and azimuth angle $\mathrm{AZ}_{ant} = 0°$. A prime focus point, F_0, and a secondary focus point, F_1, are defined for this ideal antenna. The ground and alidade track are represented together by a horizontal plane. The optical geometry of the optical telescope is embedded into the design telescope. An ideal main reflector surface, the "parent paraboloid", is defined for the configuration. This is just the main reflector paraboloid, as defined for the optical telescope, embedded into the design configuration. In like manner one defines the "parent ellipsoid" as the subreflector ellipsoid for the optical telescope, embedded into the design configuration.

In the design configuration, six local coordinate frames have been defined, together with a local Cartesian coordinate system associated with each frame. Here a frame is a set of three mutually perpendicular unit direction vectors based at a well-defined point fixed to one of the rigid subassemblies (or the ground, in one case) and is fixed in direction with respect to the geometry of this subassembly. That is, each frame is considered to be embedded in a fixed way into a rigid solid object.

Locations of the design telescope origin points are indicated in Fig. 2.

For the design configuration ($EL_{ant} = 90°, AZ_{ant} = 0°$), the six frames are:

- Frame #1.
  The Base Frame.
  Origin Point - B_d
  Unit Frame Vectors: $\widehat{X}$, $\widehat{Y}$, $\widehat{Z}$

- Frame #2.
  The Alidade Frame.
  Origin Point - A_d
  Unit Frame Vectors: $\widehat{X}_{ad}$, $\widehat{Y}_{ad}$, $\widehat{Z}_{ad}$

- Frame #3.
  The Elevation Frame.
  Origin Point - E_d
  Unit Frame Vectors: $\widehat{X}_{ed}$, $\widehat{Y}_{ed}$, $\widehat{Z}_{ed}$

- Frame #4.
  The Reflector Frame.
  Origin Point - R_d $(= V_0)$
  Unit Frame Vectors: $\widehat{X}_{rd}$, $\widehat{Y}_{rd}$, $\widehat{Z}_{rd}$

- Frame #5.
  The Prime Focus Frame.
  Origin Point - P_d $(= F_0)$
  Unit Frame Vectors: $\widehat{X}_{pd}$, $\widehat{Y}_{pd}$, $\widehat{Z}_{pd}$

- Frame #6.
  The Subreflector Frame.
  Origin Point - S_d $(= I_1)$
  Unit Frame Vectors: $\widehat{X}_{sd}$, $\widehat{Y}_{sd}$, $\widehat{Z}_{sd}$

* INDICATES DIMENSIONAL DESIGN

CENTIMETERS
(INCHES)

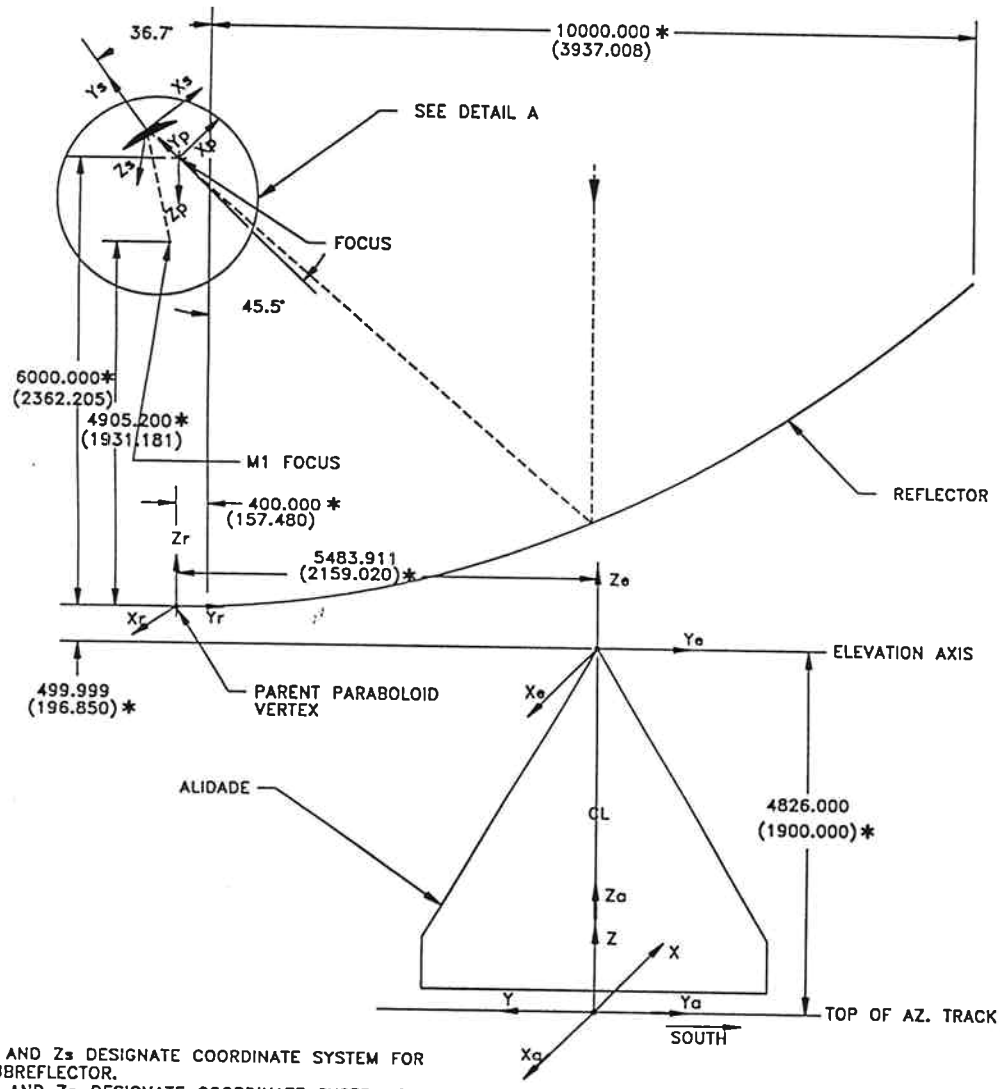

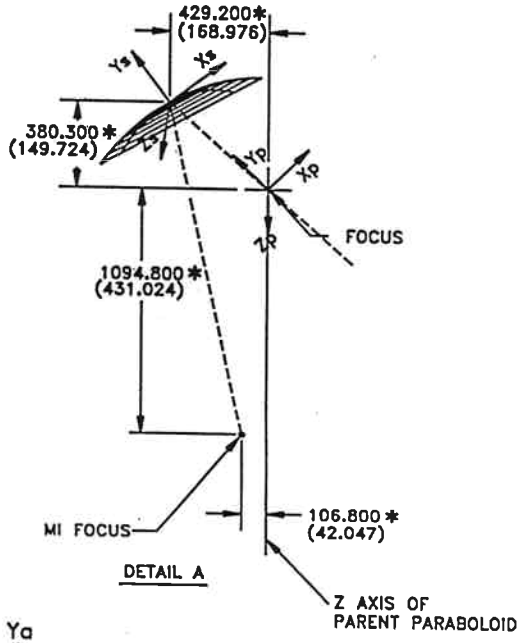

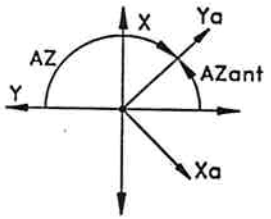

NOTES:
1. Xs, Ys AND Zs DESIGNATE COORDINATE SYSTEM FOR THE SUBREFLECTOR.
2. Xp, Yp AND Zp DESIGNATE COORDINATE SYSTEM FOR THE PRIME FOCUS.
3. Xr, Yr AND Zr DESIGNATE COORDINATE SYSTEM FOR THE REFLECTOR STRUCTURE.
4. Xe, Ye AND Ze DESIGNATE COORDINATE SYSTEM FOR THE ELEVATION STRUCTURE.
5. Xa, Ya AND Za DESIGNATE COORDINATE SYSTEM FOR THE ALIDADE.
6. X, Y AND Z DESIGNATE THE BASE COORDINATE SYSTEM.
7. SEE SHEETS 2 THRU 5 FOR COORDINATE TRANSFORMATION EQUATIONS.

NO.	DATE	BY
B	GM	1/94

REVISIONS

NATIONAL RADIO ASTRONOMY OBSERVATORY
ASSOCIATED UNIVERSITIES INC.
GREEN BANK, W. VA.

TITLE: FOCI ARRANGEMENT AND COORDINATE SYSTEMS FOR THE GBT

UNLESS OTHERWISE SPECIFIED DIMENSIONS ARE IN INCHES
TOLERANCES ANGLES ± 3 PLACE DECIMALS (.xxx)± 2 PLACE DECIMALS (.xx)± 1 PLACE DECIMALS (.x)± FRACTIONS: ±
MATERIAL:
FINISH:

	NAME	DATE		NAME	DATE
DESIGN			RECOMMENDED BY		
DRAWN	GMORRIS	12/93	ENGINEER	L.KING	12/93
CHECKED			APPROVED		
				SIGNATURE	DATE

SCALE	SHEET	NO.	REVISION
1:500	1 of 5	C35102M081	B

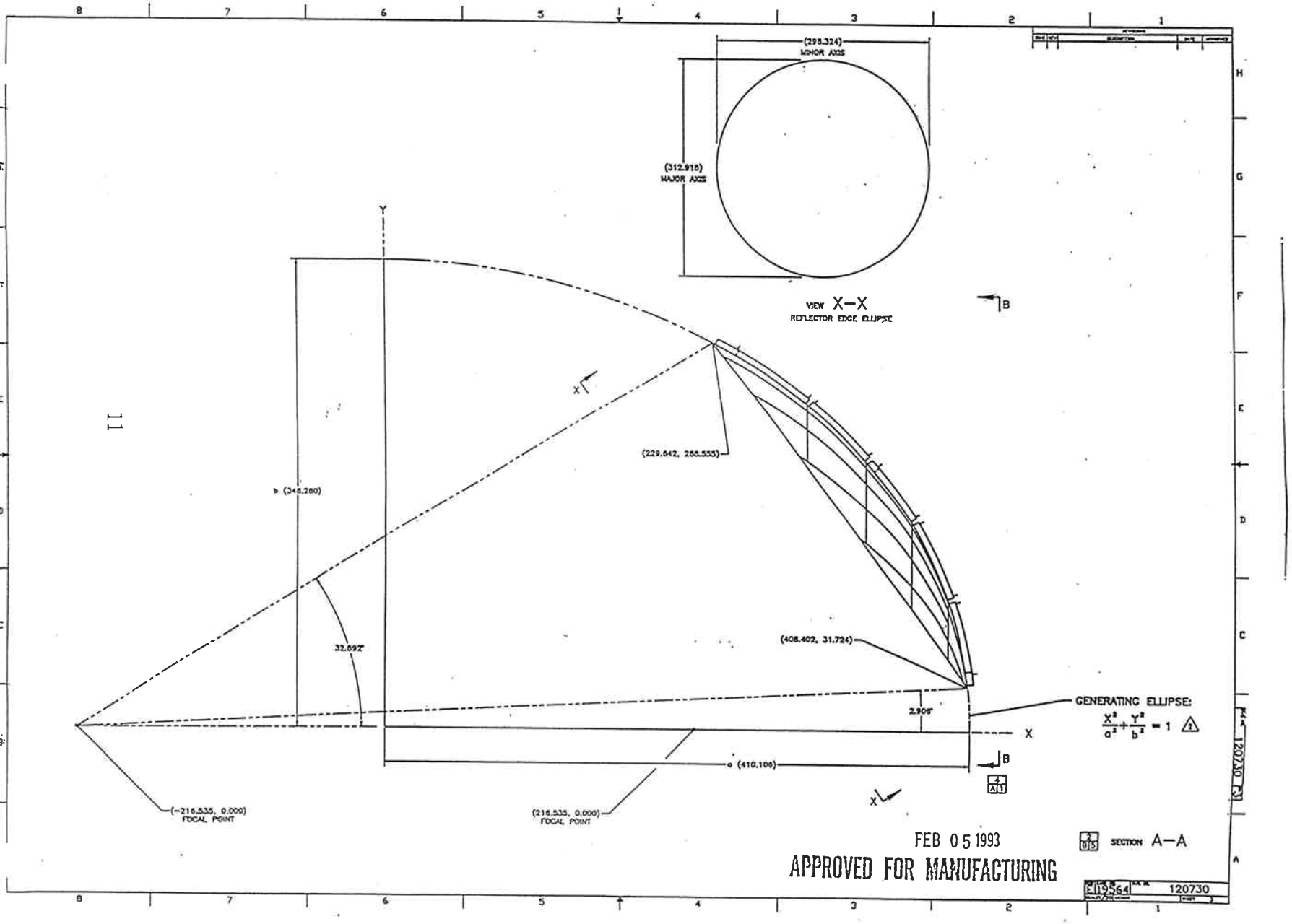
(298.324)
MINOR AXIS
(312.918)
MAJOR AXIS
VIEW X–X
REFLECTOR EDGE ELLIPSE
B
Y
X
(229.642, 256.555)
b (345.280)
32.692°
(408.402, 31.724)
2.906"
GENERATING ELLIPSE:
$\frac{X^2}{a^2}+\frac{Y^2}{b^2}=1$
a (410.106)
(-216.535, 0.000)
FOCAL POINT
(216.535, 0.000)
FOCAL POINT
FEB 05 1993
APPROVED FOR MANUFACTURING
SECTION A–A
119564
120730

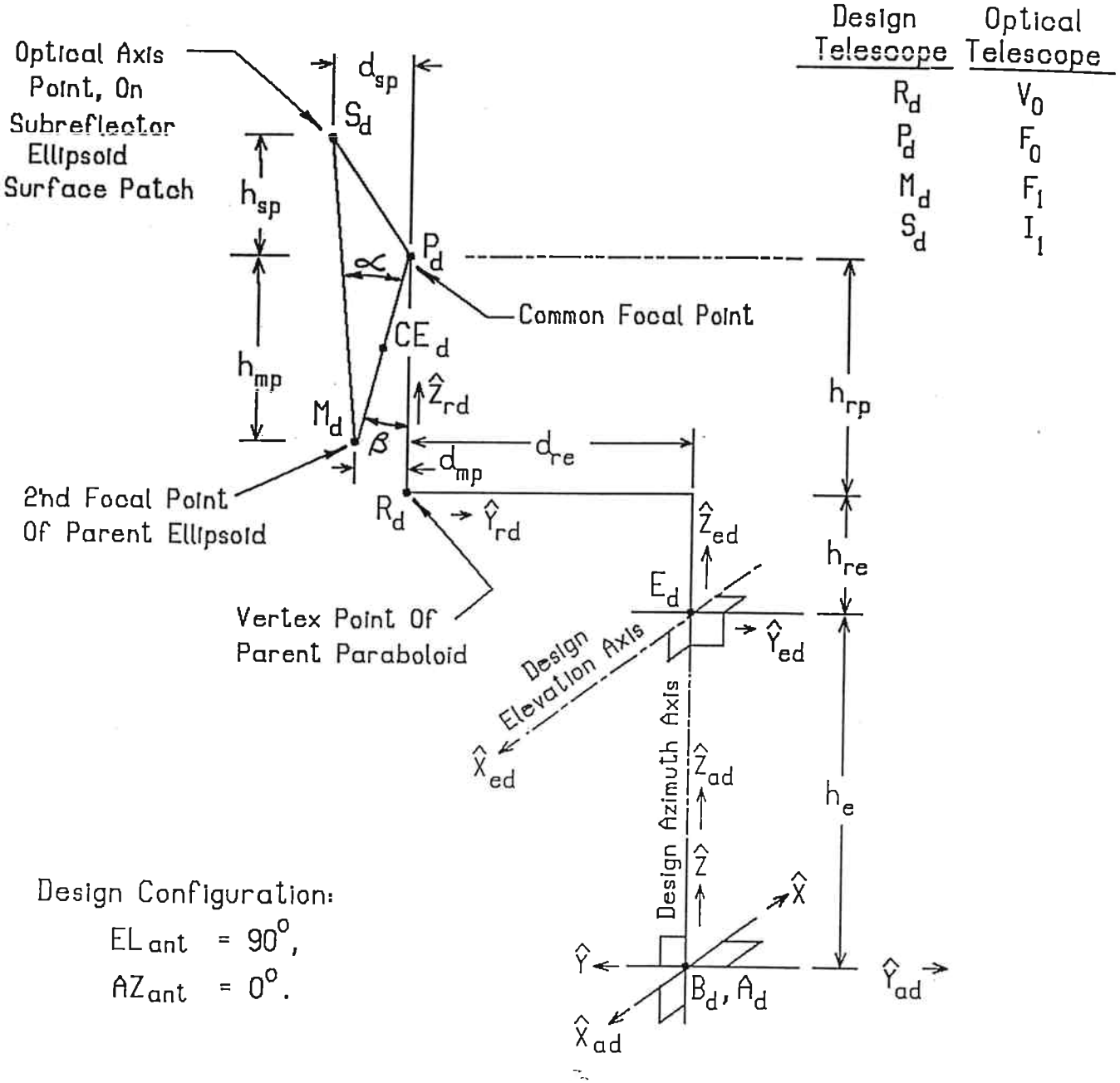

Design Configuration:

$EL_{ant} = 90^{\circ}$,

$AZ_{ant} = 0^{\circ}$.

Figure 2. Design Telescope Reference Points

GBT Prime Focus Receiver Mount
Adjustment Specifications

NOTES:
1. Xp AND Yp LIE IN ANTENNA PLANE OF SYMMETRY.
2. REF: RSI DWG 121039

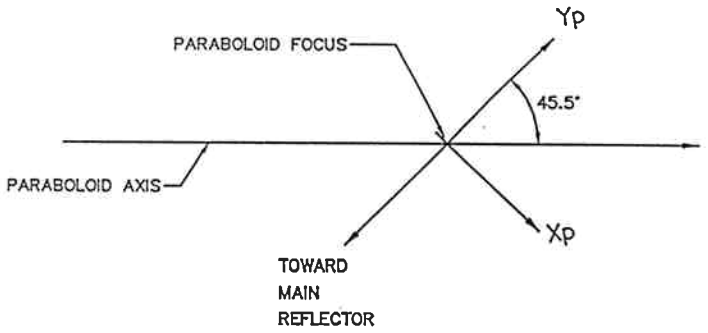

GBT Subreflector Mount
Adjustment Specifications

NOTES:
1. Xs AND Ys LIE IN ANTENNA PLANE OF SYMMETRY.
2. Zs IS PERPENDICULAR TO Xs AND Ys.
3. REF: RSI DWG 121038

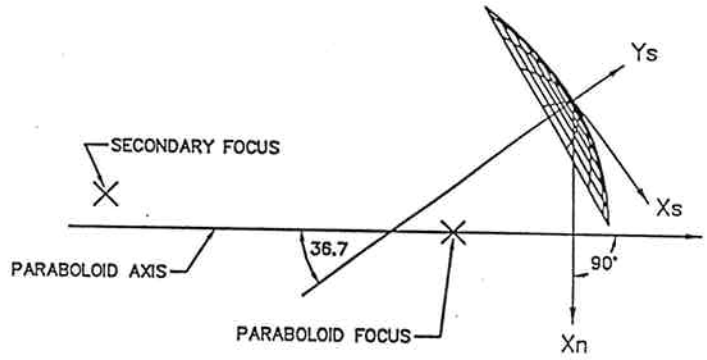

Figure 3.

The base frame must be related to the ground. We will introduce a new frame, the "ground frame", frame #0, after a control monument network has been installed and surveyed. Its unit vector $\widehat{X}_G$ will point horizontally east, unit vector $\widehat{Y}_G$ will point horizontally north (astronomical), unit vector $\widehat{Z}_G$ will point up along local gravity vertical. Its origin point, O_G, will be tied by the control survey to the West Virginia state grid. The base and ground frames are distinct. Effects of track waviness, alidade thermal expansion, structural distortion and tilt will be included in the appropriate telescope model by including them in the transformation matrices relating the alidade, base and ground frames.

The base coordinate system is Cartesian, with X, Y, Z axes respectively along the $\widehat{X}, \widehat{Y}, \widehat{Z}$ unit frame vectors. Its origin has coordinates:

(3.1) $X(B_d) = 0,\ Y(B_d) = 0,\ Z(B_d) = 0$.

The azimuth axis of the design telescope is a line through the origin of the base coordinate system, pointing along the Z axis. This design telescope axis is considered to be embedded in the alidade structure, as the axis of the pintle bearing. For the design configuration, the unit alidade frame vectors are:

(3.2 a) $\widehat{X}_{ad} = -\widehat{X}$, $\widehat{Y}_{ad} = -\widehat{Y}$, $\widehat{Z}_{ad} = \widehat{Z}$. The alidade origin is:

(3.2 b) $A_d = B_d$, $X(A_d) = 0,\ Y(A_d) = 0,\ Z(A_d) = 0$.

The point of attachment E_d of the elevation frame, which is the origin of the elevation coordinate system of the design telescope, lies on the azimuth axis:

(3.3 a) $X(E_d) = 0,\ Y(E_d) = 0,\ Z(E_d) = h_e \equiv 1900.000\,\text{inches}.$

For the design configuration, the unit elevation frame vectors are:

(3.3 b) $\widehat{X}_{ed} = -\widehat{X}$, $\widehat{Y}_{ed} = -\widehat{Y}$, $\widehat{Z}_{ed} = \widehat{Z}$.

The elevation axis of the design telescope passes through E_d and is directed along $\widehat{X}_{ed}$. Length h_e is the design height from the top of the azimuth track to the elevation axis.

The attrachment point R_d of the reflector frame is the origin of the reflector coordinate system and is the vertex of the parent paraboloid of the design telescope. Its base system coordinates are

(3.4 a) $\quad X(R_d) = 0\,,\; Y(R_d) = d_{re}\,,\; Z(R_d) = (h_e + h_{re})\,,$

where $d_{re} \equiv 5843.911\,\text{cm}$, $h_{re} \equiv 499.999\,\text{cm}$. For the design configuration, the unit reflector frame vectors are:

(3.4 b) $\quad \widehat{X}_{rd} = -\widehat{X}\,,\; \widehat{Y}_{rd} = -\widehat{Y}\,,\; \widehat{Z}_{rd} = \widehat{Z}\,.$

The equation of the parent paraboloid is:

(3.4 c) $\quad X_{rd}^2 + Y_{rd}^2 = (4f_p)(Z_{rd})$, where $f_p \equiv 6000\,\text{cm}$.

The design telescope's prime focus point, P_d , is the point of attachment of the prime focus frame, and origin of the prime focus coordinate system. It is the focal point of the parent paraboloid, and is also one of the focal points of the design ellipsoid surface of the secondary reflector (the parent ellipsoid). Its base system coordinates are:

(3.5 a) $\quad X(P_d) = 0\,,\; Y(P_d) = d_{re}\,,\; Z(P_d) = (h_e + h_{re} + h_{rp})\ \text{cm},$

where $h_{rp} = f_p \equiv 6000\,\text{cm}$.

For the design configuration, the unit prime focus frame vectors are:

(3.5 b) $\quad \begin{aligned} \widehat{X}_{pd} &\equiv -\widehat{Y}(\cos 45.5^\circ) + \widehat{Z}(\sin 45.5^\circ)\,, \\ \widehat{Y}_{pd} &\equiv +\widehat{Y}(\sin 45.5^\circ) + \widehat{Z}(\cos 45.5^\circ)\,, \\ \widehat{Z}_{pd} &\equiv -\widehat{X}\,. \end{aligned}$

The prime focus frame of the design telescope tilts exactly 45.5° to the axis of the parent paraboloid (Fig. 3). This frame is used to describe motions of the prime focus receiver mount. The frame is considered to be embedded in the prime focus receiver mount. The optical prime focus point , F_0 , is coincident with the origin of the prime focus frame, P_d . We consider the optical prime focus to be distinct

from the origin of the prime focus frame; the latter point is considered to be a reference point embedded in the prime focus receiver mount and moves together with this mount.

The gregorian focus of the parent ellipsoid is located at:

(3.5 c) $X(M_d) = 0\,,\; Y(M_d) = (d_{re} + d_{mp})\,,\; Z(M_d) = (h_e + h_{re} + h_{rp} - h_{mp})\,.$

Distances $d_{mp} = 106.800\,\text{cm}$ and $h_{mp} = 1094.800\,\text{cm}$ are called out on the reference drawing [King-1]. The distance between the two ellipsoid foci is $|P_d\ M_d| \equiv 2\,f_{ed} = \sqrt{h_{mp}^2 + d_{mp}^2}$. If one used these values, which are the reference optical values rounded to the nearest millimeter, one would obtain a distance from the design ellipsoid's center to either focus as $f_e = 549.9985\,\text{cm}$, rather than the exact value of 550 cm specified by the reference optical design. The geometry of the gregorian ellipsoid surface as approved for manufacture is specified by RSI contractor's drawing 120730, sheet 3.

In the March 1996 updated optical design, [Nor-1] , the distance between focal points F_0 and F_1 is specified to be exactly

$$|F_0\ F_1| \equiv 2\,f_e = \sqrt{h_{mp}^2 + d_{mp}^2} \equiv 1100\ \text{cm}\,.$$

The angle α , with vertex F_1 , between the segment I_1F_1 and the major axis of the design ellipsoid (the line $F_0\ F_1$) is defined to be exactly 17.899°.

Distances d_{mp} and h_{mp} should be: $d_{mp} = 1100 \sin\beta$ cm and $h_{mp} = 1100 \cos\beta$ cm, to locate the gregorian focus correctly relative to the parent paraboloid. These distances, computed previously for the reference optical telescope, are slightly different than the values called out in [King-1]. For the design telescope we will use the derived values for the optical reference design in [Nor-1] , rather than the earlier values called out in [King-1], which are the optical design values rounded to the nearest millimeter.

The point of attachment S_d of the subreflector frame of the design telescope, which is the origin of the subreflector coordinate system, has base system coordinates:

(3.6 a) $X(S_d) = 0\,,\ Y(S_d) = (d_{re} + d_{sp})\,,\ Z(S_d) = (h_e + h_{re} + h_{rp} + h_{ps})\,.$

Values $d_{sp} = 429.200\,\text{cm}$, $h_{ps} = 380.300\,\text{cm}$ are called out in [King-1] . Again, here we will also use values implied by the reference optical telescope for the design telescope

For the design configuration, the unit subreflector frame vectors are:

(3.6 b) $$\begin{aligned} \widehat{X}_{sd} &\equiv -\widehat{Y}(\cos 36.7°) + \widehat{Z}(\sin 36.7°)\,, \\ \widehat{Y}_{sd} &\equiv +\widehat{Y}(\sin 36.7°) + \widehat{Z}(\cos 36.7°)\,, \\ \widehat{Z}_{sd} &\equiv -\widehat{X}\,. \end{aligned}$$

In the design telescope, the subreflector frame tilts exactly 36.7° to the parent paraboloid's axis (Fig. 3). This frame's orientation is selected to describe motions of the subreflector. The frame is considered to be embedded in the subreflector mount structure. The $\widehat{X}_{sd}$ direction is along the common nominal direction of the axes of Stewart platform actuators #4, #5. The $\widehat{Y}_{sd}$ direction is along the common nominal direction of the axes of actuators #1, #2, #3. Note that $\widehat{Y}_{sd}$ does <u>not</u> point along the normal to the subreflector surface at S_d.

The gregorian focus point of the design telescope, F_1, happens to lie on the point of origin, M_d, of the subreflector frame. We consider the optical prime focus point to be distinct from the origin of the subreflector frame; the latter point is considered to be embedded in the subreflector support structure and move together with that structure.

Besides the six local reference frames defined by drawings C35102M081, other local reference frames may be useful for describing the GBT. Frames associated with the gregorian design ellipsoid, feed turret platter, individual receivers, and receiver room will be defined.

The additional reference frames are:

- Frame #7.
  The Gregorian Ellipsoid Frame.
  Origin Point - CE_d (Midpoint of ray F_0F_1).
  Unit Frame Vectors: $\widehat{X}_{cd}$, $\widehat{Y}_{cd}$, $\widehat{Z}_{cd}$

The point of attachment, CE_d , of the gregorian ellipsoid frame is the center of the parent ellipsoid, which is the midpoint of the line segment between foci M_d and P_d. The frame vector $\widehat{X}_{gd}$ is directed from the ellipsoid center CE_d , along the ellipsoid major axis towards P_d , the common focus point of the ellipsoid and the parent paraboloid. The angle $\beta = \tan^{-1}(\frac{d_{mp}}{h_{mp}}) = 5.57°$. For the design configuration the unit gregorian ellipsoid frame vectors and the origin are then given by:

(3.7)

$$\begin{aligned}
&\widehat{X}_{cd} \equiv -\widehat{Y}(\sin\beta) + \widehat{Z}(\cos\beta) \quad , \quad X(CE_d) = 0 \,, \\
&\widehat{Y}_{cd} \equiv +\widehat{Y}(\cos\beta) + \widehat{Z}(\sin\beta) \quad , \quad Y(CE_d) = (d_{re} + (d_{mp}/2)) \,, \\
&\widehat{Z}_{cd} \equiv -\widehat{X} \qquad\qquad\qquad\quad , \quad Z(CE_d) = (h_e + h_{re} + h_{rp} - (h_{mp}/2)) \ .
\end{aligned}$$

Frame #8.
The Turret Frame.
Origin Point - T_d
Unit Frame Vectors: $\widehat{X}_{td}$, $\widehat{Y}_{td}$, $\widehat{Z}_{td}$.

(3.8.1)

$$\begin{aligned}
&\widehat{X}_{td} \equiv -\widehat{Y}(\cos(\alpha-\beta)) + \widehat{Z}(\sin(\alpha-\beta)) \ , \\
&\widehat{Y}_{td} \equiv +\widehat{Y}(\sin(\alpha-\beta)) + \widehat{Z}(\cos(\alpha-\beta)) \ , \\
&\widehat{Z}_{td} \equiv -\widehat{X} \ , \quad \text{where } \alpha \equiv 17.899° \ , \ \beta \equiv 5.570° \ .
\end{aligned}$$

The turret frame is embedded in the platter. The origin, T_d, is intersection point of the platter's flange plane with the turret axis. The Y_{td} axis is defined to coincide with the platter axis, outwards from the platter. In the design telescope, the Y_{td} axis points coincidentally along the central optical ray M_dS_d. The X_{td} axis is perpendicular to the Y_{td} axis, and lies in the plane of the receiver flanges. It points in a radially outward direction to the receiver circle. It would be convenient if it also were in the telescope's plane of symmetry and pointed towards the main reflector when the index pin in the feed room ceiling was engaged, so the phase center of one of the receivers (which we arbitrarily choose to be the L-band receiver, N1), the origin point T_d , and the center of the engaged index pin slot were all co-linear. [The receiver flange on the platter could have locating pins, set precisely so that the midpoint between the hole centers on the mating feed

horn mount flange surface was the phase center of the inserted L-band receiver. To accomplish this one would need a survey of the receiver house and platter, to determine locating pin hole centers on the platter flanges.]

The gregorian focus M_d and the turret origin point T_d each lie in the plane of symmetry of the telescope and the gregorian focus plane. They are separated by a distance $d_{mt} \equiv 56$ inches (142.240 cm), which is the radius of the receiver circle on the turret. Considering the locations of these points as described by position vectors, with respect to an arbitrary origin, we have, for the design telescope:

(3.8.2)

$$\overrightarrow{M}_d = \overrightarrow{T}_d + (d_{mt}) \cdot (\widehat{X}_{td}) \ , \quad \text{which gives}$$

$$X(T_d) = 0 \ , \quad Y(T_d) = d_{re} + d_{mp} + (d_{mt}) \cos(\alpha - \beta) \ ,$$

$$Z(T_d) = h_e + h_{re} + h_{rp} - h_{mp} - (d_{mt}) \cos(\alpha - \beta) \ .$$

Frame #9.
The Receiver House Frame.
Origin Point - H_d
Unit Frame Vectors: $\widehat{X}_{hd}$, $\widehat{Y}_{hd}$, $\widehat{Z}_{hd}$

This is a frame embedded in the receiver house structure, used to describe the location and orientation of the feed room. To physically realize this frame and make use of it, the receiver house and the rotating turret platter should each be provided with fiducial marker survey targets. During initial alignment of the GBT, the receiver house should be positioned so that the turret axis becomes parallel to the desired central optical ray from subreflector to gregorian focus, and displaced from it by distance d_{mt}. The center of each receiver's locating flange, when rotated to the active position, should lie on the symmetry plane of the telescope. To achieve the latter requirement, the plane in the receiver house defined by the platter axis together with the center point of the index pin mounted on the ceiling of the feed room should coincide with the symmetry plane of the telescope.

The unit frame vector $\widehat{Y}_{hd}$ should lie parallel to the turret axis. The plane defined by frame vectors $\widehat{X}_{hd}$ and $\widehat{X}_{hd}$ should be parallel to the plane defined by

the center of the index pin and turret axis. The origin point H_d should be a point in the feed room at the center of a survey target in a survey target bushing affixed rigidly to the house structure. That is, H_d and other fiducial markers tied to the house structure, both inside and outside, should generate a local survey control net to tie the platter, receiver locating flanges, receiver house structure to one another and to the outside world.

- Frames #10.1 to 10.8 .
  Receiver Flange Frames.
  Origin Points - N_i
  Unit Frame Vectors: $\widehat{X}_{ni}$, $\widehat{Y}_{ni}$, $\widehat{Z}_{ni}$ $(i = 1, \ \ldots \ , 8)$.

These are frames embedded in the mount flanges for the individual receivers and their feed horns. The flange for each receiver module should be provided with two pin holes which insert into locating pins on the mating turret platter flange, to position the receiver flange with respect to the turret. Ideally, the pins on the platter flange should be oriented so that each feed horn's phase center could be brought to lie on the 56" radius receiver circle, diametrically opposite the index pin on the feed room ceiling, when the turret and intermediate feed horn rotator flange (if one is used) are rotated to the feed horn's active receiving position.

The local coordinate axis Y_{ni} is defined to be perpendicular to the receiver flange surface. The axis X_{ni} is defined to lie in the plane of the flange and to point along the line of the two alignment pin footprint points on the flange.

Feed horns should be aligned on their mount flange so each feed horn's electromagnetic axis is perpendicular to the flange, unless a squint offset is explicitly required. If possible, it would be advantageous to center a feed horn's phase center midway between the locating pins, in the plane of the mating flange surfaces, for flanges containing a single feed horn. For flanges containing multiple feed horns one might either want the individual feed horn phase centers to be rotatable, by a flange rotator, onto the 56" radius receiver circle, or one might want the centroid of the feed horn group to lie on this circle.

One or more feed horns mount on each of the eight receiver mount structures. Feed horn offsets with respect to the receiver flange center and surface normal direction should be determined before the receivers are mounted on the receiver

house turret. For each of the horns mounted on a common flange one should measure its phase center location, the direction of the unit outward vector along the horn's electrical axis, and the direction of the unit $\overrightarrow{E}$ field vector of the horn (if defined) with respect to the local flange frame coordinate system. (This could be done by antenna range measurements or local surveying of the receiver). Components of those two unit vectors in the local flange frame, and also local distance offset coordinates of the phase center from the flange frame origin point, should be entered into a data base for the horn. The databased information would then be available to provide pointing offset information for each horn, with respect to the gregorian focus optics of the telescope.

In the case where multiple feed horns mount on a common flange and that flange is placed on an intermediate rotator flange (so the feed horn array on the flange can rotate about the Y_{ni} axis), it is suggested that receiving pin holes be placed in the intermediate rotator flange and locating pins be provided for the feed horn array flange. The rotator flange would be pinned to the platter flange and the feed horn array flange would be pinned to the rotator flange. Pins would be located so that, on installation, when the platter is rotated to the active receiver position, the local frame X_{ni} axis coincides with the X_{tg} axis of the turret frame (when the reference rotation angle of the intermediate rotator flange is at zero). It is suggested that the origin point of the feed horn array flange be fiducialized by insertion of a survey target bushing, and that this point be surveyed relative to the platter's local coordinate system and receiver house local frame.

This completes our description of the design model. In the next section we extend it to provide for rotations of the antenna tipping structure about the azimuth and elevation axes of the telescope.

4. The Tilted Geometric Telescope.

At the next level of description, "the ideal tilted geometric telescope", the earth and alidade track are still represented together by a horizontal plane. The alidade structure of the telescope is still assumed to be rigid. It may now rotate in azimuth about the fixed Z axis, together with the embedded alidade frame and elevation axis. The feed arm and main reflector (together), prime focus receiver mount, and subreflector structure, together with their embedded frames, can now also rotate as a rigid unit in elevation, about the new elevation axis.

The reference optical design is still embedded in the tilted geometric telescope.

Local coordinate frames can move by individual congruence transformations, that is rotations combined with translations but without deformation. The frame attachment points (which remain origins of local Cartesian coordinate systems) and the unit frame vectors are now described as functions of the antenna elevation angle EL_{ant}, and antenna azimuth angle AZ_{ant} which is the counterclockwise alidade rotation angle, about the design azimuth axis, from the design configuration.

Descriptions of the coordinate system origins and unit coordinate frame vectors as functions of EL_{ant} and AZ_{ant} for the ideal tilted geometric telescope are given in the following paragraphs. We denote coordinate frames and frame origin points with the subscript "g" instead of "d" to indicate that we now refer to the tilted geometric telescope, rather than the design telescope. The alidade can rotate in azimuth and the tilt structure can rotate in elevation.

At this level of description we do yet not include the possibility that the alidade structure has any motions other than rotation about the design telescope's azimuth axis, the Z axis. Additional translation and rotation of the ideal tilted geometric telescope due, for example, to a wavy azimuth track is not yet allowed. Non-perpendicularity of the azimuth and elevation axes is not yet allowed.

Corresponding Local Frame Origins:

Design Telescope	Geometric Telescope
A_d	A_g
E_d	E_g
R_d	R_g
P_d	P_g
S_d	S_g
M_d	M_g

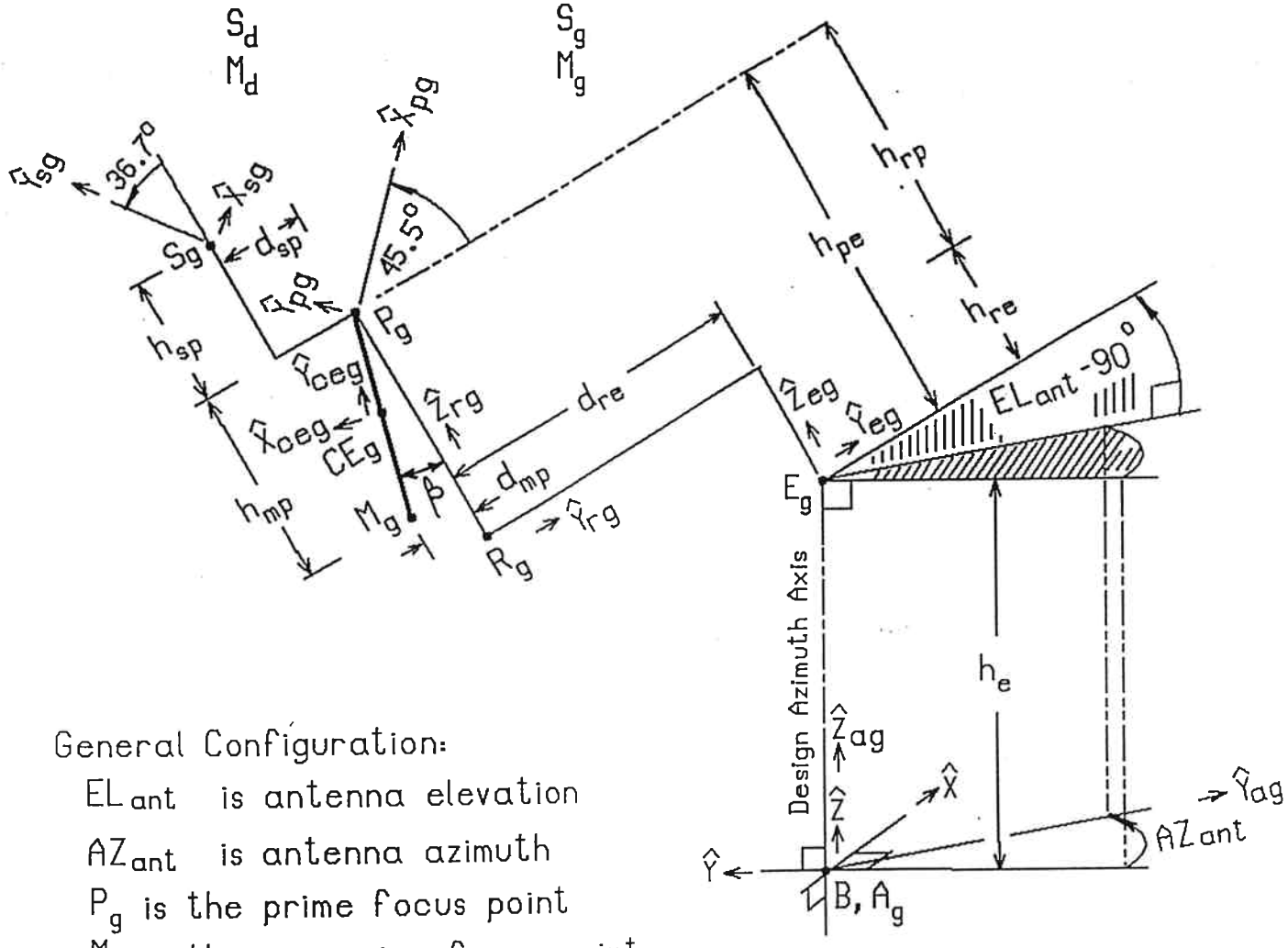

General Configuration:

- EL_{ant} is antenna elevation
- AZ_{ant} is antenna azimuth
- P_g is the prime focus point
- M_g is the gregorian focus point

Figure 4. Geometric Telescope Reference Points

Coordinate transformations defining the first six frames are given in [King 1]. We present them here, together with additional transformations relating each frame to the base frame, and also provide transformations for the frames #7 to #10. The unit frame vectors transform in the same manner as the local coordinates.A correction is required for the rotation matrix [R_{23}], and is given in Appendix I..

The reference geometry for the ideal tilted geometric telescope is shown in Figure 4.

Reference Frames For The Geometric Telescope.

We discuss the frame transformations between the alidade and base frames in some detail. Transformations between other frames follow in a similar manner. We do not reproduce computations in detail for those frames, but list the results in Appendix I.

For the geometric tilted telescope, alidade and base frames are related by:

$$(4.1.1)\quad \begin{bmatrix} X \\ Y \\ Z \end{bmatrix} = [R_{12}] \begin{bmatrix} X_{ag} \\ Y_{ag} \\ Z_{ag} \end{bmatrix}, \quad [R_{12}] = \begin{bmatrix} -1 & 0 & 0 \\ 0 & -1 & 0 \\ 0 & 0 & 1 \end{bmatrix} \begin{bmatrix} CA & -SA & 0 \\ SA & CA & 0 \\ 0 & 0 & 1 \end{bmatrix}$$
$$= \begin{bmatrix} -CA & SA & 0 \\ -SA & -CA & 0 \\ 0 & 0 & 1 \end{bmatrix}$$

where $CA = \cos(AZ_{ant})$, $SA = \sin(AZ_{ant})$ and AZ_{ant} is the counter-clockwise alidade azimuth rotation angle from the reference direction "South".

The above equation gives the transformation of coordinates for a point in space. That is, given a point Q then

$$(4.1.2)\quad \begin{bmatrix} X(Q) \\ Y(Q) \\ Z(Q) \end{bmatrix} = [R_{12}] \begin{bmatrix} X_{ag}(Q) \\ Y_{ag}(Q) \\ Z_{ag}(Q) \end{bmatrix}$$

gives the base frame coordinates of Q as a linear transformation of the alidade frame coordinates of Q .

We can also consider point Q to be described as a position vector, $\overrightarrow{Q}$, from the origin of the base frame (considered a fixed point) to the point Q . Then

$$\overrightarrow{Q} = X(Q)\cdot\widehat{X} + Y(Q)\cdot\widehat{Y} + Z(Q)\cdot\widehat{Z}\ . \tag{4.1.3}$$

The alidade frame of the geometric telescope co-rotates with the alidade structure, and is considered to be embedded in it. Unit frame vectors of the alidade structure and unit base frame vectors are related by linear transformations:

$$\begin{bmatrix}\widehat{X}\\ \widehat{Y}\\ \widehat{Z}\end{bmatrix} = [R_{12}]\begin{bmatrix}\widehat{X}_{ag}\\ \widehat{Y}_{ag}\\ \widehat{Z}_{ag}\end{bmatrix},\quad \begin{bmatrix}\widehat{X}_{ag}\\ \widehat{Y}_{ag}\\ \widehat{Z}_{ag}\end{bmatrix} = [R_{21}]\begin{bmatrix}\widehat{X}\\ \widehat{Y}\\ \widehat{Z}\end{bmatrix}\ , \text{ where} \tag{4.1.4}$$

$$[R_{21}] = [R_{12}]^{-1} = [R_{12}]^{Tr} = \begin{bmatrix}-CA & -SA & 0\\ SA & -CA & 0\\ 0 & 0 & 1\end{bmatrix}. \tag{4.1.5}$$

With respect to the geometric alidade frame:

$$\overrightarrow{Q} = X_{ag}(Q)\cdot\widehat{X}_{ag} + Y_{ag}(Q)\cdot\widehat{Y}_{ag} + Z_{ag}(Q)\cdot\widehat{Z}_{ag}\ ,\ \text{and} \tag{4.1.6}$$

$$\begin{bmatrix}X_{ag}(Q)\\ Y_{ag}(Q)\\ Zag(Q)\end{bmatrix} = [R_{21}]\begin{bmatrix}X(Q)\\ Y(Q)\\ Z(Q)\end{bmatrix}. \tag{4.1.7}$$

For the geometric telescope, the base frame coordinates of the alidade frame's origin point are

$$X(A_g) = 0,\ Y(A_g) = 0,\ Z(A_g) = 0\ . \tag{4.1.8}$$

The unit geometric alidade frame vectors, in terms of unit base frame vectors, are:

$$
\begin{aligned}
&\widehat{X}_{ag} = (-CA)(\widehat{X}) + (-SA)(\widehat{Y}) \\
&\widehat{Y}_{ag} = (SA)(\widehat{X}) + (-CA)(\widehat{Y}) \\
&\widehat{Z}_{ag} = (\widehat{Z}) \quad .
\end{aligned}
\tag{4.1.9}
$$

Geometric alidade frame coordinates of an arbitrary point in space are given in terms of its base frame coordinates by:

$$
\begin{aligned}
&X_{ag} = (-CA)(X) + (-SA)(Y) \\
&Y_{ag} = (SA)(X) + (-CA)(Y) \\
&Z_{ag} = (Z) \quad .
\end{aligned}
\tag{4.1.10}
$$

Base frame coordinates of an arbitrary point in space are given in terms of its geometric alidade frame coordinates by:

$$
\begin{aligned}
&X = (-CA)(X_{ag}) + (SA)(Y_{ag}) \\
&Y = (-SA)(X_{ag}) + (-CA)(Y_{ag}) \\
&Z = (Z_{ag}) \quad .
\end{aligned}
\tag{4.1.11}
$$

For each coordinate frame we will supply: the base system coordinates of the frame's origin point; components of each unit frame vector, in terms of the base frame unit vectors; base system coordinates of an arbitrary point, in terms of the local frame coordinates of the point; inversely, the local frame coordinates of an arbitrary point in terms of the base system coordinates of that point. For selected pairs of frames we will provide the corresponding transformations between these frames. For example it will be useful to possess transformations between the reflector frame and the frames belonging to structures on the feed arm. The general scheme to generate the desired information is the following.

Let i, j, k be coordinate frames among the frames #1 through #8 classified earlier. Let the basis vectors of frame i be $\widehat{X}_i\,,\widehat{Y}_i\,,\widehat{Z}_i$. Let the coordinates of an arbitrary point in space be: $X_i\,,Y_i\,,Z_i$ with respect to the coordinate system of that frame. We write these triples as 3×1 column matrices:

$$(4.1.12)\quad [\mathbf{X}_i] = \begin{bmatrix} X_i \\ Y_i \\ Z_i \end{bmatrix} \quad , \quad \{\widehat{\mathbf{X}_i}\} = \begin{bmatrix} \widehat{X}_i \\ \widehat{Y}_i \\ \widehat{Z}_i \end{bmatrix} .$$

For other frames, we write corresponding expressions for point coordinates and frame vectors similarly as column matrices.

Linear transformations relate the corresponding quantities in the different frames:

$$(4.1.13a)\quad [\mathbf{X}_j] = [R_{ji}][\mathbf{X}_i] + [T_{ji}] \quad , \quad \{\widehat{\mathbf{X}_j}\} = [R_{ji}]\{\widehat{\mathbf{X}_i}\} .$$

$$(4.1.13b)\quad [\mathbf{X}_k] = [R_{kj}][\mathbf{X}_j] + [T_{kj}] \quad , \quad \{\widehat{\mathbf{X}_k}\} = [R_{kj}]\{\widehat{\mathbf{X}_j}\} ,$$

where terms $[R_{pq}]$ are 3×3 rotation matrices and $[T_{pq}]$ are 3×1 column matrices representing translations.

Inverse transformations exist:

$$(4.1.13c)\quad [\mathbf{X}_i] = [R_{ij}][\mathbf{X}_j] + [T_{ij}] \quad , \quad \{\widehat{\mathbf{X}_i}\} = [R_{ij}]\{\widehat{\mathbf{X}_j}\} .$$

$$(4.1.13d)\quad [\mathbf{X}_j] = [R_{jk}][\mathbf{X}_k] + [T_{jk}] \quad , \quad \{\widehat{\mathbf{X}_j}\} = [R_{jk}]\{\widehat{\mathbf{X}_k}\} , \text{ where}$$

$$(4.1.14)\quad [R_{ij}] = [R_{ji}]^{-1} = [R_{ji}]^{Tr} \quad \text{and} \quad [T_{ij}] = [R_{ij}](-1)[T_{ji}] .$$

From (4.1.12) one obtains linear transformations relating frames k and i:

$$(4.1.15)\quad [\mathbf{X}_k] = [R_{ki}][\mathbf{X}_i] + [T_{ki}] \quad , \quad \{\widehat{\mathbf{X}_k}\} = [R_{ki}]\{\widehat{\mathbf{X}_i}\} ,$$

from the relations

$$(4.1.16)\quad [R_{ki}] = [R_{kj}][R_{ji}] , \quad [T_{ki}] = [T_{kj}] + [R_{kj}][T_{ji}] .$$

The transformation matrices and the numerical parameter values defining their elements are given explicitly in Appendix I.

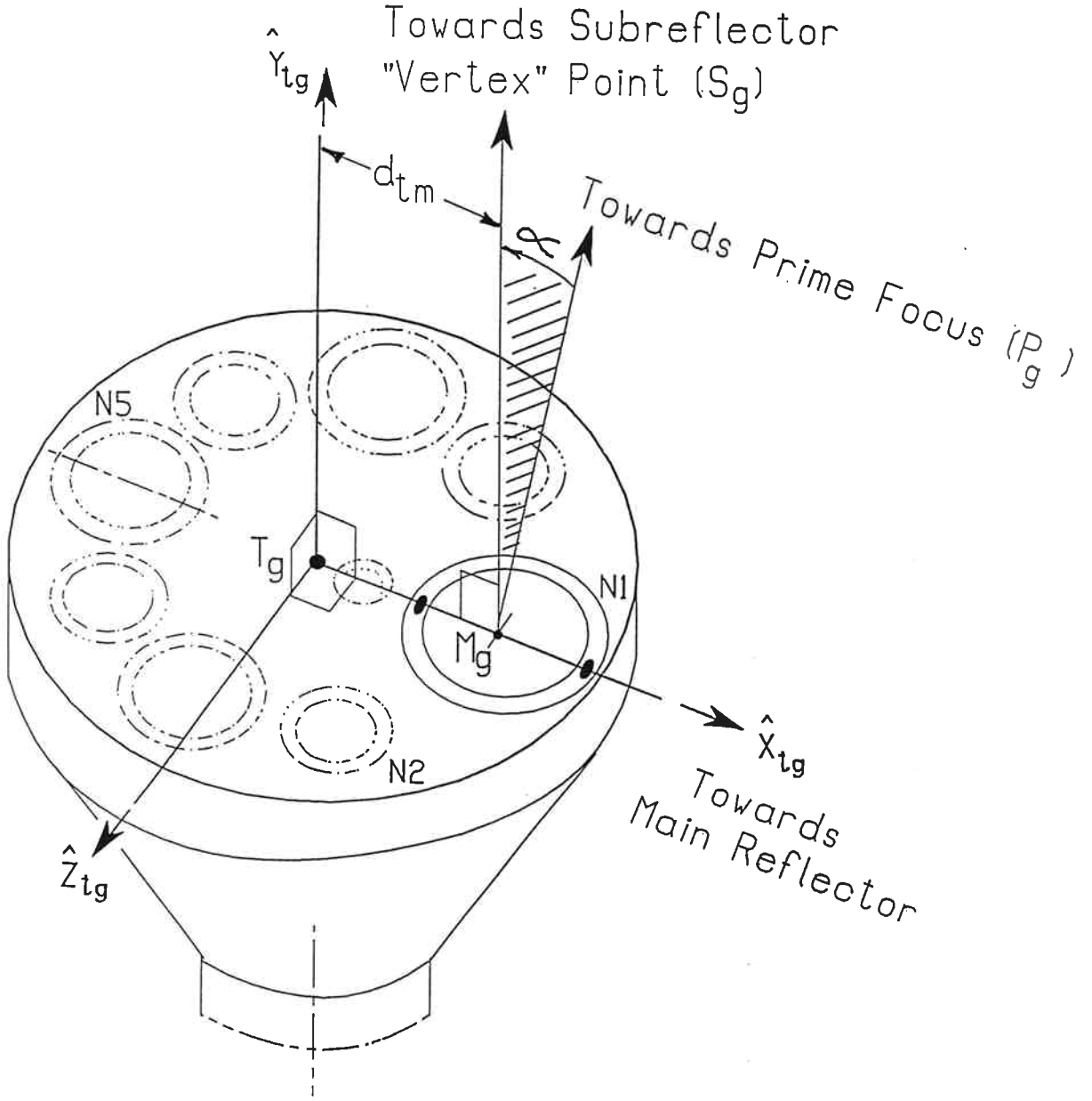

Figure 5. The Turret Frame.

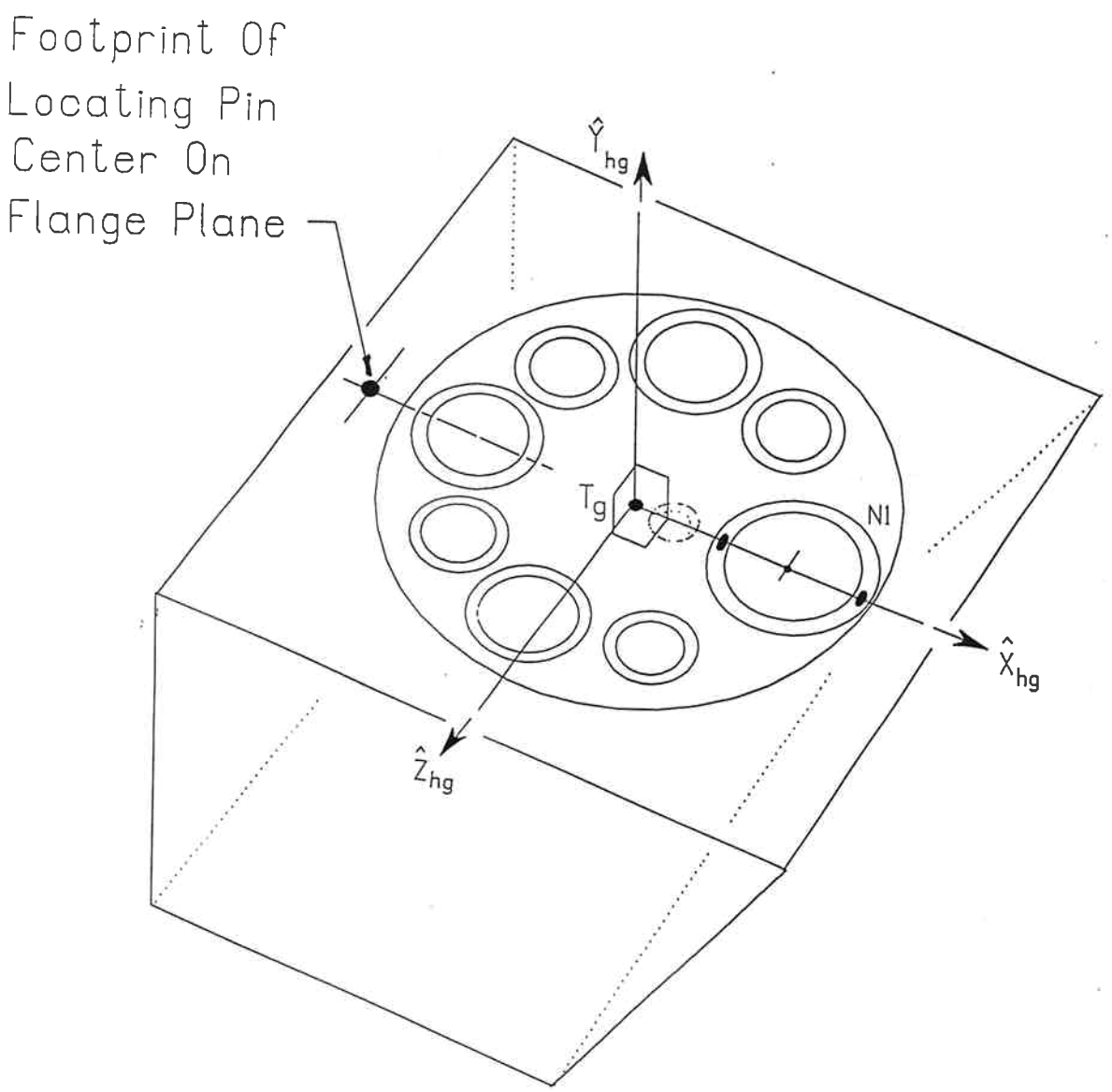

Figure 6. The Receiver House Frame.

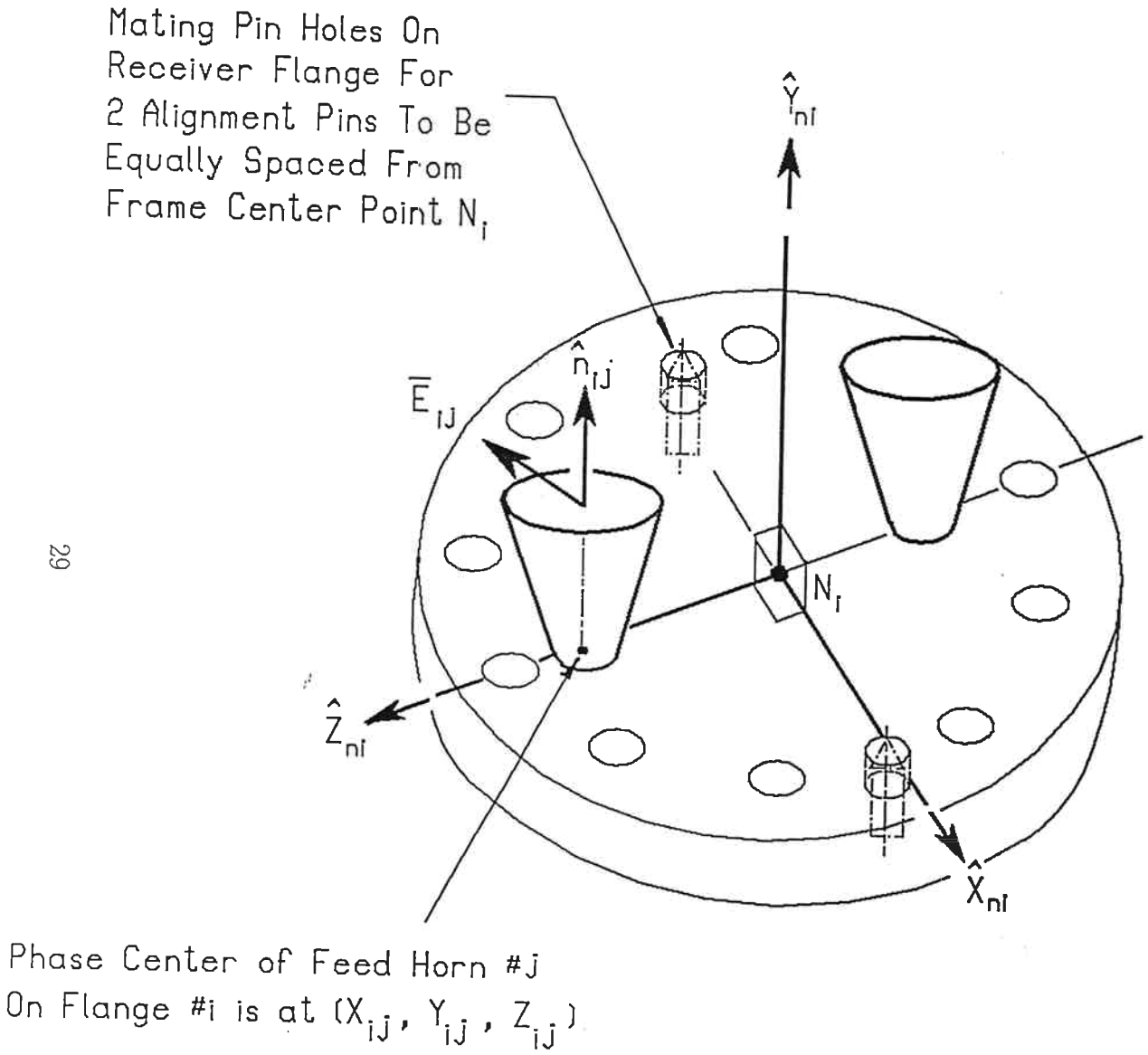

Figure 7. Suggested Receiver Flange Reference Frame

5. The Tilted Deformed Telescope.

The ideal tilted deformed telescope model to be described in this section is that described in GBT Memo 124, "The GBT Tipping-Structure Model in C", by Don Wells and Lee King [Wells-1]. Their model will be developed here in detail to find locations of fiducial reference marker points embedded in the tipping structure or in other structures above the telescope alidade, when elastic deformations of the tipping structure due to gravity loading of this structure are incorporated into telescope modeling. It will also be used to describe the gravitationally-caused shift in orientation of laser ranging platforms joined to the telescope feed arm. Effects of weight loading on the geometry of the alidade structure are not considered in [Wells-1]. The alidade geometry is still assumed to be that of the ideal tilted geometric telescope.

In the model of Wells and King, the telescope's tipping structure is described by a list of nodal points and structural members joining subsets of the nodal points. A nodal point is described by an index number and "undisplaced" Cartesian position coordinates $X_{grid}, Y_{grid}, Z_{grid}$ with respect to a local coordinate frame for the tipping structure.

This local frame is the elevation frame of the ideal tilted geometric telescope. The origin point of this frame is E_g , which is a fixed point in this model. The unit basis vectors are $\widehat{X}_{eg}$, $\widehat{Y}_{eg}$, $\widehat{Z}_{eg}$. When referred to the base frame of the telescope, these basis vectors are functions of antenna elevation EL_{ant} and azimuth AZ_{ant} . The origin point and unit frame vectors are, explicitly, as functions of EL_{ant} and AZ_{ant}:

$$(5.1) \quad \begin{bmatrix} X(E_g) \\ Y(E_g) \\ Z(E_g) \end{bmatrix} = [T_{13}] = \begin{bmatrix} 0 \\ 0 \\ h_e \end{bmatrix}$$

$$(5.2)\quad \begin{bmatrix} \widehat{X}_{eg} \\ \widehat{Y}_{eg} \\ \widehat{Z}_{eg} \end{bmatrix} = [R_{31}] \begin{bmatrix} \widehat{X} \\ \widehat{Y} \\ \widehat{Z} \end{bmatrix}, \quad \text{where}$$

$$(5.3)\quad [R_{31}] = \begin{bmatrix} -\cos AZ_{ant} & -\sin AZ_{ant} & 0 \\ \sin AZ_{ant} \cdot \sin EL_{ant} & -\cos AZ_{ant} \cdot \sin EL_{ant} & -\cos EL_{ant} \\ \sin AZ_{ant} \cdot \cos EL_{ant} & -\cos AZ_{ant} \cdot \cos EL_{ant} & \sin EL_{ant} \, . \end{bmatrix}$$

Elastic deformations to be included in the deformed telescope model are computational results of a finite element analysis of the tipping structure. In the finite element analysis the cross sectional area, moment of inertia, elastic coefficients, and weight loading are input data provided for each structural member. Our discussion will presume that the telescope tipping structure nodes at a reference antenna elevation $EL_{ant} = EL_{surf\_rig}$ (nominally 43.8° , the "surface rigging angle") are "undisturbed". Local elevation frame coordinates of each structural node will be assumed to be those belonging to that node in the geometric telescope model, for this elevation. Given initial structural data and weight loading for the tipping structure, and assuming that appropriate balancing forces and moments are added to hold the tipping structure in equilibrium with the elevation shaft at elevation angle EL_{ant}, the axial twist, transverse flexures, forces and moments can be calculated for the structural members. Displacement increments and "node rotation vectors" are calculated for each node point.

A structural model of the connecting joints for the structural members is included in the finite element analysis. Two or more structural columns may connect to one another by hinge or fully welded joints. The connecting joint member, which is a massive body, will generally be moment-resisting in one or more directions. Under force loading, the centroid of the joint member will be displaced, the joint member can rotate and may undergo strain deformation of shape. Appropriate assumptions are made in the finite element analysis to allow computation of the (small amplitude) connecting joint's rotation vector.

In generating a model of the elastically deformed telescope we formally assume that mount brackets for retroreflector fiducial reference targets and laser ranging platforms are rigidly attached locally to connecting joint members on the tipping

structure. Displacement of a fiducial reference point embedded in a retroreflector prism, caused by a change of gravity loading on the tipping structure, will be assumed to be the vector sum of the displacement of the nearby structure node point (near which its mount bracket is attached) and the fiducial point displacement generated by the rotation of the line segment between fiducial point and nearby node point. That is, the line segment from fiducial point to node point is assumed to be attached rigidly to the joint member; when the connecting joint member rotates, this rotation causes a displacement of the fiducial point. The displacement of the scan point of a laser rangefinder scanning mirror is calculated in the same manner. Internal coordinate frame unit vectors embedded in the laser rangefinder platform are rotated by the same (small) rotation vector as the connecting joint member.

Given a structural node, $\mathfrak{N}_i$, the gravitational deformation of the tipping structure produces a translation, $[\Delta(EL_{ant})]_{\mathfrak{N}_i}$, of the node position. This translation is a function of antenna elevation angle EL_{ant}, and has the following form [Wells-1], [Par-2]:

$$(5.4)\quad [\Delta(EL_{ant})]_{\mathfrak{N}_i} = \begin{bmatrix} \Delta_x(EL_{ant}) \\ \Delta_y(EL_{ant}) \\ \Delta_z(EL_{ant}) \end{bmatrix}_{\mathfrak{N}_i} = \begin{bmatrix} \sigma_{x,-z} & \sigma_{x,y} \\ \sigma_{y,-z} & \sigma_{y,y} \\ \sigma_{z,-z} & \sigma_{z,y} \end{bmatrix}_{\mathfrak{N}_i} \begin{bmatrix} \sin EL_{ant} - \sin EL_{surf\_rig} \\ \cos EL_{ant} - \cos EL_{surf\_rig} \end{bmatrix},$$

or, abbreviated,

$$(5.5)\quad [\Delta(EL_{ant})]_{\mathfrak{N}_i} = [\Delta]_{\mathfrak{N}_i} = [\sigma]_{\mathfrak{N}_i} \begin{bmatrix} \sin EL_{ant} - \sin EL_{surf\_rig} \\ \cos EL_{ant} - \cos EL_{surf\_rig} \end{bmatrix}$$

where $[\sigma]_{\mathfrak{N}_i}$ is a structural matrix associated with node $\mathfrak{N}_i$ and is computed numerically by the finite element analysis code. The detailed procedure for obtaining node matrices is discussed in [Wells-1]. Numerical examples are given there. Here we have used the abbreviations: $x \Leftrightarrow X_{eg}$, $y \Leftrightarrow Y_{eg}$, $z \Leftrightarrow Z_{eg}$. That is, the x, y, z components of the translation matrix $[\Delta]_{\mathfrak{N}_i}$ are along the X_{eg}, Y_{eg}, Z_{eg} axes respectively. The unit basis vectors pointing along these axes are given by (5.2) and (5.3) as functions of tipping structure azimuth and elevation.

The result (5.5) is obtained by resolving vertical gravity loading forces into components along the $\widehat{X}_{eg}$, $\widehat{Y}_{eg}$, $\widehat{Z}_{eg}$ directions. The initial condition is used that: nominal grid coordinates correctly describe all node locations when the tipping structure is at the elevation EL_{surf_rig}.

Wells and King [Wells-1] discuss the use of (5.5) in initially setting the surface panels which form the main reflector of the telescope. Initial panel adjustments will be performed when the tipping structure is set to an elevation angle, $EL_{birdbath}$ ($\simeq 65.8°$), suitable for construction workers to perform installation tasks. Another elevation, the "surface rigging" elevation, EL_{surf_rig}, is the desired elevation at which the tipping structure should closest approximate the ideal tilted geometric telescope. When the main reflector panel positions are initially set, with the telescope in birdbath position, the panels will be given additional translations to compensate for the deformations calculated by (5.5). By introducing positional compensation in that way the telescope can be tilted to the surface rigging elevation angle, for photogrammetric and astronomical measurements of its initial surface, and have a main reflector surface compensated for the condition that the panels were set with the telescope at a "wrong" elevation angle.

When the tipping structure elevation is other than the surface rigging elevation, there is also a node rotation: $[Rot(EL_{ant})]_{\mathfrak{N}_i}$. This may be written as a vector

$$(5.6) \quad [Rot(EL_{ant})]_{\mathfrak{N}_i} = t_x \widehat{X}_{eg} + t_y \widehat{Y}_{eg} + t_z \widehat{Z}_{eg} \equiv \mathbf{t}_{\mathfrak{N}_i} ,$$

where the local elevation system rotation vector components t_x , t_y , t_y for that node are functions of the antenna elevation angle EL_{ant}. The behavior of these components versus elevation angle is similar to that of the displacement components. In place of (5.4) one has:

$$(5.7) \quad [Rot(EL_{ant})]_{\mathfrak{N}_i} = \begin{bmatrix} t_x(EL_{ant}) \\ t_y(EL_{ant}) \\ t_z(EL_{ant}) \end{bmatrix}_{\mathfrak{N}_i} = \begin{bmatrix} \tau_{x,-z} & \tau_{x,y} \\ \tau_{y,-z} & \tau_{y,y} \\ \tau_{z,-z} & \tau_{z,y} \end{bmatrix}_{\mathfrak{N}_i} \begin{bmatrix} \sin EL_{ant} - \sin EL_{surf\_rig} \\ \cos EL_{ant} - \cos EL_{surf\_rig} \end{bmatrix},$$

or, abbreviated,

$$(5.8) \quad \mathbf{t}_{\mathfrak{N}_i} = [Rot]_{\mathfrak{N}_i} = [\tau]_{\mathfrak{N}_i} \begin{bmatrix} \sin EL_{ant} - \sin EL_{surf\_rig} \\ \cos EL_{ant} - \cos EL_{surf\_rig} \end{bmatrix}$$

where $[\tau]_{\mathfrak{N}_i}$ is a structural matrix of node rotation constants associated with node $\mathfrak{N}_i$ and is computed numerically by the finite element analysis code. The unit geometric elevation frame basis vectors appearing in (5.6) are defined by equations (5.2) and (5.3).

The finite analysis output data base for each node is a row of 16 entries: the node identification number, three undisturbed position coordinates for the node, six element entries for the displacement matrix $[\sigma]$, and six element entries for the rotation matrix $[\tau]$.

Structural node points are not per se accessible to measurement. They generally lie somewhere within connecting joints of structural members and are not directly visible. To locate them one uses "fiducial reference marker points" which are directly accessible for optical measurement of location. In the present context, a fiducial reference marker point, or "fiducial point" abbreviated, is the center point of a surveyor's target or the optical center of a retroreflector prism which can be located by optical instruments such as theodolites or laser ranging stations, and which is rigidly affixed to the structure near a nodal point. If the positions of three or more fiducial points attached near a given structural node can be measured optically (for example, by laser ranging from several stations), the position of the node point can be determined, provided that the local rigid 3-dimensional positioning of the fiducials around the node was determined when the fiducial targets were mounted on the structure. When the telescope is moved in elevation, the displacements of the fiducial points associated with a structural node point will not be exactly that of the node point. Rotation of the node joint produces an additional displacement of a nearby fiducial point which is small, but not negligible. In the next paragraph we discuss the relationship between the displacement of a node and that of a nearby fiducial point.

We assume that a surveyor's target structure containing an intrinsically embedded fiducial point, $\mathfrak{F}_i$, has been rigidly attached to the tipping structure near structural node point $\mathfrak{N}_i$. We assume also that the local undisturbed displacement vector from the node to the fiducial point has been defined in some manner, which we do not specify explicitly. We are given

$$(5.9)\qquad \begin{bmatrix} X_{eg}(\mathfrak{F}_i) \\ Y_{eg}(\mathfrak{F}_i) \\ Z_{eg}(\mathfrak{F}_i) \end{bmatrix} = \begin{bmatrix} X_{eg}(\mathfrak{N}_i) + \xi_i \\ Y_{eg}(\mathfrak{N}_i) + \eta_i \\ Z_{eg}(\mathfrak{N}_i) + \zeta_i \end{bmatrix} = \begin{bmatrix} X_{eg}(\mathfrak{N}_i) \\ Y_{eg}(\mathfrak{N}_i) \\ Z_{eg}(\mathfrak{N}_i) \end{bmatrix} + [D_i] \,.$$

Here, $X_{eg}(\mathfrak{N}_i)$, $Y_{eg}(\mathfrak{N}_i)$, and $Z_{eg}(\mathfrak{N}_i)$ are the undisturbed elevation system coordinates of the node point, that is the geometric telescope elevation coordinates of $\mathfrak{N}_i$ at the rigging angle EL_{surf_rig}; $X_{eg}(\mathfrak{F}_i)$, $Y_{eg}(\mathfrak{F}_i)$, and $Z_{eg}(\mathfrak{F}_i)$ are the undisturbed

elevation system coordinates of the fiducial point. The undisturbed displacement vector of the fiducial point $\mathfrak{F}_i$ from the nodal point $\mathfrak{N}_i$ is

$$(5.10) \qquad [D_i] = \left[\begin{array}{c} \xi \\ \eta \\ \zeta \end{array} \right]_{\mathfrak{N}_i} = \left[\begin{array}{c} \xi_i \\ \eta_i \\ \zeta_i \end{array} \right] .$$

When the tipping structure rotates in elevation from the rigging angle EL_{surf_rig} to the general elevation angle EL_{ant}, node point $\mathfrak{N}_i$ moves to a position whose coordinates relative to the geometric elevation system frame are:

$$(5.11) \qquad \left[\begin{array}{c} X_e(\mathfrak{N}_i) \\ Y_e(\mathfrak{N}_i) \\ Z_e(\mathfrak{N}_i) \end{array} \right] = \left[\begin{array}{c} X_{eg}(\mathfrak{N}_i) \\ Y_{eg}(\mathfrak{N}_i) \\ Z_{eg}(\mathfrak{N}_i) \end{array} \right] + [\Delta]_{\mathfrak{N}_i} .$$

The associated fiducial point moves to the position whose coordinates are:

$$(5.12) \qquad \left[\begin{array}{c} X_e(\mathfrak{F}_i) \\ Y_e(\mathfrak{F}_i) \\ Z_e(\mathfrak{F}_i) \end{array} \right] = \left[\begin{array}{c} X_{eg}(\mathfrak{N}_i) \\ Y_{eg}(\mathfrak{N}_i) \\ Z_{eg}(\mathfrak{N}_i) \end{array} \right] + [\Delta]_{\mathfrak{N}_i} + \left[Rot(\ \mathbf{t}_{\mathfrak{N}_i}) \right] [D_i] .$$

The last term is the perturbed displacement vector between node and fiducial point. The displacement vector between node and fiducial point is rotated by $\mathbf{t}_{\mathfrak{N}_i}$ due to the rigid body rotation of the connection joint member at the node. The new position of the fiducial point is then:

$$(5.13) \qquad \left[\begin{array}{c} X_e(\mathfrak{F}_i) \\ Y_e(\mathfrak{F}_i) \\ Z_e(\mathfrak{F}_i) \end{array} \right] = \left[\begin{array}{c} X_{eg}(\mathfrak{F}_i) \\ Y_{eg}(\mathfrak{F}_i) \\ Z_{eg}(\mathfrak{F}_i) \end{array} \right] + [\Delta]_{\mathfrak{N}_i} + \left\{ \left[Rot(\ \mathbf{t}_{\mathfrak{N}_i}) \right] [D_i] - [D_i] \right\} .$$

Defining

$$(5.14) \qquad \left[Rot(\ \mathbf{t}_{\mathfrak{N}_i}) \right] [D_i] - [D_i] = [\delta Rot(\ \mathbf{t}_{\mathfrak{N}_i})] [D_i] , \text{ we get}$$

$$(5.15) \qquad \left[\begin{array}{c} X_e(\mathfrak{F}_i) \\ Y_e(\mathfrak{F}_i) \\ Z_e(\mathfrak{F}_i) \end{array} \right] = \left[\begin{array}{c} X_{eg}(\mathfrak{F}_i) \\ Y_{eg}(\mathfrak{F}_i) \\ Z_{eg}(\mathfrak{F}_i) \end{array} \right] + [\Delta]_{\mathfrak{N}_i} + [\delta Rot(\ \mathbf{t}_{\mathfrak{N}_i})] [D_i] .$$

The term $[\delta Rot(\ \mathbf{t}_{\mathfrak{N}_i})] [D_i]$ vanishes in the special case $\left| \ \mathbf{t}_{\mathfrak{N}_i} \right| = 0$.

With respect to the local elevation frame the gravity-load-induced displace-

ment of the fiducial point is the same as that of the associated node except for the additional differential rotation term (5.14). To evaluate this term let us write the displacement vector $[D_i]$ in vector notation:

$$(5.16) \qquad [D_i] = \xi_i \widehat{X}_{eg} + \eta_i \widehat{Y}_{eg} + \zeta_i \widehat{Z}_{eg} = \mathbf{D_i} \ .$$

The term $\left[Rot(\ \mathbf{t}_{\mathfrak{N}_i})\right][D_i]$ is a clockwise rotation of the vector $\mathbf{D_i}$ by an angle $\left|\ \mathbf{t}_{\mathfrak{N}_i}\right|$ radians about an axis pointing in the direction of $\mathbf{t}_{\mathfrak{N}_i}$. Calling

$$(5.17) \qquad t = \left|\ \mathbf{t}_{\mathfrak{N}_i}\right| = \sqrt{t_x^2 + t_y^2 + t_z^2} = t(\mathfrak{N}_i)\,,$$

it may be shown[1] that

$$(5.18) \qquad \left[Rot(\ \mathbf{t}_{\mathfrak{N}_i})\right][D_i] = (\cos t)(\ \mathbf{D}_i) + \frac{(1-\cos t)}{t^2}\left(\ \mathbf{t}_{\mathfrak{N}_i} \cdot\ \mathbf{D}_i\right)\left(\ \mathbf{t}_{\mathfrak{N}_i}\right) + \left(\frac{\sin t}{t}\right)\left(\ \mathbf{t}_{\mathfrak{N}_i} \times\ \mathbf{D}_i\right).$$

For $0 < t << 1$ radian, expanding (5.18) to order 3 in t,

$$(5.19) \quad \left[\delta Rot(\ \mathbf{t}_{\mathfrak{N}_i})\right][D_i] = \left(\ \mathbf{t}_{\mathfrak{N}_i} \times\ \mathbf{D}_i\right)\left(1 - \frac{t^2}{6}\right) + \left(\ \mathbf{t}_{\mathfrak{N}_i}\right)\left(\frac{\mathbf{t}_{\mathfrak{N}_i} \cdot\ \mathbf{D}_i}{2}\right) - \left(\ \mathbf{D}_i\right)\left(\frac{t^2}{2}\right)$$

$$= \begin{bmatrix} \left(1 - \dfrac{t^2}{6}\right)(t_y\zeta_i - t_z\eta_i) + \left(\dfrac{t_x}{2}\right)(t_x\xi_i + t_y\eta_i + t_z\zeta_i) - (\xi_i)\left(\dfrac{t^2}{2}\right) \\ \left(1 - \dfrac{t^2}{6}\right)(t_z\xi_i - t_x\zeta_i) + \left(\dfrac{t_y}{2}\right)(t_x\xi_i + t_y\eta_i + t_z\zeta_i) - (\eta_i)\left(\dfrac{t^2}{2}\right) \\ \left(1 - \dfrac{t^2}{6}\right)(t_x\eta_i - t_y\xi_i) + \left(\dfrac{t_z}{2}\right)(t_x\xi_i + t_y\eta_i + t_z\zeta_i) - (\zeta_i)\left(\dfrac{t^2}{2}\right) \end{bmatrix}.$$

For a retroreflector's fiducial point, located within a few meters of its associated node, the joint rotation term above is sufficiently well approximated by the first order term $\mathbf{t}_{\mathfrak{N}_i} \times \mathbf{D}_i$. Equation (5.19) can also be employed in the case where $\mathbf{D}_i$ represents not the displacement of a fiducial point from a structural node, but instead is a local unit frame vector of a feed arm laser station. In the latter situation, one may want to include terms above first order.

[1] H. Goldstein, Classical Mechanics, Addison-Wesley, 2'nd Edition 1980, pp 164-165.

Local Elevation Frames At The Structural Nodes.

The geometric elevation frame of the tipping structure is a globally defined frame:

$$\{\widehat{X}_{eg}(AZ_{ant},\, EL_{ant})\,,\, \widehat{Y}_{eg}(AZ_{ant},\, EL_{ant})\,,\, \widehat{Z}_{eg}(AZ_{ant},\, EL_{ant});\, E_g\}$$

consisting of three mutually perpendicular unit basis vectors attached to origin point E_g . These vectors, which we abbreviate as $\widehat{X}_{eg}$, $\widehat{Y}_{eg}$, $\widehat{Z}_{eg}$ respectively, are functions of tipping structure angles AZ_{ant} and EL_{ant} , and are given explicitly by (5.2) and (5.3). They are the geometric elevation frame basis vectors defined by the ideal geometric telescope model, which assumes that the feed arm and main reflector are both rigid and rigidly attached to one another. The vectors are defined for the global tipping structure geometry and do not relate to local embedding at any particular structural node.

To calculate aiming of laser beams of feed arm laser rangefinders, one requires a local model of elastic telescope deformations. The finite element model of the tipping structure generates deformation displacements $[\Delta]_{\mathfrak{N}_i}$ of structural node points $\mathfrak{N}_i$ and deformation rotations $\mathbf{t}_{\mathfrak{N}_i}$ of their associated connection joints, as functions of EL_{ant} and a reference rigging elevation angle. Laser rangefinders rest on support platforms which provide local rigid reference frames for aiming the scanning beams. A laser beam is aimed by calling out two mirror scan angles defined with respect to a local platform frame. These are the scan-azimuth angle, A_T, to a distant target point T and the scan-elevation angle, E_T, to T . Differential elastic displacements and node rotations near the target point and laser platform change the scan-azimuth and scan-elevation angles needed to aim the laser beam from a scan mirror's scan fiducial point S to target point T . (The scan fiducial point is the intersection point of the scan rotor axes). To calculate scan angle corrections it is useful to define local elevation frames at structure nodes adjacent to laser rangefinder platforms and to main reflector nodes adjacent to surface retroreflector prism targets.

Given a generic structural node point $\mathfrak{N}_i$ let us try to define a "local elevation frame" at $\mathfrak{N}_i$:

$$\{\widehat{X}_e(AZ_{ant}, EL_{ant}; \mathfrak{N}_i)\,,\ \widehat{Y}_e(AZ_{ant}, EL; \mathfrak{N}_i)\,,\ \widehat{Z}_e(AZ_{ant}, EL_{ant}; \mathfrak{N}_i); \mathfrak{N}_i\}\,.$$

This consists of a right-hand triple of mutually perpendicular unit basis vectors: $\widehat{X}_e(AZ_{ant}, EL_{ant})$, $\widehat{Y}_e(AZ_{ant}, EL_{ant})$, $\widehat{Z}_e(AZ_{ant}, EL_{ant})$ and a point of frame attachment, $\mathfrak{N}_i$. To complete the frame definition we specify its basis vectors as functions of AZ_{ant} and EL_{ant}.

We want the frame to be rigidly embedded in the structure, at point $\mathfrak{N}_i$, and to co-move with the structure joint at $\mathfrak{N}_i$. If this is to be accomplished when the deformation of the structure is provided by the finite element model we must choose:

$$(5.20.1)\quad \widehat{X}_e(AZ_{ant}, EL_{ant}; \mathfrak{N}_i) = [Rot(\ \mathbf{t}_{\mathfrak{N}_i})]\widehat{X}_{eg} = \widehat{X}_{eg} + [\delta Rot(\ \mathbf{t}_{\mathfrak{N}_i})]\widehat{X}_{eg}\,,$$

$$(5.20.2)\quad \widehat{Y}_e(AZ_{ant}\,,\ EL_{ant}\,;\mathfrak{N}_i) = [Rot(\ \mathbf{t}_{\mathfrak{N}_i})]\widehat{Y}_{eg} = \widehat{Y}_{eg} + [\delta Rot(\ \mathbf{t}_{\mathfrak{N}_i})]\widehat{Y}_{eg}\,,$$

$$(5.20.3)\quad \widehat{Z}_e(AZ_{ant}\,,\ EL_{ant}\,;\mathfrak{N}_i) = [Rot(\ \mathbf{t}_{\mathfrak{N}_i})]\widehat{Z}_{eg} = \widehat{Z}_{eg} + [\delta Rot(\ \mathbf{t}_{\mathfrak{N}_i})]\widehat{Z}_{eg}\,.$$

The rotation operator $[\delta Rot(\ \mathbf{t}_{\mathfrak{N}_i})]$ is given for an arbitrary vector by (5.19). The components of $\mathbf{t}_{\mathfrak{N}_i}$ are supplied as functions of EL_{ant}, at node $\mathfrak{N}_i$, by (5.8). The constant structure matrix $[\tau]_{\mathfrak{N}_i}$ supplied by the current finite element structural model. Let us use the abbreviations:

$$(5.21.1)\quad \widehat{X}_e(AZ_{ant}\,,\ EL_{ant}\,;\mathfrak{N}_i) = \widehat{X}_e(\mathfrak{N}_i)\,,$$

$$(5.21.2)\quad \widehat{Y}_e(AZ_{ant}\,,\ EL_{ant}\,;\mathfrak{N}_i) = \widehat{Y}_e(\mathfrak{N}_i)\,,$$

$$(5.21.1)\quad \widehat{Z}_e(AZ_{ant}\,,\ EL_{ant}\,;\mathfrak{N}_i) = \widehat{Z}_e(\mathfrak{N}_i)\,.$$

From (5.19), we get, a functions of the components of $\mathbf{t}_{\mathfrak{N}_i}$:

$$(5.22.1)\quad \widehat{X}_e(\mathfrak{N}_i) = \widehat{X}_{eg}(1-\frac{t^2}{2}+\frac{t_x^2}{2})+\widehat{Y}_{eg}(t_z+\frac{t_xt_y}{2}-\frac{t_zt^2}{6})+\widehat{Z}_{eg}(-t_y+\frac{t_xt_z}{2}+\frac{t_yt^2}{6})\,,$$

$$(5.22.2)\quad \widehat{Y}_e(\mathfrak{N}_i) = \widehat{Y}_{eg}(1-\frac{t^2}{2}+\frac{t_y^2}{2})+\widehat{Z}_{eg}(t_x+\frac{t_yt_z}{2}-\frac{t_xt^2}{6})+\widehat{X}_{eg}(-t_z+\frac{t_yt_x}{2}+\frac{t_zt^2}{6})\,,$$

$$(5.22.3)\quad \widehat{Z}_e(\mathfrak{N}_i) = \widehat{Z}_{eg}(1-\frac{t^2}{2}+\frac{t_z^2}{2})+\widehat{X}_{eg}(t_y+\frac{t_zt_x}{2}-\frac{t_yt^2}{6})+\widehat{Y}_{eg}(-t_x+\frac{t_zt_y}{2}+\frac{t_xt^2}{6})\,.$$

In the next sections we use this result to compute laser rangefinder aiming corrections.

Laser Rangefinder Platform And Scan Geometry.

We will define a local frame for a laser rangefinder platform joined rigidly to the GBT feed arm near structural node point $\mathfrak{N}_i$:

$$\{\widetilde{X}_e(AZ_{ant}\,,\,EL_{ant};\,\mathfrak{L})\,,\,\widetilde{Y}_e(AZ_{ant}\,,\,EL_{ant};\,\mathfrak{L}\,)\,,\,\widetilde{Z}_e(AZ_{ant}\,,\,EL_{ant}\,;\,\mathfrak{L})\,;\;\mathfrak{L}\}\,.$$

This consists of mutually perpendicular unit basis vectors: $\widetilde{X}_e$, $\widetilde{Y}_e$, $\widetilde{Z}_e$ embedded rigidly in the platform at platform fiducial point $\mathfrak{L}$.

We first assume that a reference orientation of the platform with respect to the geometric elevation frame of the tipping structure is specified, at the surface rigging elevation angle. This specification is provided by a linear transformation:

$$(5.23.1)\qquad \begin{bmatrix} \widetilde{X}_e(AZ_{ant}\,,\,EL_{surf\_rig};\,\mathfrak{L}\,) \\ \widetilde{Y}_e(AZ_{ant}\,,\,EL_{surf\_rig};\,\mathfrak{L}\,) \\ \widetilde{Z}_e(AZ_{ant}\,,\,EL_{surf\_rig};\,\mathfrak{L}\,) \end{bmatrix} =$$

$$\begin{bmatrix} A_{11}\widehat{X}_{eg}(AZ_{ant},EL_{surf\_rig}) + A_{12}\widehat{Y}_{eg}(AZ_{ant},EL_{surf\_rig}) + A_{13}\widehat{Z}_{eg}(AZ_{ant},EL_{surf\_rig}) \\ A_{21}\widehat{X}_{eg}(AZ_{ant},EL_{surf\_rig}) + A_{22}\widehat{Y}_{eg}(AZ_{ant},EL_{surf\_rig}) + A_{23}\widehat{Z}_{eg}(AZ_{ant},EL_{surf\_rig}) \\ A_{31}\widehat{X}_{eg}(AZ_{ant},EL_{surf\_rig}) + A_{32}\widehat{Y}_{eg}(AZ_{ant},EL_{surf\_rig}) + A_{33}\widehat{Z}_{eg}(AZ_{ant},EL_{surf\_rig}) \end{bmatrix}.$$

We abbreviate the quantities in the above equation as:

$$(5.23.2)\qquad \widetilde{\mathbf{X}}_{eg}(\,\mathfrak{L}\,) = [A]_{\mathfrak{N}_i}\;\widetilde{\mathbf{X}}_{eg}\,.$$

Coefficients in the matrix $[A]_{\mathfrak{N}_i}$ are the projections of the platform frame basis vectors onto the geometric elevation frame basis vectors, at the surface rigging elevation angle and arbitrary telescope azimuth angle. That is, the matrix elements are direction cosines,

$$(5.24) \quad [A]_{\mathfrak{N}_i} = \begin{bmatrix} \widetilde{X}_{eg} \cdot \widehat{X}_{eg} & \widetilde{X}_{eg} \cdot \widehat{Y}_{eg} & \widetilde{X}_{eg} \cdot \widehat{Z}_{eg} \\ \widetilde{Y}_{eg} \cdot \widehat{X}_{eg} & \widetilde{Y}_{eg} \cdot \widehat{Y}_{eg} & \widetilde{Y}_{eg} \cdot \widehat{Z}_{eg} \\ \widetilde{Z}_{eg} \cdot \widehat{X}_{eg} & \widetilde{Z}_{eg} \cdot \widehat{Y}_{eg} & \widetilde{Z}_{eg} \cdot \widehat{Z}_{eg} \end{bmatrix}_{(EL_{surf\_rig})}$$

Provisional feed arm scan point locations and platform orientation matrices $[A]_{\mathfrak{N}_i}$ have been computed for feed arm laser rangefinders, by F.R. Schwab. His suggested locations and orientations are presented in a limited distribution memo: "Laser Rangefinder Locations and Orientations" (March 6, 1996). Rangefinders set at the locations and orientations given in that memo have adequate scan coverage of the GBT main reflector, at small enough beam incidence angles to the surface retroreflectors to insure adequate reflected optical return. The coordinate frame used in that memo is not a standard GBT coordinate frame. The given matrix elements and coordinates require a (simple) transcription to the standard geometric elevation frame.

Each feed arm rangefinder mounts rigidly near an adjoining feed arm structural node. The node point and rangefinder fiducial reference points are assigned reference geometric frame coordinates when the telescope is at the surface rigging elevation. The assigned reference coordinates might initially be calculated ideal location coordinates, to be replaced later by measured values at the surface rigging elevation or at another elevation with finite element mode corrections. When $EL_{ant} = EL_{surf\_rig}$ the local elevation frame coordinates of node and rangefinder fiducial points are defined to coincide with the reference coordinates of these points in the geometric elevation frame. In turn, the reference coordinates of these points are included in a database file listing for distinguished telescope points. There is, however, a problem associated with the assignment of reference points to the feed arm structural node and rangefinder fiducial points. We discuss this problem and suggest a solution in the next paragraphs.

Initial joining of the upper feed arm to the telescope and measurement of its fiducial reference points will not necessarily be made at surface rigging elevation. It is possible that these operations will occur when the tipping structure is near the feed arm access elevation, $EL_{arm\_access} \simeq 77.7°$, with upper feed arm vertical. (At that time surface panels may or not be installed. Weight loading on the telescope may or may not be at its final distribution). For initial feed arm alignment and adjustment, it may be preferable to reference undisturbed coor-

dinates of feed arm nodes and fiducials to another access angle, EL_{access}, (for example either feed arm access elevation EL_{arm_access} or surface access elevation $EL_{birdbath}$) rather than EL_{surf_rig}. Node deformations and node joint rotations would reference to EL_{access} which would replace EL_{surf_rig} in (5.4)-(5.8). This is discussed in [Wells-1].

When using gravity structural deformation corrections to correct rangefinder aiming, it is desirable to have a common reference coordinate data base for all tipping structure nodes and fiducial reference points. Separate data bases and data handling procedures for feed arm and main reflector nodes and fiducials are undesirable, and present opportunity for ambiguity.

The view is expressed here that all elevation frame node and fiducial point undisturbed coordinates should refer to values when the tipping structure is at elevation angle EL_{surf_rig}. This differs from the viewpoint presented in [Wells-1], which presumes that undisturbed coordinates of feed arm nodes be defined at a different tipping structure elevation angle.

The two viewpoints can be reconciled if one databases initial reference coordinates required by [Wells-1] under another nomenclature, for example "installation coordinates" and computes the geometric elevation "undisturbed coordinates" at EL_{surf_rig} using transformations (5.5) and (5.8) but making the replacements $EL_{surf\_rig} \rightarrow EL_{access}$, $EL_{ant} \rightarrow EL_{surf\_rig}$ in those equations.

One can now compute platform basis vectors explicitly, for the gravity-loaded tipping structure. One first computes basis vectors: $\widehat{X}_e(\mathfrak{N}_i)$, $\widehat{Y}_e(\mathfrak{N}_i)$, $\widehat{Z}_e(\mathfrak{N}_i)$ of the local elevation frame at $\mathfrak{N}_i$ defined by (5.21), using equations (5.22). Because the local elevation frame at $\mathfrak{N}_i$ and the platform frame at $\mathfrak{L}$ are rigidly joined to each other, the same linear transformation matrix $[A]_{\mathfrak{N}_i}$ that relates their basis vectors at surface rigging elevation (cf. (5.23)) also relates their basis vectors at arbitrary elevation and azimuth. One then computes platform basis vectors for the gravity-loaded structure: $\widetilde{X}_e(AZ_{ant}, EL_{ant};\, \mathfrak{L})$, $\widetilde{Y}_e(AZ_{ant}, EL_{ant};\, \mathfrak{L})$, $\widetilde{Z}_e(AZ_{ant}, EL_{ant};\, \mathfrak{L})$, using the same linear transformation:

$$(5.25) \qquad \begin{bmatrix} \widetilde{X}_e(AZ_{ant}, EL_{ant};\, \mathfrak{L}) \\ \widetilde{Y}_e(AZ_{ant}, EL_{ant};\, \mathfrak{L}) \\ \widetilde{Z}_e(AZ_{ant}, EL_{ant};\, \mathfrak{L}) \end{bmatrix} = [A]_{\mathfrak{N}_i} \begin{bmatrix} \widehat{X}_e(\mathfrak{N}_i) \\ \widehat{Y}_e(\mathfrak{N}_i) \\ \widehat{Z}_e(\mathfrak{N}_i) \end{bmatrix}.$$

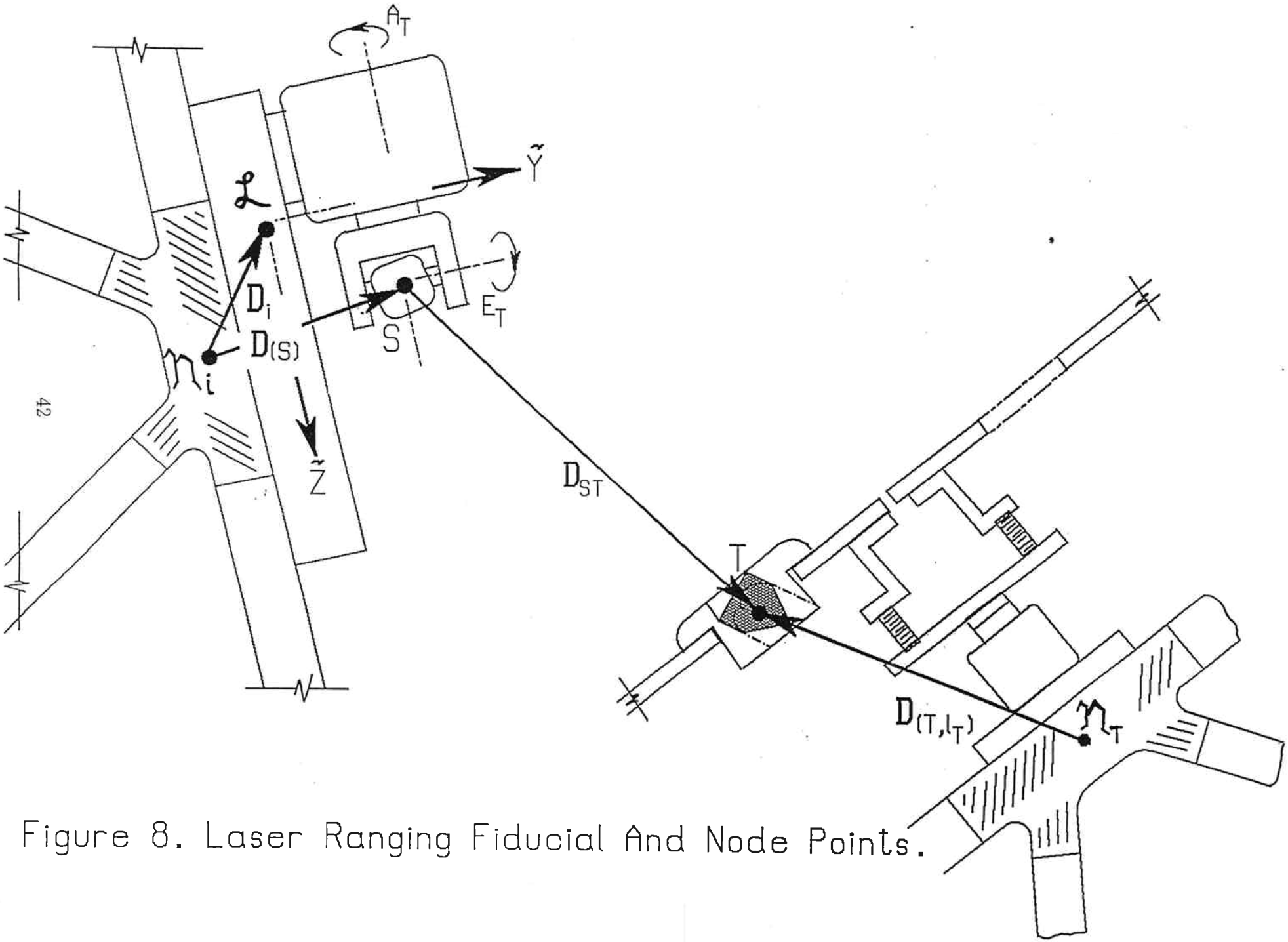

Figure 8. Laser Ranging Fiducial And Node Points.

Rangefinder Scan Angle Corrections.

We now discuss the correction of laser rangefinder scan angles for gravity-loading changes when the telescope tilts in elevation.

Assume that a rangefinder platform is rigidly attached to the feed arm near structure node point $\mathfrak{N}_i$. Let $\mathfrak{L}$ be the origin point of the rangefinder's platform frame, and S be the rangefinder's scan center point. As before, we let $\widetilde{X}$, $\widetilde{Y}$, $\widetilde{Z}$ be unit basis vectors for the platform frame. (Cf. Figure 8).

Given a laser target fiducial point, T, on the tipping structure, which is to be scanned by the rangefinder's laser beam, we let $\widetilde{x}_T$, $\widetilde{y}_T$, $\widetilde{z}_T$ be the platform frame coordinates of T. Typically T would be the optical center of a cube corner retroreflector prism on a surface panel of the telescope's main reflector.

Introduce local spherical polar coordinates in the laser platform frame, so that

$$\text{(5.26)} \qquad \begin{bmatrix} \widetilde{x}_T \\ \widetilde{y}_T \\ \widetilde{z}_T \end{bmatrix} = \begin{bmatrix} R(\sin\Phi)(\cos\Theta) \\ R(\sin\Phi)(\sin\Theta) \\ R(\cos\Phi) \end{bmatrix} .$$

Inversely,

$$\text{(5.27.1)} \qquad \Phi = \cos^{-1}(\frac{\widetilde{z}_T}{R}) \ , \quad 0 \le \Phi \le \pi \ ,$$

$$\text{(5.27.2)} \qquad \Theta = (a\tan_2)(\frac{\widetilde{z}_T}{R}) \ , \quad -\frac{\pi}{2} \le \Phi < \frac{3\pi}{2} \ ,$$

$$\text{(5.27.3)} \qquad R = \sqrt{(\widetilde{x}_T)^2 + (\widetilde{y}_T)^2 + (\widetilde{z}_T)^2} \ .$$

Assuming that the rangefinder scan axes are properly zeroed, intersect, are mutually perpendicular, and the scan-azimuth axis is aligned along the platform basis vector $\widetilde{Z}$, the rangefinder rotor angles required to aim the laser beam from scan center point S to target point T are:

$$\text{(5.28.1)} \qquad A_T = \Theta - \frac{\pi}{2} \ , \ -\pi \le A_T < \pi \ , \text{ the scan-azimuth angle, and}$$

$$\text{(5.28.2)} \qquad E_T = (-1)(\frac{\Phi}{2}) \ , \ -\frac{\pi}{2} \le E_T \le 0 \ , \text{ the scan-elevation angle.}$$

The rangefinder platform frame coordinates of T are then:

$$(5.29)\qquad \begin{bmatrix} \widetilde{x}_T \\ \widetilde{y}_T \\ \widetilde{z}_T \end{bmatrix} = \begin{bmatrix} R(\sin 2E_T)(\sin A_T) \\ (-1)R(\sin 2E_T)(\cos A_T) \\ R(\cos 2E_T) \end{bmatrix} .$$

When the telescope's tipping structure is in general position, specified by angles EL_{ant} and AZ_{ant}, the "undisturbed" geometric elevation coordinates of the points $\mathfrak{N}_i$, $\mathfrak{L}$, S are the elevation coordinates of these points which would be attained in the absence of gravity load deformation of the telescope. The displacement vectors of these points from the geometric elevation frame origin point, E_g , are:

$$\begin{aligned}(5.30)\qquad \mathbf{X}_{eg}(\mathfrak{N}_i) \equiv\ & X_{eg}(EL_{surf\_rig};\, \mathfrak{N}_i)\, \widehat{X}_{eg}(AZ_{ant}, EL_{ant}) \\ & + Y_{eg}(EL_{surf\_rig};\, \mathfrak{N}_i)\, \widehat{Y}_{eg}(AZ_{ant}, EL_{ant}) \\ & + Z_{eg}(EL_{surf\_rig};\, \mathfrak{N}_i)\, \widehat{Z}_{eg}(AZ_{ant}, EL_{ant}) ,\end{aligned}$$

$$\begin{aligned}(5.31)\qquad \mathbf{X}_{eg}(\mathfrak{L}) \equiv\ & \mathbf{X}_{eg}(\mathfrak{N}_i) + \xi(\mathfrak{L})\, \widehat{X}_{eg}(AZ_{ant}, EL_{ant}) \\ & + \eta(\mathfrak{L})\, \widehat{Y}_{eg}(AZ_{ant}, EL_{ant}) + \zeta(\mathfrak{L})\, \widehat{Z}_{eg}(AZ_{ant}, EL_{ant}) ,\end{aligned}$$

$$\begin{aligned}(5.32)\qquad \mathbf{X}_{eg}(S) \equiv\ & \mathbf{X}_{eg}(\mathfrak{N}_i) + \xi(S)\, \widehat{X}_{eg}(AZ_{ant}, EL_{ant}) \\ & + \eta(S)\, \widehat{Y}_{eg}(AZ_{ant}, EL_{ant}) + \zeta(S)\, \widehat{Z}_{eg}(AZ_{ant}, EL_{ant}) .\end{aligned}$$

Here we have written

$$(5.33)\qquad \mathbf{X}_{eg}(\mathfrak{L}) \equiv\ \mathbf{X}_{eg}(\mathfrak{N}_i) + \ \mathbf{D}_{eg}(\mathfrak{L}) ,$$

$$(5.34)\qquad \mathbf{X}_{eg}(S) \equiv\ \mathbf{X}_{eg}(\mathfrak{N}_i) + \ \mathbf{D}_{eg}(S) \text{ , where}$$

$$(5.35)\qquad \mathbf{D}_{eg}(\mathfrak{L}) = \xi(\mathfrak{L})\, \widehat{X}_{eg}(AZ_{ant}, EL_{ant}) + \eta(\mathfrak{L})\, \widehat{Y}_{eg}(AZ_{ant}, EL_{ant}) + \zeta(\mathfrak{L})\ \widehat{Z}_{eg}(AZ_{ant}, EL_{ant}),$$

$$(5.36)\qquad \mathbf{D}_{eg}(S) = \xi(S)\, \widehat{X}_{eg}(AZ_{ant}, EL_{ant}) + \eta(S)\, \widehat{Y}_{eg}(AZ_{ant}, EL_{ant}) + \zeta(S)\ \widehat{Z}_{eg}(AZ_{ant}, EL_{ant}).$$

Coefficients of the basis vectors in (5.30)-(5.33) are reference coordinates, and are listed in elevation frame reference data base for these points. Note that we express the displacements of the laser frame origin and the laser scan center points

as the sum of a displacement from E_g to the adjacent structural node point plus a displacement from the node point to the point in question.

The displacement of the main reflector target point T from its associated structural node point, $\mathfrak{N}_T$, depends on the extension of the surface actuator driving the motion of T. It is possible to describe the position of this target point as follows. Displacements of T vary linearly with the extension of the nearby actuator from a home position of the actuator. Let l_T be the actuator extension from its home position. We may write

$$(5.37)\quad \mathbf{X}_{eg}(T) = \mathbf{X}_{eg}(\mathfrak{N}_T) + \mathbf{D}^0_{eg}(T) + l_T\ \mathbf{D}^1_{eg}(T) = \mathbf{X}_{eg}(\mathfrak{N}_T) + \mathbf{D}_{eg}(T, l_T)\,.$$

Resolving (5.37) into component vectors we have

$$\begin{aligned}(5.38)\quad \mathbf{X}_{eg}(T) \equiv\ & \mathbf{X}_{eg}(\mathfrak{N}_T) + (\xi_0(T) + l_T\,\xi_1(T))\,\widehat{X}_{eg}(AZ_{ant}, EL_{ant}) \\ & +(\eta_0(T) + l_T\,\eta_1(T))\,\widehat{Y}_{eg}(AZ_{ant}, EL_{ant}) \\ & +(\zeta_0(T) + l_T\,\zeta_1(T))\,\widehat{Z}_{eg}(AZ_{ant}, EL_{ant})\,.\end{aligned}$$

We are now able to express the displacement vector from rangefinder scan point S to main reflector surface target point T, for the general case of an elastically deformed tipping structure at elevation EL_{ant} and azimuth AZ_{ant}.

Let $\mathbf{D}_{ST}(EL_{ant}, AZ_{ant})$ be the displacement vector from scan point S to surface target point T, when the tipping structure is at elevation EL_{ant} and azimuth AZ_{ant}. Collecting our earlier results we find:

$$\begin{aligned}(5.39)\quad \mathbf{D}_{ST}(EL_{ant}, AZ_{ant}) =\ & \mathbf{X}_{eg}(T) - \mathbf{X}_{eg}(S) + [\Delta]_{\mathfrak{N}_T} - [\Delta]_{\mathfrak{N}i} \\ & + [\delta Rot(\ \mathbf{t}_{\mathfrak{N}_T})]\ \mathbf{D}_{eg}(T, l_T) - [\delta Rot(\ \mathbf{t}_{\mathfrak{N}i})]\ \mathbf{D}_{eg}(S)\,.\end{aligned}$$

The node joint rotations $\mathbf{t}_{\mathfrak{N}_T}$ and $\mathbf{t}_{\mathfrak{N}i}$ are obtained by postmultiplying the constant finite element analysis matrices $[\tau]_{\mathfrak{N}_T}$ and $[\tau]_{\mathfrak{N}_i}$ by the 2×1 column matrix $\begin{bmatrix} \sin EL_{ant} - \sin EL_{surf\_rig} \\ \cos EL_{ant} - \cos EL_{surf\_rig} \end{bmatrix}$.

Gravity-load node displacements $[\Delta]_{\mathfrak{N}_T}$ and $[\Delta]_{\mathfrak{N}i}$ are obtained by postmultiplying the constant finite element analysis matrices $[\sigma]_{\mathfrak{N}_T}$ and $[\sigma]_{\mathfrak{N}i}$ by the same 2×1 column matrix . Differential rotation operators $[\delta Rot(\ \mathbf{t}_{\mathfrak{N}_T})]$ and $[\delta Rot(\ \mathbf{t}_{\mathfrak{N}i})]$ are computed using (5.19).

Having calculated $\mathbf{D}_{ST}(EL_{ant}, AZ_{ant})$, the displacement vector from rangefinder scan point S to surface retroreflector fiducial point T, one finds the rangefinder platform frame coordinates of T by projecting this vector onto the platform frame basis vectors:

$$\widetilde{x}_T = \mathbf{D}_{ST}(EL_{ant}, AZ_{ant}) \cdot \widetilde{X}_e(AZ_{ant}, EL_{ant}; \mathfrak{L}) \ , \tag{5.40}$$

$$\widetilde{y}_T = \mathbf{D}_{ST}(EL_{ant}, AZ_{ant}) \cdot \widetilde{Y}_e(AZ_{ant}, EL_{ant}; \mathfrak{L}) \ , \tag{5.41}$$

$$\widetilde{z}_T = \mathbf{D}_{ST}(EL_{ant}, AZ_{ant}) \cdot \widetilde{Z}_e(AZ_{ant}, EL_{ant}; \mathfrak{L}) \ . \tag{5.42}$$

Scan-elevation angle E_T and scan-azimuth angle A_T, corrected for gravity loading of the tipping structure, are then obtained from $\widetilde{x}_T$, $\widetilde{y}_T$, $\widetilde{z}_T$ by transforming to platform spherical coordinates and converting polar angles to scan angles, using (5.26) and (5.27).

The computations presented in the preceding sections are intrinsically complicated. The telescope's tipping structure can rotate in azimuth and elevation. Structural joints near the feed arm laser platforms are both displaced and rotated due to gravity weight-loading of the tipping structure, which is presumed to deform elastically according to whatever finite element model is employed. Rangefinder platforms co-rotate with their nearby feed arm structure joints, and have additional displacements because they are somewhat distant from those joints. Each main reflector retroprism is displaced from its nearby structural joint by a piston actuator, which is presumed to have the capability of linear displacement in a fixed direction relative to the nearby structural joint. Structural joint displacements and rotations at nodes near the main reflector retroprisms are different from those of the feed arm rangefinder platforms. All of these considerations enter into the computations of feed arm rangefinder scan point positions and scan aiming angles.

The computations outlined in this chapter present a model of a telescope whose

tipping structure is elastically deformed by gravity loading. One can compute ideal locations of fiducial reference points on the feed arm and main reflector structures and the positions and orientations of laser rangefinder platforms as functions of ideal telescope elevation and azimuth angles. These computations can in principle be converted into object-oriented computer codes. But the model is incomplete, as an ideal model of an elastically deformed telescope. Departures of the telescope's alidade structure from the extremely oversimplified rigid alidade model used here will be significant. Some of them can be modelled theoretically, to provide useful extensions to the ideal elastic deformation model presented in this chapter.

In the next chapter we discuss extensions of the ideal elastically deformed telescope which take into account the fact that the alidade structure is much more than a rigid vertical rotation shaft. In some sense we will try to correct the model thus far, to include effects of alidade elastic deformation, misalignment and offset of the elevation and azimuth shafts, unevenness of the alidade track.

6. Alidade Structure Corrections.

The GBT telescope structure was modeled previously as an ideal geometric telescope elastically deformed by gravity-load forces. This model of the telescope does not include: elastic deformation of the alidade structure, offset between the azimuth and elevation axes, non-verticality of the azimuth axis caused by an imperfectly level azimuth track or truck wheels, lack of perpendicularity of azimuth and elevation shafts. At present, there is no elastic model of the alidade structure which corresponds to the elastic model of the tipping structure. Additional features must be incorporated into our present model of the gravity-loaded telescope to include these and other departures of the alidade structure and azimuth track from the ideal.

It is worthwhile retaining the earlier formalism which allows positions of structural node and fiducial points to be computed in terms of coordinate transforms among the previously defined coordinate frames. The question then presents itself: how does one include alidade structure imperfections in the formalism, without requiring complete revision and redefinition?

Here, to include alidade structure modifications, we introduce a "ground" coordinate frame, frame #0. We provide frame origin shifts and translations and rotations between the ground frame and the base frame, frame #1, and the azimuth and elevation frames, frames #2 and #3, to include alidade deviations from the trivial alidade structure design model. The ground frame lies coincident with the base frame initially. Transformations between ground frame and the other frames are then modified to include alidade structure departures from the ideal.

Elevation Shaft Offset

In the ideal geometric telescope model, the azimuth shaft and axis are vertical and the elevation axis and shaft are horizontal. The two axes intersect at point E_g. Let us suppose that the physical telescope is constructed so that the two shaft rotation axes remain perpendicular but are skew, separated by a distance d_{off}. That is, the elevation bearings, elevation shaft, and the attached tipping structure are horizontally translated by a displacement vector $d_{off}\,\widehat{Y}_{ag}$. The geometric elevation frame and base point E_g are translated by this displacement. Relative to the ground frame,

$$(6.1) \qquad \overrightarrow{E}_g \longrightarrow \overrightarrow{E}_g + d_{off}\,\widehat{Y}_{ag}\ .$$

For the ideal geometric telescope without this shaft offset, if $\mathcal{F}$ is a fiducial point embedded in the tipping structure, the ground frame coordinates of $\mathcal{F}$ are related to elevation frame coordinates of $\mathcal{F}$ by the transformation:

$$(6.3) \qquad \begin{bmatrix} X_G(\mathcal{F}) \\ Y_G(\mathcal{F}) \\ Z_G(\mathcal{F}) \end{bmatrix}_{\text{ideal}} = \left[R_{03}^{(0)}\right] \begin{bmatrix} X_{eg}(\mathcal{F}) \\ Y_{eg}(\mathcal{F}) \\ Z_{eg}(\mathcal{F}) \end{bmatrix} + \left[T_{03}^{(0)}\right] \equiv \begin{bmatrix} X_G^{(0)}(\mathcal{F}) \\ Y_G^{(0)}(\mathcal{F}) \\ Z_G^{(0)}(\mathcal{F}) \end{bmatrix}$$

where

$$\left[R_{03}^{(0)}\right] = \begin{bmatrix} -CA & SA.SE & SA.CE \\ -SA & -CA.SE & -CA.CE \\ 0 & -CE & SE \end{bmatrix}\ ,\ [T_{03}]^{(0)} = \begin{bmatrix} 0 \\ 0 \\ h_e \end{bmatrix}\ ,\ \text{and}$$

$$CA = \cos AZ_{ant}\ ,\ SA = \sin AZ_{ant}\ ,\ CE = \cos EL_{ant}\ ,\ SE = \sin EL_{ant}\ .$$

The transformation (6.3) is just that between elevation frame coordinates and base frame coordinates, which initially are the same as ground frame coordinates. That is, $\left[R_{03}^{(0)}\right] = [R_{13}]$ and $\left[T_{03}^{(0)}\right] = [T_{13}]$.

When the elevation bearings, shaft and tipping structure are offset, the elevation frame coordinates of fiducial point $\mathcal{F}$ do not change, since $\mathcal{F}$ is embedded in the tipping structure. That is,

$$
\begin{array}{ll}
 & X_{eg}(\mathcal{F}) \longrightarrow X_{eg}(\mathcal{F}) \\
(6.3) & Y_{eg}(\mathcal{F}) \longrightarrow Y_{eg}(\mathcal{F}) \quad . \\
 & Z_{eg}(\mathcal{F}) \longrightarrow Z_{eg}(\mathcal{F})
\end{array}
$$

But the ground frame coordinates of $\mathcal{F}$ are displaced (Cf. Figure 9):

$$
\begin{array}{ll}
 & X_G^{(0)}(\mathcal{F}) \longrightarrow X_G(\mathcal{F}) + d_{off} \cdot SA \equiv X_G^{(1)}(\mathcal{F}) \\
(6.5) & Y_G^{(0)}(\mathcal{F}) \longrightarrow Y_G(\mathcal{F}) - d_{off} \cdot CA \equiv Y_G^{(1)}(\mathcal{F}) \quad . \\
 & Z_G^{(0)}(\mathcal{F}) \longrightarrow Z_G(\mathcal{F}) \qquad\qquad\quad \equiv Z_G^{(1)}(\mathcal{F})
\end{array}
$$

After the offset by $d_{off}\,\widehat{Y}_{ag}$ (which is a horizontal displacement moving the vertical feed arm closer to the pintle bearing when d_{off} is positive) the equation (6.2) must be replaced by

$$
(6.5) \quad \left[\begin{array}{c} X_G(\mathcal{F}) \\ Y_G(\mathcal{F}) \\ Z_G(\mathcal{F}) \end{array}\right]_{\text{offset\_shaft}} = \left[R_{03}^{(0)}\right] \left[\begin{array}{c} X_{eg}(\mathcal{F}) \\ Y_{eg}(\mathcal{F}) \\ Z_{eg}(\mathcal{F}) \end{array}\right] + \left[T_{03}^{(0)}\right] + \left[\begin{array}{c} d_{off} \cdot SA \\ -d_{off} \cdot CA \\ 0 \end{array}\right], \text{ or}
$$

$$
(6.6) \quad \left[\begin{array}{c} X_G^{(1)}(\mathcal{F}) \\ Y_G^{(1)}(\mathcal{F}) \\ Z_G^{(1)}(\mathcal{F}) \end{array}\right] = \left[R_{03}^{(0)}\right] \left[\begin{array}{c} X_{eg}(\mathcal{F}) \\ Y_{eg}(\mathcal{F}) \\ Z_{eg}(\mathcal{F}) \end{array}\right] + \left[T_{03}^{(1)}\right], \text{ where}
$$

$$
(6.7) \quad \left[T_{03}^{(1)}\right] = \left[\begin{array}{c} d_{off} \cdot SA \\ -d_{off} \cdot CA \\ h_e \end{array}\right].
$$

It is convenient to rewrite (6.5) in the condensed notation:

$$
(6.8) \quad \left[\, \mathbf{X}_G^{(1)}(\mathcal{F}) - \mathbf{T}_{03}^{(1)}\right] = \left[R_{03}^{(0)}\right] \left[\, \mathbf{X}_{eg}(\mathcal{F})\right].
$$

Equation (6.6) provides equations to convert elevation coordinates to ground frame coordinates when offset is introduced between the elevation and azimuth shafts. These equations will be extended to a more general situation where additional rotations and translations appear between the ground and elevation frames, caused by additional departures of physical telescope from the ideal.

$$X_G^{(1)}(E_g) = d_{off} \cdot SA$$

$$Y_G^{(1)}(E_g) = -d_{off} \cdot CA$$

$$Z_G^{(1)}(E_g) = h_e$$

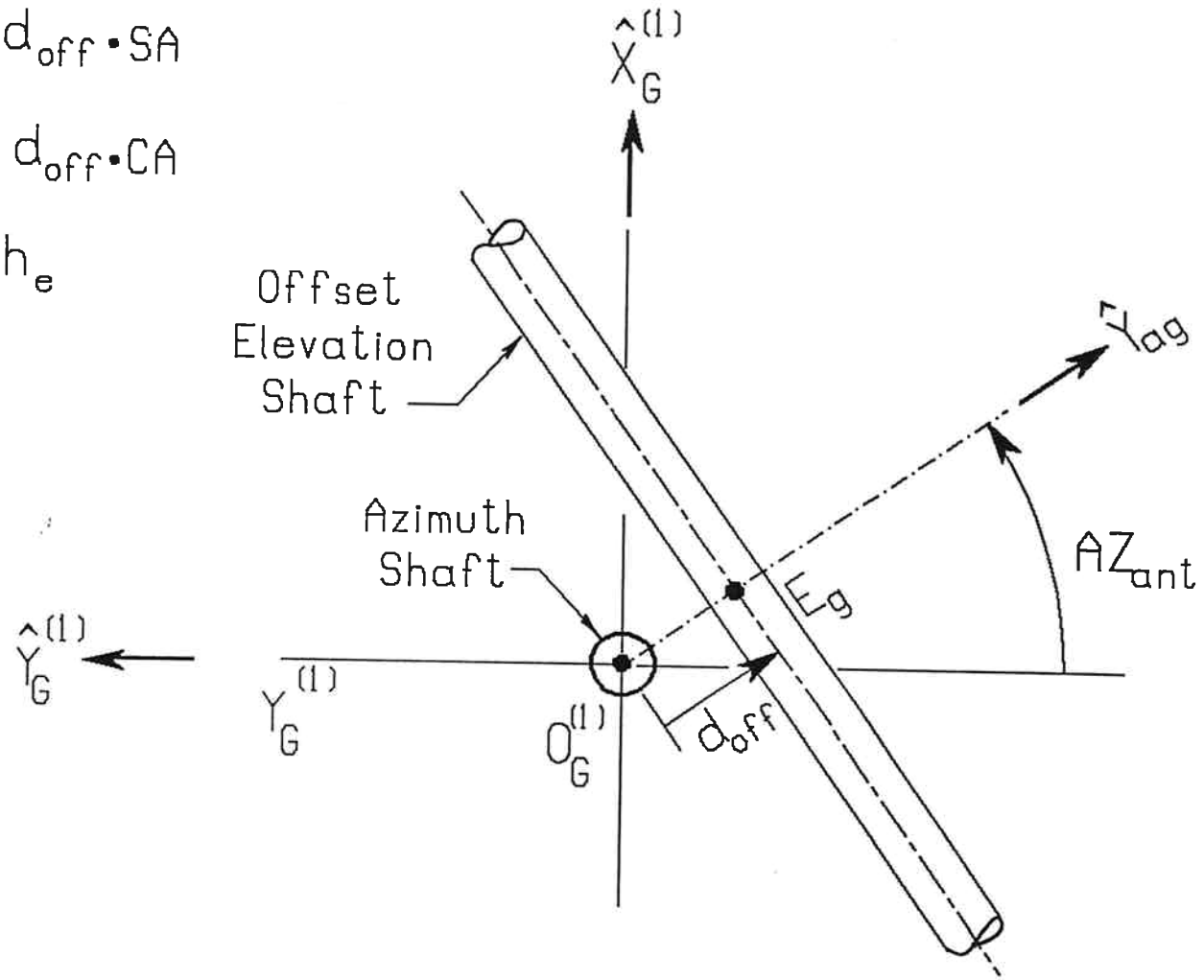

Figure 9. Ground Frame Coordinates Of The Offset Elevation Frame's Origin Point

Non-Perpendicularity Of The Elevation And Azimuth Shafts

After the telescope's elevation and aximuth axes have been offset by distance d_{off}, the Y_{ag} axis still passes through the offset elevation frame origin point E_g. If the elevation shaft, elevation bearings, and the entire tipping structure were rotated by a small angle, $\vartheta_\perp$, about the Y_{ag} axis, this would introduce a departure from perpendicularity of amount $\vartheta_\perp$ between the elevation and azimuth axes.

The azimuth and elevation axes of the telescope are no longer considered to be exactly perpendicular. This non-orthogonality is the collimation error. The angle between the azimuth axis (direction of $\widehat{Z}_{ag}$) and the observer's left end of the elevation axis (direction of $\widehat{X}_{eg}$) is now $90° + \vartheta_\perp$. This shaft misalignment is expected to be small, and constant with time.

To model this effect, a rotation of the elevation shaft and tipping structure by $\vartheta_\perp$ about the Y_{ag} axis, we can instead rotate the ground frame rigidly by $-\vartheta_\perp$ about the Y_{ag} axis. The point E_g and the basis vectors $\widehat{X}_{eg}$, $\widehat{Y}_{eg}$, $\widehat{Z}_{eg}$ would remain fixed. The reflector, prime focus, subreflector and alidade frames and their origin points would also remain fixed. But the ground frame's origin point $O_G^{(0)}$ and basis vectors $\widehat{X}_G^{(0)}$, $\widehat{Y}_G^{(0)}$, $\widehat{Z}_G^{(0)}$ would be rotated by $-\vartheta_\perp \widehat{Y}_{ag}$.

In terms of the geometric elevation frame's basis vectors the initial unrotated ground frame has basis vectors

$$
\begin{aligned}
\widehat{X}_G^{(0)} &= (-CA)\widehat{X}_{eg} + (SA \cdot SE)\widehat{Y}_{eg} + (SA \cdot CE)\widehat{Z}_{eg} \\
\widehat{Y}_G^{(0)} &= (-SA)\widehat{X}_{eg} + (-CA \cdot SE)\widehat{Y}_{eg} + (-CA \cdot CE)\widehat{Z}_{eg} \\
\widehat{Z}_G^{(0)} &= (-CE)\,\widehat{Y}_{eg} + (SE)\,\widehat{Z}_{eg} \quad ,
\end{aligned}
\tag{6.9}
$$

which can also be written as

$$
\widehat{\mathbf{X}}_G^{(0)} = \left[R_{03}^{(0)}\right] \widehat{\mathbf{X}}_{eg} \, , \tag{6.10}
$$

where $\left[R_{03}^{(0)}\right]$ is the matrix of coefficients in (6.9).

We wish to find the rotated ground frame basis vectors and origin point after the rotation $-\vartheta_\perp \widehat{Y}_{ag}$. As a first step, we compute the displacement vector $\mathbf{X}_{eg}\,(O_G^{(0)})$ of the origin point $O_G^{(0)}$ of the unrotated ground frame from the offset

origin point E_g of the geometric elevation frame. To accomplish this, we use (6.7) to compute the displacement vector from $O_G^{(0)}$ to the offset origin point of the geometric elevation frame.

$$(6.11.1) \qquad \mathbf{X}_G\,(E_g) = (d_{off} \cdot SA)\,\widehat{X}_G^{(0)} + (-d_{off} \cdot CA)\,\widehat{Y}_G^{(0)} + (h_e)\;\widehat{Z}_G^{(0)}\;.$$

The negative of this vector is the displacement vector from E_g to $O_G^{(0)}$.

$$(6.11.2) \qquad \mathbf{X}_{eg}\,(O_G^{(0)}) = (-d_{off} \cdot SA)\,\widehat{X}_G^{(0)} + (d_{off} \cdot CA)\,\widehat{Y}_G^{(0)} + (-h_e)\;\widehat{Z}_G^{(0)}\;.$$

Expressing $\mathbf{X}_{eg}\,(O_G^{(0)})$ in components relative to the geometric elevation frame basis, using (6.9), one gets

$$(6.12) \qquad \mathbf{X}_{eg}\,(O_G^{(0)}) = (h_e \cdot CE - d_{off} \cdot CE)\,\widehat{Y}_{eg} + (-h_e \cdot SE - d_{off} \cdot CE)\;\widehat{Z}_{eg}\;.$$

We now rotate $\mathbf{X}_{eg}\,(O_G^{(0)})$ by the angle $-\vartheta_\perp$ about an axis through E_g which is parallel to $\widehat{Y}_{ag}$, to give a new origin point of the ground frame, $O_G^{(1)}$. The displacement vector of this point from E_g is:

$$(6.13) \qquad \mathbf{X}_{eg}\,(O_G^{(1)}) = \left[Rot(-\vartheta_\perp\,\widehat{Y}_{ag})\right]\;\mathbf{X}_{eg}\,(O_G^{(0)})\;.$$

Using (5.18), we can show that, for an arbitrary displacement vector, $\mathbf{D}$,

$$(6.14) \quad \left[Rot(-\vartheta_\perp\,\widehat{Y}_{ag})\right]\;\mathbf{D} = (\cos\vartheta_\perp)\;\mathbf{D} +$$

$$(1 - \cos\vartheta_\perp)(\;\mathbf{D}\cdot\widehat{Y}_{ag})\widehat{Y}_{ag} + (\sin\vartheta_\perp)\;(\;\mathbf{D}\times\widehat{Y}_{ag}),$$

when $\widehat{Y}_{ag}$ is a unit vector. We also have

$$(6.15) \qquad \widehat{Y}_{ag} = (CE)\,\widehat{Y}_{eg} + (-SE)\;\widehat{Z}_{eg}\;.$$

Equations (6.14) and (6.15) applied to (6.13) give

$$(6.16.1) \quad \mathbf{X}_{eg}\,(O_G^{(1)}) \;=\; (d_{off} \cdot \sin\vartheta_\perp)\,\widehat{X}_{eg}$$

$$+(h_e \cdot CE - d_{off} \cdot SE \cdot \cos\vartheta_\perp)\widehat{Y}_{eg} + (-h_e \cdot SE - d_{off} \cdot CE \cdot \cos\vartheta_\perp)\widehat{Z}_{eg}.$$

The shaft offset d_{off} and the shaft misalignment angle $\vartheta_\perp$ are both sufficiently small that we make negligible error by replacing (6.16.1) by

$$(6.16.2)\quad \mathbf{X}_{eg}\,(O_G^{(1)}) \;=\; (d_{off}\cdot\vartheta_\perp)\,\widehat{X}_{eg}$$
$$+(h_e\cdot CE - d_{off}\cdot SE)\widehat{Y}_{eg} + (-h_e\cdot SE - d_{off}\cdot CE)\widehat{Z}_{eg}.$$

We apply (6.14) to find the rotated basis vectors of the ground frame:

$$(6.17)\qquad \begin{aligned} \widehat{X}_G^{(1)} &= \left[Rot(-\vartheta_\perp\,\widehat{Y}_{ag})\right]\widehat{X}_G^{(0)} \\ \widehat{Y}_G^{(1)} &= \left[Rot(-\vartheta_\perp\,\widehat{Y}_{ag})\right]\widehat{Y}_G^{(0)} \\ \widehat{Z}_G^{(1)} &= \left[Rot(-\vartheta_\perp\,\widehat{Y}_{ag})\right]\widehat{Z}_G^{(0)}\ , \end{aligned}$$

gives

$$(6.18)\qquad \begin{aligned} \widehat{X}_G^{(1)} &= (-CA\cdot\cos\vartheta_\perp)\widehat{X}_{ag} + (SA)\,\widehat{Y}_{ag} \;+(-CA\cdot\sin\vartheta_\perp)\,\widehat{Z}_{ag} \\ \widehat{Y}_G^{(1)} &= (-SA\cdot\cos\vartheta_\perp)\widehat{X}_{ag} + (-CA)\,\widehat{Y}_{ag} + (-SA\cdot\sin\vartheta_\perp)\,\widehat{Z}_{ag} \\ \widehat{Z}_G^{(1)} &= \qquad\qquad (-\sin\vartheta_\perp)\,\widehat{Y}_{ag} \quad + \quad (\cos\vartheta_\perp)\,\widehat{Z}_{ag}\ , \end{aligned}$$

and using (6.15) then gives

$$(6.19.1)\qquad \begin{bmatrix} \widehat{X}_G^{(1)} \\ \widehat{Y}_G^{(1)} \\ \widehat{Z}_G^{(1)} \end{bmatrix} = \left[R_{03}^{(1)}\right] \begin{bmatrix} \widehat{X}_{eg} \\ \widehat{Y}_{eg} \\ \widehat{Z}_{eg} \end{bmatrix} \qquad \text{where}$$

$$(6.19.1)\qquad \left[R_{03}^{(1)}\right] =$$

$$\begin{bmatrix} (-CA\cdot C_\perp) & (SA\cdot SE + CA\cdot CE\cdot S_\perp) & (SA\cdot CE - CA\cdot SE\cdot S_\perp) \\ (-SA\cdot C_\perp) & (-CA\cdot SE + CE\cdot SA\cdot S_\perp) & (-CA\cdot CE - SA\cdot SE\cdot S_\perp) \\ (-S_\perp) & (-CE\cdot C_\perp) & (SE\cdot C_\perp)\ . \end{bmatrix}$$

where we use the abbreviations $C_\perp \equiv \cos\vartheta_\perp$ and $S_\perp \equiv \sin\vartheta_\perp$.

We have now obtained the rotation matrix relating the geometric elevation

frame to the ground frame, for the model of a telescope where the azimuth and elevation shafts are offset and have a small angular misalignment from perpendicularity. We can now find the translation vector relating the origins of the two frames, and this will allow us to obtain the relation between the ground and geometric elevation coordinates of fiducial points on the telescope's tipping structure.

7. Determination Of Azimuth And Elevation.

So far, in this memo, the telescope orientation angles AZ_{ant}, EL_{ant} are only mathematical variables, not physical objects. They, together with EL_{surf_rig}, are the independent real variables used to describe analytical transformations of points and vectors associated with an ideal geometric complex, the geometric model of the Green Bank Telescope. These transformations describe positions and motions of structural node points, fiducial reference points and local unit frame vectors on the telescope when the ideal telescope rotates in azimuth, tips in elevation and deforms under gravity loading.

One starts with a set of structure node points:

$$\{\mathfrak{N}_i\,;\ i = 1, 2..., i_{\max}\}$$

and a set of fiducial reference points:

$$\{\mathfrak{F}_k\,;\ k = 1, 2..., k_{\max}\}$$

in a 3-dimensional abstract Euclidean space, E^3, which is not yet related to geographic or astronomical space. Each of the points is defined by three Cartesian reference coordinates in this space:

$$(X_{eg}(EL_{surf\_rig};\ \mathfrak{N}_i),\ Y_{eg}(EL_{surf\_rig};\ \mathfrak{N}_i),\ Z_{eg}(EL_{surf\_rig};\ \mathfrak{N}_i))$$

for the node point $\mathfrak{N}_i$, and

$$(X_{eg}(EL_{surf\_rig};\ \mathfrak{F}_k),\ Y_{eg}(EL_{surf\_rig};\ \mathfrak{F}_k),\ Z_{eg}(EL_{surf\_rig};\ \mathfrak{F}_k))$$

for the fiducial point $\mathfrak{F}_k$.

These coordinates are cataloged in a data base list of "ideal" geometric elevation frame coordinates for the structure node points and a separate data base list of "ideal" geometric elevation coordinates for the fiducial reference points. These listed coordinates are interpreted as initial position coordinates in E^3 for node and fiducial points of the ideal geometric telescope. Later, data base lists will be prepared for "measured" geometric elevation frame coordinates of node and fiducial points of the as-built physical telescope. The "measured" geometric elevation coordinates will be coordinates corresponding to a particular reference orientation of the telescope: EL_{surf_rig} .

There is a mapping:

(7.1)

$$\mathbf{X}_e(\mathfrak{N}_i) = \mathbf{X}_e(AZ_{ant},\, EL_{ant};\, EL_{surf\_rig};\, \mathfrak{N}_i) :\; R^2 \times R \times E^3 \rightarrow E^3$$

defined by

$$(X_{eg}(EL_{surf\_rig};\, \mathfrak{N}_i),\, Y_{eg}(EL_{surf\_rig};\, \mathfrak{N}_i),\, Z_{eg}(EL_{surf\_rig};\, \mathfrak{N}_i)) \rightarrow$$

$$(X_e(AZ_{ant}, EL_{ant};\, \mathfrak{N}_i),\, Y_e(AZant, EL_{ant};\, \mathfrak{N}_i),\, Z_e(AZ_{ant}, EL_{ant};\, \mathfrak{N}_i))$$

which predicts, on the basis of the ideal elastic model of the telescope, the coordinates of $\mathfrak{N}_i$ in the geometric elevation frame to be expected when the ideal telescope is moved to azimuth angle AZ_{ant} and elevation angle EL_{amt}.

Likewise, there is a mapping:

(7.2)

$$\mathbf{X}_e(\mathfrak{F}_k) = \mathbf{X}_e(AZ_{ant}, EL_{ant}; EL_{surf-Rig};\, \mathfrak{F}_k) :\; R^2 \times R \times E^3 \rightarrow E^3$$

defined by

$$(X_{eg}(EL_{surf\_rig};\, \mathfrak{F}_k),\, Y_{eg}(EL_{surf\_rig};\, \mathfrak{F}_k),\, Z_{eg}(EL_{surf\_rig};\, \mathfrak{F}_k)) \rightarrow$$

$$(X_e(AZ_{ant}, EL_{ant};\, \mathfrak{N}_i),\, Y_e(AZant, EL_{ant};\, \mathfrak{N}_i),\, Z_e(AZ_{ant}, EL_{ant};\, \mathfrak{N}_i))$$

which predicts, on the basis of the ideal elastic model of the telescope, the coordinates of $\mathfrak{F}_k$ in the geometric elevation frame to be expected when the ideal telescope is moved to azimuth AZ_{ant} and elevation EL_{ant}.

At node points associated with either feed arm laser stations or main reflector target retroprisms one defines transformations of local coordinate frame basis vectors in a similar way.

The orientation of the as-built Green Bank Telescope could be described by pointing and elevation angles: AZ_{shaft} and EL_{shaft}. These would represent, in some sense, best estimators for the telescope azimuth and elevation shaft angles of the as-built telescope relative, respectively, to astronomical South and the local gravity horizon. Physical definitions for these angles are not intuitively obvious. To define them, should be able to measure them. Direct measurement is nontrivial.

Two conventional candidate measurement procedures are available. One can measure shaft orientations by reading electromagnetic shaft encoder angle readouts. Or, one can orient the telescope to observe well-known celestial objects at well-defined times, pointing the telescope to observe maximum received radio signal at the telescope's prime focus. Neither of these methods is direct. Angle encoders may have readout error. Corrections for atmospheric refraction must be made, including corrections for azimuth and elevation, and the atmospheric variables: temperature, pressure, and relative humidity. Corrections for shaft imperfections must be made.

A third candidate method of measuring AZ_{shaft} and EL_{shaft} is to determine best estimator angles: AZ_{ant} and EL_{ant} for these angles, by range distance measurements using laser rangefinders, followed by a best fitting of the observed° and adjusted set of ranges to the the ideal mathematical model of the deformable telescope.

Antenna Azimuth, Astronomical Azimuth, Encoder Azimuth: Their Ranges And Sign Conventions.

The telescope models given in this memo use the variable AZ_{ant} to describe the antenna structure. This variable was defined in the reference drawings [King-1]. AZ_{ant} is measured counter-clockwise from astronomical South, looking down on the telescope. That is, when $AZ_{ant} = 0$, the Y_{ag} axis points to South, and when $AZ_{ant} = \frac{\pi}{2}$ radian, the Y_{ag} axis points to East.

This is not the azimuth convention preferred by astronomers, when employing a topocentric azimuth/elevation horizon system of coordinates to describe celestial radio sources, or pointing radio telescopes. The preferred astronomical azimuth is measured clockwise from astronomical North, looking down to ground from the sky. That is, when the true astronomical azimuth of a radio source is zero, the observer looks to astronomical North, and when true astronomical azimuthof a radio source is equal to $\frac{\pi}{2}$ radian, the observer looks to astronomical East. The range of astronomical azimuth is conventionally 0° to 360°.

When discussing the telescope model in relation to observation of radio sources it will be convenient to work with not AZ_{ant}, but with its supplement. Define

(7.3) $$AZ \equiv \pi - AZ_{ant} \ .$$

When applying laser ranging measurements to telescope pointing problems it will be convenient to work with the variable AZ in place of AZ_{ant} . The variable AZ has the same rotational sense, and the same zero direction as astronomical azimuth.

The variable AZ is a variable associated with mathematical models of the telescope, and is not yet defined defined for an as-built physical telescope. A correspondiing azimuth variable must be defined for the physical telescope to describe azimuth orientation of the alidade structure of the GBT, a variable which can be measured optically.

When defining the *physical* rotational position of the alidade structure, it is most convenient to use the same rotation sense and zero direction as for astronomical azimuth. Let us use a new variable: AZ_{shaft} , to describe the rotation angle of the alidade shaft (defined by the local alidade structure aligned by the pintle bearing). It increases in the same sense as astronomical azimuth. We use

the following criterion to define the zero direction of: AZ_{shaft}: when the telescope tipping structure is set to the rigging elevation angle and the main reflector surface is shaped as the parent paraboloid, the horizontal component of the direction of the paraboloid axis is towards astronomical North when $AZ_{shaft} = 0$.

One of the measurement instruments used to measure AZ_{shaft} is the azimuth angle encoder. The azimuth encoder is an optical analog-to-digital angular measurement transducer that divides a circle into a specific number (2^{22}) of discrete shaft positions; its output signal amplitude increases linearly with increasing azimuth shaft angle for a correctly manufactured encoder. (For the GBT encoder, output count and azimuth shaft angle increase as astronomical azimuth of an observed source increases). For an imperfect encoder one can generally find a correction function to convert output count to shaft angle. Let us call the nominal angle readout (linear with count) of the encoder $AZ_{encoder}$. The readout angle of the azimuth encoder increases in the same sense as astronomical azimuth. The GBT azimuth encoder is designed to have an angular range of operation $-270° < AZ_{encoder} < 270°$. The encoder angle readout when $AZ_{shaft} = 0$ is called the zero offset angle of the azimuth encoder.

We can define corresponding quantities to describe elevation of the tipping structure. The range of the elevation encoder is $0 < EL_{encoder} < \left(\frac{95}{180}\right)\pi$.

When laser ranging measurements are used in the determination of pointing variables of the GBT, by determining coordinates of appropriate sets of fiducial reference points, the measured ground frame coordinates of these fiducial points are used to fit the tilted deformed model of the telescope, and the calculated values obtained, by fitting, for EL_{ant} and $\pi - AZ_{ant}$ are used as estimated measured values for EL_{shaft} and AZ_{shaft}.

Telescope Pointing.

Call the output readings of the azimuth and elevation shaft angle encoders $AZ_{encoder}$ and $EL_{encoder}$ respectively. Let us write:

(7.4.1) $$AZ_{shaft} = AZ_{encoder} + AZ^{(1)} + AZ^{(2)} + AZ^{(3)} + AZ^{(4)} + \ldots .$$

(7.4.2) $$EL_{shaft} = EL_{encoder} + EL^{(1)} + EL^{(2)} + EL^{(3)} + EL^{(4)} + \ldots .$$

The terms $AZ^{(k)}$ and $EL^{(k)}$ are pointing correction terms, to be determined, and are functions of encoder readout angles $AZ_{encoder}$ and $EL_{encoder}$.

The angles AZ_{shaft} and EL_{shaft} do not include atmospheric refraction. They specify best-estimate spatial orientations of the alidade and tipping structures with respect to a local terrestrial topographic frame (the ground frame).

We wish to observe an astronomical point source emitter, at local apparent sidereal time: LAST, and true local terrestrial azimuth (neglecting atmospheric refraction): $AZ_{true}(Source, LAST)$ and elevation $EL_{true}(Source, LAST)$. At the telescope, because of atmospheric refraction, the apparent azimuth and elevation of this sky object are different from true azimuth and elevation. We may call them $AZ_{apparent}$ and $EL_{apparent}$. The apparent direction of the radio source depends upon the atmospheric refractivity profile along the ray-optical path from sky to earth for radio propagation from the direction AZ_{true}, EL_{true} at the time of observation. We may write:

$$(7.5) \quad EL_{apparent} = EL_{true} + \Delta_{EL}^{(refraction)}, \; AZ_{apparent} = AZ_{true} + \Delta_{AZ}^{(refraction)}.$$

In general, the azimuth refraction correction term is small and is usually negligible. The elevation correction $\Delta_{EL}^{(refraction)}$, below 100 GHz observing frequency, is given in section 1.2.5 of [Wells-2].

To point the telescope, in the absence of elastic gravity-load deformation, the apparent azimuth and elevation of a radio source would be set to coincide, respectively, with the azimuth and elevation shaft angles of the telescope. But the main reflector will be deformed from a parabolic shape, unless reshaped using the main surface acuators. In the present discussion, telescope operation is assumed to occur so that the main reflector will be reshaped into a best fit paraboloid which is a function of the telescope's shaft elevation angle, EL_{shaft}. Detailed computations of the configuration of the best fit paraboloid have been given in GBT Memo 131, by D. Wells and L. King [Wells-2], including the C-language computer codes to implement these calculations. There is an elevation-shaft-angle dependent shift of the best fit paraboloid's axis from the elevation angle of the shaft.

$$(7.6) \quad EL_{bfp} = EL_{shaft} + \Delta_{EL}^{(bfp)}.$$

The current elastic model of the telescope tipping structure does not indicate an azimuth shift due to gravity loading, but we may formally include such a term, in case the elastic model requires a later update if construction asymmetries arise during telescope construction. Formally we can write,

$$(7.7) \quad AZ_{bfp} = AZ_{shaft} + \Delta_{AZ}^{(bfp)} .$$

The incremental term in (7.6) is calculated from the elastic model of the tipping structure, and has been given in [Wells-2]. The incremental term in (7.7) is assumed to be zero, unless a non-zero term is required by an updated elastic model.

To point the telescope, allowing for elastic gravity-load deformation, the apparent azimuth and elevation of the radio source are set to coincide, respectively, with the azimuth and elevation angles of the best fit paraboloid.

When the telescope has been pointed:

$$(7.8) \quad EL_{true} + \Delta_{EL}^{(refraction)} = EL_{bfp} \ , \ AZ_{true} = AZ_{bfp} .$$

The pointing equations for the telescope are then:

$$(7.9) \quad EL_{true}(Source, LAST) + \Delta_{EL}^{(refraction)} = EL_{encoder} + \Delta_{EL}^{(bfp)} + \sum_k EL^{(k)} ,$$

$$(7.10) \quad AZ_{true}(Source, LAST) = AZ_{encoder} + \Delta_{AZ}^{(bfp)} + \sum_k AZ^{(k)} .$$

One wishes to solve these equations for $EL_{encoder}$ and $AZ_{encoder}$; their solutions are the setpoint values for the shaft encoder angle outputs to be read out when the telescope points to the radio source. That is, encoder outputs $EL_{encoder}$ and $AZ_{encoder}$ which satisfy (7.9) and (7.10) are, respectively, the commanded elevation and azimuth encoder outputs $EL_{command}$ and $AZ_{command}$ required for pointing to

be achieved. Angles EL_{true} and AZ_{true} are given input parameters in the equations; they are obtained by converting celestial coordinates of the radio source into terrestrial topographic direction coordinates in the local horizon coordinate system.

The equations are complicated, because the sum terms are themselves functions of $EL_{encoder}$ and $AZ_{encoder}$. The refraction terms are functions of the true azimuth and elevation of the radio source. This complication is mitigated by the fact that the correction terms are slowly-varying functions of their arguments. Negligible error should be generated by replacing the independent variables $EL_{encoder}$ and $AZ_{encoder}$ in the sum terms by EL_{true} and AZ_{true}. (If one wishes to correct such small errors one can compute the encoder angles, making such a replacement, and then modify the solution by adding additional terms corresponding to the Taylor's series expansions of the sum terms about the encoder angles. This will not be attempted here.).

The sum terms in (7.9) and (7.10) are usually obtained by associating each term with a particular mechanical or thermal deviation of the telescope structure or encoders from their nominal design characteristics. Examples of mechanical effects to be corrected are: are encoder angle index offsets, encoder eccentricity, encoder cyclic errors, deviation of the azimuth shaft from verticality , lack of perpendicularity between elevation and azimuth shafts, offset error due to non-intersection of the azimuth and elevation shaft axes, elevation-dependent flexure of the alidade structure, main reflector flexure. An example of a thermal expansion effect is a roll of the tipping structure about the horizontal feed arm due to unequal solar heating of the two alidade legs.

Equations of the form (7.9) and (7.10) describe a "traditional" pointing model of the telescope. Traditional pointing models were developed for the following azimuth-elevation instruments, among others: the Haystack telescope [Meeks-1]; the 36-foot millimeter wave telescope at Kitt Peak [Schr-1], [Ulich-1]; the 30-meter IRAM millimeter wave telescope [Greve-1]; the ESSCO 45-foot antenna at Green Bank [Ghigo-1]. Von Hoerner [Hoe-1] suggested a traditional pointing model for the GBT.

The terms in von Hoerner's traditional pointing model for the GBT are:

Term	Cause	Value
$EL^{(1)}$	Azimuth axis offset to North by P_1	$P_1 \cos(AZ)$
$AZ^{(1)}$	Azimuth axis offset to North by P_1	$P_1 \tan(EL) \sin(AZ)$
$EL^{(2)}$	Azimuth axis offset to East by P_2	$P_2 \sin(AZ)$
$AZ^{(2)}$	Azimuth axis offset to East by P_2	$-P_2 \tan(EL) \cos(AZ)$
$EL^{(3)}$	Elevation axis deviates from $\perp$	0
$AZ^{(3)}$	to Azimuth axis by P_3	$P_3 \tan(EL)$
$EL^{(4)}$	Zero elevation offset, feed offset to Y	P_4
$AZ^{(4)}$	Zero elevation offset, feed offset to Y	0
$EL^{(5)}$	Beam not $\perp$ to Elevation axis, feed	0
$AZ^{(5)}$	offset to X	$P_5 \sec(EL)$
$EL^{(6)}$	Zero azimuth offset	0
$AZ^{(6)}$	Zero azimuth offset	P_6
$EL^{(7)}$	Gravity, symmetrical	$P_7 \cos(EL)$
$AZ^{(7)}$	Gravity, symmetrical	0
$EL^{(8)}$	Gravity, asymmetrical	$P_8 \sin(EL)$
$AZ^{(8)}$	Gravity, asymmetrical	0
$\Delta_{EL}^{(refraction)}$	Refraction	(Form not given)
$\Delta_{AZ}^{(refraction)}$	Refraction	0

A series of memos is available presenting the pointing model for the equatorial 140-foot telescope at Green Bank, and its modifications over two decades of telescope operation. ([Gor-1], [Hoe-2] to [Hoe-6], [Madd-1], [Pau-1]). In particular, memos by von Hoerner give an in-depth presentation of the problem of differential thermal effects on telescope pointing, and methods used to overcome them.

Alternatively, one can present encoder setpoint elevation and azimuth angles as a two-dimensional Fourier series expansion in true elevation and azimuth angles, to model radiotelescope pointing. Individual terms in a Fourier series model of the telescope are not given unique physical interpretation. A model of this type has been given for the GBT by J.J.Condon [Con-1]. Condon's model is currently scheduled for implementation on the GBT. In Condon's pointing model, equations (7.9) and (7.10) are replaced by series of the form:

$$(7.11)\quad EL_{true}(Source, LAST) + \Delta_{EL}^{(refraction)} - EL_{command} =$$

$$d_{00}^{(EL)} + \sum_{q=1}^{q\max} \sum_{p=1}^{p\max} a_{pq}^{(EL)} \sin(p \cdot AZ) \sin(q \cdot EL) + b_{pq}^{(EL)} \cos(p \cdot AZ) \sin(q \cdot EL)$$
$$+ c_{pq}^{(EL)} \sin(p \cdot AZ) \cos(q \cdot EL) + d_{pq}^{(EL)} \cos(p \cdot AZ) \cos(q \cdot EL).$$

$$(7.12)\quad AZ_{true}(Source, LAST) - AZ_{command} = d_{00}^{(AZ)} +$$

$$+ \sec(EL) \cdot \sum_{q=1}^{q\max} \sum_{p=1}^{p\max} a_{pq}^{(AZ)} \sin(p \cdot AZ) \sin(q \cdot EL) + b_{pq}^{(AZ)} \cos(p \cdot AZ) \sin(q \cdot EL)$$
$$+ c_{pq}^{(AZ)} \sin(p \cdot AZ) \cos(q \cdot EL) + d_{pq}^{(AZ)} \cos(p \cdot AZ) \cos(q \cdot EL)\,.$$

One can use angles EL_{true} and AZ_{true} in the right hand sides of the above equations, to sufficient accuracy. (These are determined by the calibration sky object, at the time of observation). The commanded elevation and azimuth angles are computed using these equations. It is possible to partition and reserve certain terms in the above series to represent explicitly those pointing corrections which are due to waviness of the alidade track. Also, some of the low order Fourier terms correspond uniquely to physically defined terms in the traditional pointing model. This is discussed in [Con-1].

In Condon's GBT Memo 75, the source of the Fourier coefficients is not discussed. Passing reference is made to astronomical measurements of calibrator radio source positions and laser ranging measurements, but no detailed suggestions are given for coefficient determination. If sky radio source positions are used to determine telescope pointing, effects of subreflector and feed arm motions on the pointing determination must be removed or corrected. That is, feed arm motions and deformations and subreflector position and orientation should not enter into the pointing equations as additional variables or error sources.

The modular software and control implementation of the GBT Pointing System, which is to perform antenna pointing and focus tracking tasks, is described in GBT Memos 103 [Fisher-1] and 122 [Hogg-1].

In [Hogg-1] a distinction is made between "pointing" which involves bringing

radiation from a sky object to a prime focus, and "focus tracking", which deals with bringing the radiation from prime focus to a receiver, via the subreflector. In Condon's pointing model such a distinction is not defined. If pointing coefficients of Condon's model are to be determined by astronomical measurement procedures, it is important to understand the practical effects of focus tracking considerations on these measurements. That is (for example), receiver feed positioning, feed arm elastic deformations, subreflector position and orientation should either not affect the pointing coefficient measurements or should be compensated or removed. Possible effects of focus tracking interactions involving the feed arm, subreflector and receiver feed positioning on pointing coefficient determination need some examination. One should insure that pointing is in fact determined independently of the behavior of components on the feed arm.

Laser metrology could be of help in determining pointing, independent of feed arm component behavior. We discuss this and give examples in the paragraphs which follow.

It should be practical to use laser rangefinder measurements of structural fiducial reference point positions, when the GBT telescope is moved in elevation and azimuth, to obtain individual terms in a traditional pointing model of the GBT. By including pointing terms which are both assignable to a particular structural deviation and measurable by laser rangefinding explicitly in the pointing model one could decrease the contributions of *arbitrary* terms to the pointing model. It is also possible to measure separately the translational and rotational motions of the alidade structure due to waviness of the alidade track when telescope azimuth is varied. During the initial calibration of the GBT, measurements of the following types would be made:

Measurement 1. The tipping structure is fixed in elevation. The telescope is rotated 360° in azimuth. Orbit curves, in space, with respect to the ground, are measured for fiducial reference points of retroreflectors attached to the alidade structure. In particular orbit curves are measured for diametrally opposite retroreflector pairs at approximately the same height above ground. If the alidade track is flat and horizontal, these orbit curves should be horizontal circles. If the track has a mean tilt from the horizontal the orbit circles will display this tilt. If the track is wavy or if the alidade truck wheels are nonuniform the orbit curves will show a wave departure from circularity. One can also determine the effect of

track waviness in generating azimuthal twist of the elevation shaft with respect to the alidade base (a deformation considered significant by Condon) by looking at differential changes in the azimuthal orientation of displacement vectors between diametrally opposite alidade fiducial point pairs near the top and bottom respectively of the alidade structure, as azimuth is varied.

Measurement 2. The alidade is fixed in azimuth. The tipping structure is rotated 90° in elevation. The orbit curves in space, with respect to the ground, are measured for fiducial reference points of retroreflectors on the feed arm and box structure. If the elevation shaft is horizontal, the retroreflector fiducial point orbit curves will be (approximately 90°) arcs of vertical circles. If the elevation shaft is tilted from the horizontal, the orbit curve planes will no longer be vertical, and will show this tilt. Deviations of the elevation shaft from the horizontal can be caused either by non-perpendicularity of the elevation and azimuth axes, or by alidade track waviness. By making these measurements at each of several different azimuths, and also using the results of Measurement 1, the effects of track waviness and axis non-perpendicularity can be separated.

Measurement 3. The alidade is fixed in azimuth. The tipping structure is rotated 90° in elevation. The orbit curves in space, with respect to the ground, are measured for fiducial reference points of retroreflectors high on the alidade, located beneath the elevation shaft bearings, and also for alidade retroreflector fiducial points located near the base of the alidade. If the alidade were perfectly rigid, and the tipping structure were balanced so that it exerted no large bending moments on the alidade, these alidade fiducial reference points would not move. If they are observed to move, the bending of the alidade structure can be determined from their orbit curves.

It seems likely that these and other laser measurement schemes can be developed in detail as practical aids to achieve GBT pointing. But laser measurements can also be used to observe changes in the pointing model of the telescope as the telescope ages, and can flag when the model needs updating or upgrade.

8. DISCUSSION.

We now discuss the motivation and applications for the telescope coordinate modeling presented in the earlier chapters. The GBT possesses features which are unusual or unique among radio telescopes. It has an actively driven main reflector, gregorian configuration with offset feed, and an active laser ranging metrology system which will dynamically measure reflector surface shape and subreflector position, monitor pointing, vibrations and structural features to provide information about dynamic telescope behavior. For the ranging system to achieve these goals, it must dynamically aim feed arm laser ranging beams at moving target reflectors, while possibly in motion as these targets are scanned.

Range measurements are made as follows [Payne-1]. An intensity-modulated light beam is transmitted over the measurement path, reversed by a target retroreflector, and returned to the scan instrument. The phase of the return beam's modulation envelope is measured and compared to that of the outgoing beam. A corresponding phase measurement is made over a comparison path, to remove common mode path [from the laser output face to the scan mirror center (outgoing) and from scan mirror center to photodetector surface (return)]. Corrections relating target prism optical center to the telescope surface are discussed in [Gol-1]. The difference between measurement path and comparison path phase delays is $2\pi \left(\frac{2d_{opt}}{\lambda_{\mathrm{mod}}} \right)$, where d_{opt} is the optical path length from the scan mirror center to the optical center of the retroreflector. Phase detector output is the phase delay, modulo 2π. Distance from scan center to target center is determined modulo the modulation wavelength λ_{mod}, after the path length is corrected for refraction. Range measurement is modular, not absolute. There is ambiguity of a multiple of $\lambda_{\mathrm{mod}}/2$ in each measurement. GBT ranging instruments do not provide multiple modulation frequency capability, to resolve the ambiguity. Distances to be measured should therefore be known *a-priori* to $\lambda_{\mathrm{mod}}/2$.

During GBT operation, feed arm displacements at the ranging stations varies by several modulation wavelengths, as telescope elevation changes. Distances from range scan centers to targets changes by several modulation lengths. Attitude changes of range station platforms to the main reflector are also significant, requiring changes in commanded scan angles. Additionally, actuators may move to alter the main reflector surface. *A-priori* information concerning scan mirror position and attitude and main reflector target center must be accurate enough to avoid ambiguity. The model of the deformed telescope (with alidade corrections) presented in this memo is intended to supply computational tools to get the needed *a-priori* information. It is expected that the model will be coded in object oriented language, and that data bases of fiducial and node point coordinates, at some reference elevation, will be supplied. Computed distances and attitudes can then be used to remove distance ambiguity and correct commanded scan aiming angles so that each demanded range measurement is achieved.

Reference Optical Telescope, Design Telescope and Tilted Geometric Telescope.

The first two models were developed to trace how basic design dimensions for the GBT are derived from fundamental optical parameters, and to present a self consistent set of design dimensions (Appendix I) and relate them to GBT design drawings. The geometric telescope model was developed to define geometric reference frames used to describe a more general, as-built telescope. In section 6, this model is extended to allow shaft offset and misalignment. Coordinate and basis vector transformations relating local reference frames are given in Appendix I. Transformation matrices are given symbolically, to allow substitution of as-built telescope dimensions in place of design dimensions. Additional reference frames, besides those appearing in the GBT design drawings, are defined for the feed house, turret, and receiver feed flanges, to provide a nomenclature and framework for description of microwave receiver component locations.

The Tilted Deformed Telescope.

Using frames defined for the tilted geometric telescope as reference frames for the telescope whose tipping structure is deformed in accord with the Finite Element Model, position shifts of structure node points and retroreflector fiducial points were calculated. Attitude shifts of laser platforms were calculated, to find

laser beam aiming corrections as a function of tipping structure elevation. The model also provides equations to predict range changes between station scan mirrors and main reflector target centers, as elevation varies. It also allows one to calculate improved distances between feed arm scan centers and ground retroreflector fiducials, to get ground frame coordinates of the feed arm laser scan centers.

Determination of Azimuth and Elevation.

Use of laser ranging to assist with pointing of the GBT was discussed in [Payne-2] and [Wells-2] , and is mentioned in passing as an aid to determination of Fourier coefficients for Condon's pointing model [Con-1].

If laser metrology is to assist with pointing, the laser range measurement tasks and range distance analyses for this purpose must be defined carefully. We briefly review the pointing process, and then discuss possible use of laser ranging to assist with this task.

We start with an astronomical source which is to appear at known apparent horizon system elevation and azimuth, at a known time. To best observe this source, the telescope primary must be shaped to an appropriate paraboloid. (This is preferably the best fit paraboloid corresponding to the source elevation, but might also be the most recently available paraboloid if surface actuators can not be adjusted for this measurement). The telescope is driven in elevation and azimuth until the axis of the available paraboloid coincides with the apparent direction of the radio source. This is done by entering commanded position angles into the telescope servo system and driving $(EL_{encoder} - EL_{command})$ and $(AZ_{encoder} - AZ_{command})$ to zero, so the telescope points to a direction in space corresponding to the condition that the encoder angle readouts are the commanded angles. Angles $EL_{command}$ and $AZ_{command}$ are near to but not equal to the apparent radio source angles. Proper command angles can be obtained from the source angles if one has a pointing model of the telescope (e.g., either a traditional or Condon's). The pointing model consists of a trigonometric series expansion in source elevation and azimuth (as independent variables) for the commanded elevation, and a trigonometric series in source elevation and azimuth for commanded azimuth. The usual procedure used for determining a pointing model for a radio telescope is to use microwave holography with a radio source which is either a stationary satellite or a celestial maser. At the GBT, holography can be supplemented with laser ranging metrology.

Considerations for applying laser metrology to pointing are given in [Wells-2]. Wells suggests using retroreflectors at several heights on the alidade legs to detect and measure thermal distortion, and retroreflectors near the elevation axle bearings to determine axle orientation. Alidade retroreflectors can also be used to find alidade azimuth rotations from an azimuth reference. We note that they may also be placed beneath opposite ends of the box structure supporting the main reflector, along a line perpendicular to the elevation shaft. Rotation of the line joining these retroreflectors can be used to find changes in tipping structure elevation from an elevation reference angle, for example EL_{surf_rig}. Use of laser rangers to determine alidade track pointing variation due to track waviness was discussed in section 8.

Determination of the Fiducial Point Coordinate Data Base.

To use laser ranging for telescope metrology one must possess a data base list of fiducial reference point coordinates. It can be acquired as follows.

One first performs a ground control survey. Using theodolites and a total station equipped with a boresighted Electronic Distance Measurement laser, one measures and adjusts a survey control network. (A TOPCON total station is available at Green Bank). The EDM ranging laser has frequency diversity operation and measures absolute distance to within three millimeters. The control net includes ground based retroreflector fiducials, metrology laser scan center fiducials, and reference monument fiducials. The adjusted network distances will be accurate to three millimeters, which is much shorter than the laser beam 10 cm modulation half wavelength. The network is then resurveyed by trilateration using metrology ranging station lasers. The needed modular distance corrections are now available from the preliminary survey results. Adjusted distances of the resurveyed network are expected to have accuracy near 50 μm. One then has accurate position coordinates available for the ground based fiducial reference points, and has accurate distances between range station mirror scan centers.

One independently determines orientations, with respect to the ground frame, of the kelvin mounts and the laser scan axes of the ground ranging stations using conventional surveying methods. One can then use scan elevation and azimuth readouts of a ranging beam to find direction cosines of the beam's direction vector

with respect to ground reference frame coordinate axes. One can then triangulate from a pair of laser ranging stations at known separation from one another to a target retroreflector on the telescope, to obtain an unambiguous range from that target to each of the laser scan centers, to an accuracy near one centimeter. That is, one uses scan angle readouts, when a target is ranged, to compute the angles between the laser beam directions and the line segment between the scan centers, and then uses the accurately known distance between scan centers to compute ranges, using the law of sines for the triangle whose vertices are the scan centers and target fiducial point. Scan angle readouts on the laser stations are accurate to about $2\pi \times 10^{-5}$ so they can be used to compute range to an accuracy of about 1 cm. A triangulation range is accurate enough to supply the modular part of the range distance from laser scan center to target. Accurate distance is then obtained from range phase output, after triangulation range information is made available.

For fiducial points associated with ground based lasers and target retroreflectors, the data based coordinates are the fixed ground frame coordinates obtained from the control survey.

For alidade based retroreflectors, data base coordinates are measured when the tipping structure is set at a selected reference elevation, preferably EL_{surf_rig}. Coordinates are measured by ranging when the alidade is set to an arbitrarily selected azimuth reference angle. Those reference angles can initially, during telescope commissioning, be shaft encoder output angles and can be corrected subsequently to true source angles, after a pointing model has been obtained. If time permits, during commissioning, it would be valuable to obtain coordinates of targets on the alidade, with the alidade set at its reference azimuth and the tipping structure set to the upper and lower extremes of elevation.

Alidade fiducial retroreflector coordinates, at reference azimuth, can be listed as either ground frame coordinates or (after transformation) as geometric alidade coordinates.

Measurement of feed arm fiducial reference point coordinates should be done by laser ranging from ground based lasers and by ranging from feed arm lasers to ground based retroreflectors, with tipping structure set to the surface rigging elevation angle, EL_{surf_rig} . If direct laser-to-laser ranging can be done, range

measurements between laser scan center points should be made separately in each direction, feed arm to ground and ground to feed arm. Feed arm retroreflector fiducial point coordinates should be data based as geometric elevation coordinates.

Summary.

The GBT was modelled geometrically to provide a framework to locate positions of fiducial reference points on the telescope structure and to describe their expected position changes as the antenna moves. Corrections in position due to gravity load deformation of the tipping structure, as calculated by the tipping structure's finite element model, were derived to provide aiming corrections for feed arm lasers used for main reflector surface determination.

Laser ranging measurements are modular, and are not unambiguous. Initial estimates of position, good to one half modulation wavelength (near 10 cm) are needed to eliminate ambiguity. It is practical to obtain a measured data base of fiducial point coordinates for a single telescope pointing position and then use a geometric model of the GBT to compute coordinates of any selected fiducial point at arbitrary elevation and azimuth. Model computations developed in this memo provide a way to do this.

It is expected that computations developed in this memo will be coded in object oriented code, and a data base of measured fiducial point coordinates will be developed during commissioning of the telescope. Subsequently, a data base of fiducial positions and the telescope model will be available to evaluate laser range measurements used to improve the pointing and study the dynamic behavior of the telescope.

As a final comment, I express the hope that this memo can serve as a basis to stimulate discussion and innovation with regard to use of laser metrology as a tool for diagnostics and operation of the GBT. Dynamic laser metrology is a new and promising tool for radiotelescopes. It should be used to to the full extent of its capabilities.

Appendix I. Matrix Relations For The Ideal Geometric Telescope.

We use the following abbreviations:

AZant is the antenna azimuth angle.
ELant is the antenna elevation angle

SA = sin AZant
CA = cos AZant

SE = sin ELant
CE = cos ELant

Spf = sin 45.5 degrees
Cpf = cos 45.5 degrees

Ss = sin 36.7 degrees
Cs = cos 36.7 degrees .

S_{pfE} = sin (ELant + 45.5 degrees)
C_{pfE} = cos (ELant + 45.5 degrees)

S_{sE} = sin (ELant + 36.7 degrees)
C_{sE} = cos (ELant + 36.7 degrees)

S_{2A} = sin (2 AZant)
C_{2A} = cos (2 AZant)

SB = sin β
CB = cos β

ST = sin $(\alpha - \beta)$
CT = cos $(\alpha - \beta)$

SET = sin (ELant + $\alpha - \beta$)
CET = cos (ELant + $\alpha - \beta$)

$$h_{pe} = h_{rp} + h_{re}$$
$$d_{pe} = d_{re}$$

$$h_{rs} = h_{rp} + h_{sp}$$
$$d_{rs} = d_{sp}$$

$$h_{se} = h_{rs} + h_{re}$$
$$d_{se} = d_{rs} + d_{re}$$

$$d_{rce} = \frac{d_{mp}}{2}$$
$$h_{rce} = h_{rp} - \left(\frac{h_{mp}}{2}\right)$$

$$d_{mr} = d_{mp}$$
$$h_{mr} = h_{rp} - h_{mp}$$

$$d_{tr} = d_{mr} + CT \cdot d_{tm}$$
$$h_{tr} = h_{rp} - h_{mp} - ST \cdot d_{tm}$$

$$d_{te} = d_{tr} + d_{re}$$
$$h_{te} = h_{tr} + h_{re}$$

Numerical Values Of The Transformation Parameters.

The following parameters are functions of the antenna angles, AZant and ELant :

SA , CA , SE , CE ,

SET = sin (ELant + 12.329 degrees) , CET = cos (ELant + 12.329 degrees) ,

S_{pfE} , C_{pfE} , S_{2A} , C_{2A} , S_{sE} , C_{sE} .

The numerical values of the trigonometric parameters are:

S_{pf} = 0.713250449

C_{pf} = 0.700909264

S_{s} = 0.597625147

C_{s} = 0.801775644

SB = 0.097061786

CB = 0.995278357

ST = 0.213524886

CT = 0.977271823

Two sets of values for the length parameters are provided. The table to the left gives values derived from the reference optical telescope model. The table to the right gives values derived from from design values stated on the GBT drawing C35102M081-B, which are the optical telescope values rounded to the nearest millimeter .

Length Parameter	Reference Optical Telescope Value (centimeters)	Design Drawing Value (centimeters)
d_{mp}	106.7680	106.8000
h_{mp}	1094.8062	1094.800
d_{sp}	429.1726	429.2000
h_{sp}	380.2874	380.3000

h_e	4826.0000	4826.0000
h_{re}	499.9990	499.9990
d_{re}	5843.9110	5843.9110
h_{rp}	6000.0000	6000.0000
h_{pe}	6499.9990	6499.9990
d_{pe}	5843.9110	5843.9110
h_{rs}	6429.1726	6429.2000
d_{rs}	429.1726	429.2000
h_{se}	6929.1716	6929.1990
d_{se}	6273.0836	6273.1110
d_{rce}	53.3840	53.4000
h_{rce}	5452.5969	5452.6000
d_{mr}	106.7680	106.8000
h_{mr}	4905.1938	4905.2000
d_{tm}	142.2400	142.2400
d_{tr}	245.7751	245.7681
h_{tr}	4874.8220	4874.8282
d_{te}	6089.6861	6089.6791
h_{te}	5374.8210	5374.8272

Alidade To Base Transformation:

$$\begin{pmatrix} X \\ Y \\ Z \end{pmatrix} = [R12] \begin{bmatrix} X_{ag} \\ Y_{ag} \\ Z_{ag} \end{bmatrix} + [T12]$$

$$[R12] = \begin{pmatrix} -CA & SA & 0 \\ -SA & -CA & 0 \\ 0 & 0 & 1 \end{pmatrix} \quad , \qquad [T12] = \begin{pmatrix} 0 \\ 0 \\ 0 \end{pmatrix}$$

$$\begin{pmatrix} X \\ Y \\ Z \end{pmatrix} = \begin{bmatrix} -CA \cdot X_{ag} + SA \cdot Y_{ag} \\ -SA \cdot X_{ag} - CA \cdot Y_{ag} \\ Z_{ag} \end{bmatrix}$$

Alidade Frame Origin:

$$\begin{pmatrix} X(Ag) \\ Y(Ag) \\ Z(Ag) \end{pmatrix} = \begin{pmatrix} 0 \\ 0 \\ 0 \end{pmatrix}$$

Base To Alidade Transformation:

$$\begin{bmatrix} X_{ag} \\ Y_{ag} \\ Z_{ag} \end{bmatrix} = [R21] \begin{bmatrix} X \\ Y \\ Z \end{bmatrix} + [T21]$$

$$[R21] = \begin{pmatrix} -CA & -SA & 0 \\ SA & -CA & 0 \\ 0 & 0 & 1 \end{pmatrix} \quad , \qquad [T21] = \begin{pmatrix} 0 \\ 0 \\ 0 \end{pmatrix}$$

$$\begin{bmatrix} X_{ag} \\ Y_{ag} \\ Z_{ag} \end{bmatrix} = \begin{bmatrix} -CA \cdot X - SA \cdot Y \\ SA \cdot X - CA \cdot Y \\ Z \end{bmatrix}$$

Elevation To Alidade Transformation:

$$\begin{bmatrix} X_{ag} \\ Y_{ag} \\ Z_{ag} \end{bmatrix} = [R23] \begin{bmatrix} X_{eg} \\ Y_{eg} \\ Z_{eg} \end{bmatrix} + [T23]$$

$$[R23] = \begin{pmatrix} 1 & 0 & 0 \\ 0 & SE & CE \\ 0 & -CE & SE \end{pmatrix} \quad , \quad [T23] = \begin{bmatrix} 0 \\ 0 \\ h_e \end{bmatrix}$$

$$\begin{bmatrix} X_{ag} \\ Y_{ag} \\ Z_{ag} \end{bmatrix} = \begin{bmatrix} X_{eg} \\ SE \cdot Y_{eg} + CE \cdot Z_{eg} \\ -CE \cdot Y_{eg} + SE \cdot Z_{eg} + h_e \end{bmatrix}$$

Alidade to Elevation Transformation:

$$\begin{bmatrix} X_{eg} \\ Y_{eg} \\ Z_{eg} \end{bmatrix} = [R32] \begin{bmatrix} X_{ag} \\ Y_{ag} \\ Z_{ag} \end{bmatrix} + [T32] \quad , \quad [T32] = [R32](-1)[T23]$$

$$[R32] = \begin{pmatrix} 1 & 0 & 0 \\ 0 & SE & -CE \\ 0 & CE & SE \end{pmatrix} \quad , \quad [T32] = \begin{bmatrix} 0 \\ CE \cdot h_e \\ -SE \cdot h_e \end{bmatrix}$$

$$\begin{bmatrix} X_{eg} \\ Y_{eg} \\ Z_{eg} \end{bmatrix} = \begin{bmatrix} X_{ag} \\ SE \cdot Y_{ag} - CE \cdot Z_{ag} + CE \cdot h_e \\ CE \cdot Y_{ag} + SE \cdot Z_{ag} - SE \cdot h_e \end{bmatrix}$$

Elevation To Base Transformation:

$$\begin{bmatrix} X \\ Y \\ Z \end{bmatrix} = [R13] \begin{bmatrix} X_{eg} \\ Y_{eg} \\ Z_{eg} \end{bmatrix} + [T13] \quad , \qquad \begin{aligned} [R13] &= [R12][R23] \\ [T13] &= [T12] + [R12][T23] \end{aligned}$$

$$[R13] = \begin{pmatrix} -CA & SA \cdot SE & SA \cdot CE \\ -SA & -CA \cdot SE & -CA \cdot CE \\ 0 & -CE & SE \end{pmatrix} \quad , \qquad [T13] = \begin{bmatrix} 0 \\ 0 \\ h_e \end{bmatrix}$$

$$\begin{bmatrix} X \\ Y \\ Z \end{bmatrix} = \begin{bmatrix} -CA \cdot X_{eg} + SA \cdot SE \cdot Y_{eg} + SA \cdot CE \cdot Z_{eg} \\ -SA \cdot X_{eg} - CA \cdot SE \cdot Y_{eg} - CA \cdot CE \cdot Z_{eg} \\ -CE \cdot Y_{eg} + SE \cdot Z_{eg} + h_e \end{bmatrix}$$

Elevation Frame Origin:

$$\begin{pmatrix} X(Eg) \\ Y(Eg) \\ Z(Eg) \end{pmatrix} = \begin{bmatrix} 0 \\ 0 \\ h_e \end{bmatrix} \qquad (= [T13])$$

Base to Elevation Transformation:

$$\begin{bmatrix} X_{eg} \\ Y_{eg} \\ Z_{eg} \end{bmatrix} = [R31] \begin{bmatrix} X \\ Y \\ Z \end{bmatrix} + [T31] \quad , \qquad [T31] = [R31](-1)[T13]$$

$$[R31] = \begin{pmatrix} -CA & -SA & 0 \\ SA \cdot SE & -CA \cdot SE & -CE \\ SA \cdot CE & -CA \cdot CE & SE \end{pmatrix} \quad , \qquad [T31] = \begin{bmatrix} 0 \\ CE \cdot h_e \\ -SE \cdot h_e \end{bmatrix}$$

$$\begin{bmatrix} X_{eg} \\ Y_{eg} \\ Z_{eg} \end{bmatrix} = \begin{bmatrix} -CA \cdot X - SA \cdot Y \\ SA \cdot SE \cdot X - CA \cdot SE \cdot Y - CE \cdot Z + CE \cdot h_e \\ SA \cdot CE \cdot X - CA \cdot CE \cdot Y + SE \cdot Z - SE \cdot h_e \end{bmatrix}$$

Reflector To Elevation Transformation:

$$\begin{bmatrix} X_{eg} \\ Y_{eg} \\ Z_{eg} \end{bmatrix} = [R34] \begin{bmatrix} X_{rg} \\ Y_{rg} \\ Z_{rg} \end{bmatrix} + [T34]$$

$$[R34] = \begin{pmatrix} 1 & 0 & 0 \\ 0 & 1 & 0 \\ 0 & 0 & 1 \end{pmatrix}, \quad [T34] = \begin{bmatrix} 0 \\ -d_{re} \\ h_{re} \end{bmatrix}$$

$$\begin{bmatrix} X_{eg} \\ Y_{eg} \\ Z_{eg} \end{bmatrix} = \begin{bmatrix} X_{rg} \\ Y_{rg} - d_{re} \\ Z_{rg} + h_{re} \end{bmatrix}$$

Elevation To Reflector Transformation:

$$\begin{bmatrix} X_{rg} \\ Y_{rg} \\ Z_{rg} \end{bmatrix} = [R43] \begin{bmatrix} X_{eg} \\ Y_{eg} \\ Z_{eg} \end{bmatrix} + [T43], \quad [T43] = [R43](-1)[T34]$$

$$[R43] = \begin{pmatrix} 1 & 0 & 0 \\ 0 & 1 & 0 \\ 0 & 0 & 1 \end{pmatrix}, \quad [T43] = \begin{bmatrix} 0 \\ d_{re} \\ -h_{re} \end{bmatrix}$$

$$\begin{bmatrix} X_{rg} \\ Y_{rg} \\ Z_{rg} \end{bmatrix} = \begin{bmatrix} X_{eg} \\ Y_{eg} + d_{re} \\ Z_{eg} - h_{re} \end{bmatrix}$$

Reflector To Base Transformation:

$$\begin{bmatrix} X \\ Y \\ Z \end{bmatrix} = [R14] \begin{bmatrix} X_{rg} \\ Y_{rg} \\ Z_{rg} \end{bmatrix} + [T14] \quad , \qquad \begin{aligned} [R14] &= [R13][R34] \\ [T14] &= [T13] + [R13][T34] \end{aligned}$$

$$[R14] = \begin{pmatrix} -CA & SA \cdot SE & SA \cdot CE \\ -SA & -CA \cdot SE & -CA \cdot CE \\ 0 & -CE & SE \end{pmatrix} \quad , \qquad [T14] = \begin{bmatrix} -SA \cdot SE \cdot d_{re} + SA \cdot CE \cdot h_{re} \\ CA \cdot SE \cdot d_{re} - CA \cdot CE \cdot h_{re} \\ CE \cdot d_{re} + SE \cdot h_{re} + h_e \end{bmatrix}$$

$$\begin{bmatrix} X \\ Y \\ Z \end{bmatrix} = \begin{bmatrix} -CA \cdot X_{rg} + SA \cdot SE \cdot Y_{rg} + SA \cdot CE \cdot Z_{rg} - SA \cdot SE \cdot d_{re} + SA \cdot CE \cdot h_{re} \\ -SA \cdot X_{rg} - CA \cdot SE \cdot Y_{rg} - CA \cdot CE \cdot Z_{rg} + CA \cdot SE \cdot d_{re} - CA \cdot CE \cdot h_{re} \\ -CE \cdot Y_{rg} + SE \cdot Z_{rg} + CE \cdot d_{re} + SE \cdot h_{re} + h_e \end{bmatrix}$$

Reflector Frame Origin:

$$\begin{pmatrix} X(Rg) \\ Y(Rg) \\ Z(Rg) \end{pmatrix} = \begin{bmatrix} -SA \cdot SE \cdot d_{re} + SA \cdot CE \cdot h_{re} \\ CA \cdot SE \cdot d_{re} - CA \cdot CE \cdot h_{re} \\ CE \cdot d_{re} + SE \cdot h_{re} + h_e \end{bmatrix} \qquad (= [T14])$$

Base to Reflector Transformation:

$$\begin{bmatrix} X_{rg} \\ Y_{rg} \\ Z_{rg} \end{bmatrix} = [R41] \begin{bmatrix} X \\ Y \\ Z \end{bmatrix} + [T41] \quad , \qquad [T41] = [R41](-1)[T14]$$

$$[R41] = \begin{pmatrix} -CA & -SA & 0 \\ SA \cdot SE & -CA \cdot SE & -CE \\ SA \cdot CE & -CA \cdot CE & SE \end{pmatrix}$$

$$[T41] = \begin{pmatrix} -CA & -SA & 0 \\ SA \cdot SE & -CA \cdot SE & -CE \\ SA \cdot CE & -CA \cdot CE & SE \end{pmatrix} \cdot \begin{bmatrix} SA \cdot SE \cdot d_{re} - SA \cdot CE \cdot h_{re} \\ -CA \cdot SE \cdot d_{re} + CA \cdot CE \cdot h_{re} \\ -CE \cdot d_{re} - SE \cdot h_{re} - h_e \end{bmatrix} = \begin{bmatrix} 0 \\ d_{re} + CE \cdot h_e \\ -h_{re} - SE \cdot h_e \end{bmatrix}$$

$$\begin{bmatrix} X_{rg} \\ Y_{rg} \\ Z_{rg} \end{bmatrix} = \begin{bmatrix} -CA \cdot X - SA \cdot Y \\ SA \cdot SE \cdot X - CA \cdot SE \cdot Y - CE \cdot Z + d_{re} + CE \cdot h_e \\ SA \cdot CE \cdot X - CA \cdot CE \cdot Y + SE \cdot Z - h_{re} - SE \cdot h_e \end{bmatrix}$$

Prime Focus To Reflector Transformation:

$$\begin{bmatrix} X_{rg} \\ Y_{rg} \\ Z_{rg} \end{bmatrix} = [R45] \begin{bmatrix} X_{pg} \\ Y_{pg} \\ Z_{pg} \end{bmatrix} + [T45]$$

$$[R45] = \begin{bmatrix} 0 & 0 & 1 \\ C_{pf} & -S_{pf} & 0 \\ S_{pf} & C_{pf} & 0 \end{bmatrix}, \quad [T45] = \begin{bmatrix} 0 \\ 0 \\ h_{rp} \end{bmatrix}$$

$$\begin{bmatrix} X_{rg} \\ Y_{rg} \\ Z_{rg} \end{bmatrix} = \begin{bmatrix} Z_{pg} \\ C_{pf}X_{pg} - S_{pf}Y_{pg} \\ S_{pf}X_{pg} + C_{pf}Y_{pg} + h_{rp} \end{bmatrix}$$

Reflector To Prime Focus Transformation:

$$\begin{bmatrix} X_{pg} \\ Y_{pg} \\ Z_{pg} \end{bmatrix} = [R54] \begin{bmatrix} X_{rg} \\ Y_{rg} \\ Z_{rg} \end{bmatrix} + [T54], \quad [T54] = [R54](-1)[T45]$$

$$[R54] = \begin{bmatrix} 0 & C_{pf} & S_{pf} \\ 0 & -S_{pf} & C_{pf} \\ 1 & 0 & 0 \end{bmatrix}, \quad [T54] = \begin{bmatrix} -S_{pf}h_{rp} \\ -C_{pf}h_{rp} \\ 0 \end{bmatrix}$$

$$\begin{bmatrix} X_{pg} \\ Y_{pg} \\ Z_{pg} \end{bmatrix} = \begin{bmatrix} C_{pf}Y_{rg} + S_{pf}Z_{rg} - S_{pf}h_{rp} \\ -S_{pf}Y_{rg} + C_{pf}Z_{rg} - C_{pf}h_{rp} \\ X_{rg} \end{bmatrix}$$

Prime Focus To Base Transformation:

$$\begin{bmatrix} X \\ Y \\ Z \end{bmatrix} = [R15] \begin{bmatrix} X_{pg} \\ Y_{pg} \\ Z_{pg} \end{bmatrix} + [T15] \quad , \quad \begin{array}{l} [R15] = [R14][R45] \\ [T15] = [T14] + [R14][T45] \end{array}$$

$$[R15] = \begin{bmatrix} SA \cdot S_{pfE} & SA \cdot C_{pfE} & -CA \\ -CA \cdot S_{pfE} & -CA \cdot C_{pfE} & -SA \\ -C_{pfE} & S_{pfE} & 0 \end{bmatrix}$$

$$[T15] = \begin{bmatrix} SA \cdot CE \cdot h_{pe} - SA \cdot SE \cdot d_{re} \\ -CA \cdot CE \cdot h_{pe} - CA \cdot SE \cdot d_{re} \\ SE \cdot h_{pe} + CE \cdot d_{re} + h_e \end{bmatrix}$$

$$\begin{bmatrix} X \\ Y \\ Z \end{bmatrix} = \begin{bmatrix} SA \cdot S_{pfE} \cdot X_{pg} + SA \cdot C_{pfE} \cdot Y_{pg} - CA \cdot Z_{pg} + SA \cdot CE \cdot h_{pe} - SA \cdot SE \cdot d_{re} \\ -CA \cdot S_{pfE} \cdot X_{pg} - CA \cdot C_{pfE} \cdot Y_{pg} - SA \cdot Z_{pg} - CA \cdot CE \cdot h_{pe} - CA \cdot SE \cdot d_{re} \\ -C_{pfE} \cdot X_{pg} + S_{pfE} \cdot Y_{pg} + SE \cdot h_{pe} + CE \cdot d_{re} + h_e \end{bmatrix}$$

Prime Focus Frame Origin:

$$\begin{pmatrix} X(Pg) \\ Y(Pg) \\ Z(Pg) \end{pmatrix} = \begin{bmatrix} SA \cdot CE \cdot h_{pe} - SA \cdot SE \cdot d_{re} \\ -CA \cdot CE \cdot h_{pe} - CA \cdot SE \cdot d_{re} \\ SE \cdot h_{pe} + CE \cdot d_{re} + h_e \end{bmatrix} \quad (= [T15])$$

Base to Prime Focus Transformation:

$$\begin{bmatrix} X_{pg} \\ Y_{pg} \\ Z_{pg} \end{bmatrix} = [R51] \begin{bmatrix} X \\ Y \\ Z \end{bmatrix} + [T51] \quad , \quad [T51] = [R51](-1)[T15]$$

$$[R51] = \begin{bmatrix} SA \cdot S_{pfE} & -CA \cdot S_{pfE} & -C_{pfE} \\ SA \cdot C_{pfE} & -CA \cdot C_{pfE} & S_{pfE} \\ -CA & -SA & 0 \end{bmatrix}$$

$$[T51] = \begin{bmatrix} SA \cdot S_{pfE} & -CA \cdot S_{pfE} & -C_{pfE} \\ SA \cdot C_{pfE} & -CA \cdot C_{pfE} & S_{pfE} \\ -CA & -SA & 0 \end{bmatrix} \cdot \begin{bmatrix} -SA \cdot CE \cdot h_{pe} + SA \cdot SE \cdot d_{re} \\ CA \cdot CE \cdot h_{pe} + CA \cdot SE \cdot d_{re} \\ -SE \cdot h_{pe} - CE \cdot d_{re} - h_e \end{bmatrix}$$

$$[T51] = \begin{bmatrix} C_{pfE} \cdot (SE \cdot h_{pe} + CE \cdot d_{re} + h_e) - C_{2A} \cdot S_{pfE} \cdot SE \cdot d_{re} - S_{pfE} \cdot CE \cdot h_{pe} \\ -S_{pfe} \cdot (SE \cdot h_{pe} + CE \cdot d_{re} + h_e) - C_{2A} \cdot C_{pfE} \cdot SE \cdot d_{re} - C_{pfE} \cdot CE \cdot h_{pe} \\ -S_{2A} \cdot SE \cdot d_{re} \end{bmatrix}$$

$$\begin{bmatrix} X_{pg} \\ Y_{pg} \\ Z_{pg} \end{bmatrix} = \begin{bmatrix} SA \cdot S_{pfE} \cdot X - CA \cdot S_{pfE} \cdot Y - C_{pfE} \cdot Z + C_{pfE} \cdot (SE \cdot h_{pe} + CE \cdot d_{re} + h_e) - C_{2A} \cdot S_{pfE} \cdot SE \cdot d_{re} - S_{pfE} \cdot CE \cdot h_{pe} \\ SA \cdot C_{pfE} \cdot X - CA \cdot C_{pfE} \cdot Y + S_{pfE} \cdot Z - S_{pfe} \cdot (SE \cdot h_{pe} + CE \cdot d_{re} + h_e) - C_{2A} \cdot C_{pfE} \cdot SE \cdot d_{re} - C_{pfE} \cdot CE \cdot h_{pe} \\ -CA \cdot X - SA \cdot Y - S_{2A} \cdot SE \cdot d_{re} \end{bmatrix}$$

Subreflector To Reflector Transformation:

$$\begin{bmatrix} X_{rg} \\ Y_{rg} \\ Z_{rg} \end{bmatrix} = [R46] \begin{bmatrix} X_{sg} \\ Y_{sg} \\ Z_{sg} \end{bmatrix} + [T46]$$

$$[R46] = \begin{bmatrix} 0 & 0 & 1 \\ C_s & -S_s & 0 \\ S_s & C_s & 0 \end{bmatrix}, \quad [T46] = \begin{bmatrix} 0 \\ -d_{rs} \\ h_{rs} \end{bmatrix}$$

$$\begin{bmatrix} X_{rg} \\ Y_{rg} \\ Z_{rg} \end{bmatrix} = \begin{bmatrix} Z_{sg} \\ C_s \cdot X_{sg} - S_s \cdot Y_{sg} - d_{rs} \\ S_s \cdot X_{sg} + C_s \cdot Y_{sg} + h_{rs} \end{bmatrix}$$

Reflector To Subreflector Transformation:

$$\begin{bmatrix} X_{sg} \\ Y_{sg} \\ Z_{sg} \end{bmatrix} = [R64] \begin{bmatrix} X_{rg} \\ Y_{rg} \\ Z_{rg} \end{bmatrix} + [T64], \quad [T64] = [R64](-1)[T46]$$

$$[R64] = \begin{bmatrix} 0 & C_s & S_s \\ 0 & -S_s & C_s \\ 1 & 0 & 0 \end{bmatrix}, \quad [T64] = \begin{bmatrix} C_s \cdot d_{rs} - S_s \cdot h_{rs} \\ -S_s \cdot d_{rs} - C_s \cdot h_{rs} \\ 0 \end{bmatrix}$$

$$\begin{bmatrix} X_{sg} \\ Y_{sg} \\ Z_{sg} \end{bmatrix} = \begin{bmatrix} C_s \cdot Y_{rg} + S_s \cdot Z_{rg} + C_s \cdot d_{rs} - S_s \cdot h_{rs} \\ -S_s \cdot Y_{rg} + C_s \cdot Z_{rg} - S_s \cdot d_{rs} - C_s \cdot h_{rs} \\ X_{rg} \end{bmatrix}$$

Subreflector To Base Transformation:

$$\begin{bmatrix} X \\ Y \\ Z \end{bmatrix} = [R16] \begin{bmatrix} X_{sg} \\ Y_{sg} \\ Z_{sg} \end{bmatrix} + [T16] \quad , \quad \begin{array}{l} [R16] = [R14][R46] \\ [T16] = [T14] + [R14][T46] \end{array}$$

$$[R16] = \begin{bmatrix} SA \cdot S_{sE} & SA \cdot C_{sE} & -CA \\ -CA \cdot S_{sE} & -CA \cdot C_{sE} & -SA \\ -C_{sE} & S_{sE} & 0 \end{bmatrix}$$

$$[T16] = \begin{bmatrix} -SA \cdot SE \cdot d_{se} + SA \cdot CE \cdot h_{se} \\ CA \cdot SE \cdot d_{se} - CA \cdot CE \cdot h_{se} \\ CE \cdot d_{se} + SE \cdot h_{se} + h_e \end{bmatrix}$$

$$\begin{bmatrix} X \\ Y \\ Z \end{bmatrix} = \begin{bmatrix} SA \cdot S_{sE} \cdot X_{sg} + SA \cdot C_{sE} \cdot Y_{sg} - CA \cdot Z_{sg} - SA \cdot SE \cdot d_{se} + SA \cdot CE \cdot h_{se} \\ -CA \cdot S_{sE} \cdot X_{sg} - CA \cdot C_{sE} \cdot Y_{sg} - SA \cdot Z_{sg} + CA \cdot SE \cdot d_{se} - CA \cdot CE \cdot h_{se} \\ -C_{sE} \cdot X_{sg} + S_{sE} \cdot Y_{sg} + CE \cdot d_{se} + SE \cdot h_{se} + h_e \end{bmatrix}$$

Subreflector Frame Origin:

$$\begin{pmatrix} X(Sg) \\ Y(Sg) \\ Z(Sg) \end{pmatrix} = \begin{bmatrix} -SA \cdot SE \cdot d_{se} + SA \cdot CE \cdot h_{se} \\ CA \cdot SE \cdot d_{se} - CA \cdot CE \cdot h_{se} \\ CE \cdot d_{se} + SE \cdot h_{se} + h_e \end{bmatrix} \quad (= [T16])$$

Base to Subreflector Transformation:

$$\begin{bmatrix} X_{sg} \\ Y_{sg} \\ Z_{sg} \end{bmatrix} = [R61] \begin{bmatrix} X \\ Y \\ Z \end{bmatrix} + [T61] \qquad [T61] = [R61](-1)[T16]$$

$$[R61] = \begin{bmatrix} SA \cdot S_{sE} & -CA \cdot S_{sE} & -C_{sE} \\ SA \cdot C_{sE} & -CA \cdot C_{sE} & S_{sE} \\ -CA & -SA & 0 \end{bmatrix}$$

$$[T61] = \begin{bmatrix} S_{sE} \cdot SE \cdot d_{se} - S_{sE} \cdot CE \cdot h_{se} + C_{sE} \cdot CE \cdot d_{se} + C_{sE} \cdot SE \cdot h_{se} + C_{sE} \cdot h_e \\ C_{sE} \cdot SE \cdot d_{se} - C_{sE} \cdot CE \cdot h_{se} - S_{sE} \cdot CE \cdot d_{se} - S_{sE} \cdot SE \cdot h_{se} - S_{sE} \cdot h_e \\ 0 \end{bmatrix}$$

$$\begin{bmatrix} X_{sg} \\ Y_{sg} \\ Z_{sg} \end{bmatrix} = \begin{bmatrix} SA \cdot S_{sE} \cdot X - CA \cdot S_{sE} \cdot Y - C_{sE} \cdot Z + S_{sE} \cdot SE \cdot d_{se} - S_{sE} \cdot CE \cdot h_{se} + C_{sE} \cdot CE \cdot d_{se} + C_{sE} \cdot SE \cdot h_{se} + C_{sE} \cdot h_e \\ SA \cdot C_{sE} \cdot X - CA \cdot C_{sE} \cdot Y + S_{sE} \cdot Z + C_{sE} \cdot SE \cdot d_{se} - C_{sE} \cdot CE \cdot h_{se} - S_{sE} \cdot CE \cdot d_{se} - S_{sE} \cdot SE \cdot h_{se} - S_{sE} \cdot h_e \\ -CA \cdot X - SA \cdot Y \end{bmatrix}$$

Gregorian Ellipsoid To Reflector Transformation:

$$\begin{bmatrix} X_{rg} \\ Y_{rg} \\ Z_{rg} \end{bmatrix} = [R47] \begin{bmatrix} X_{ceg} \\ Y_{ceg} \\ Z_{ceg} \end{bmatrix} + [T47]$$

$$[R47] = \begin{pmatrix} 0 & 0 & 1 \\ SB & -CB & 0 \\ CB & SB & 0 \end{pmatrix}, \quad [T47] = \begin{bmatrix} 0 \\ -d_{rce} \\ h_{rce} \end{bmatrix}$$

$$\begin{bmatrix} X_{rg} \\ Y_{rg} \\ Z_{rg} \end{bmatrix} = \begin{bmatrix} Z_{ceg} \\ SB \cdot X_{ceg} - CB \cdot Y_{ceg} - d_{rce} \\ CB \cdot X_{ceg} + SB \cdot Y_{ceg} + h_{rce} \end{bmatrix}$$

Reflector To Gregorian Ellipsoid Transformation:

$$\begin{bmatrix} X_{ceg} \\ Y_{ceg} \\ Z_{ceg} \end{bmatrix} = [R74] \begin{bmatrix} X_{rg} \\ Y_{rg} \\ Z_{rg} \end{bmatrix} + [T74], \quad [T74] = [R74](-1)[T47]$$

$$[R74] = \begin{pmatrix} 0 & SB & CB \\ 0 & -CB & SB \\ 1 & 0 & 0 \end{pmatrix}, \quad [T74] = \begin{bmatrix} SB \cdot d_{rce} - CB \cdot h_{rce} \\ -CB \cdot d_{rce} - SB \cdot h_{rce} \\ 0 \end{bmatrix}$$

$$\begin{bmatrix} X_{ceg} \\ Y_{ceg} \\ Z_{ceg} \end{bmatrix} = \begin{bmatrix} SB \cdot Y_{rg} + CB \cdot Z_{rg} + SB \cdot d_{rce} - CB \cdot h_{rce} \\ -CB \cdot Y_{rg} + SB \cdot Z_{rg} - CB \cdot d_{rce} - SB \cdot h_{rce} \\ X_{rg} \end{bmatrix}$$

Gregorian Focus Point:

$$\begin{bmatrix} X_{ceg(M_g)} \\ Y_{ceg(M_g)} \\ Z_{ceg(M_g)} \end{bmatrix} = \begin{bmatrix} -f_e \\ 0 \\ 0 \end{bmatrix}$$

Prime Focus Point:

$$\begin{bmatrix} X_{ceg(P_g)} \\ Y_{ceg(P_g)} \\ Z_{ceg(P_g)} \end{bmatrix} = \begin{bmatrix} f_e \\ 0 \\ 0 \end{bmatrix}$$

where f_e = 550 cm.

Turret To Reflector Transformation:

$$\begin{bmatrix} X_{rg} \\ Y_{rg} \\ Z_{rg} \end{bmatrix} = [R48] \begin{bmatrix} X_{tg} \\ Y_{tg} \\ Z_{tg} \end{bmatrix} + [T48]$$

$$[R48] = \begin{pmatrix} 0 & 0 & 1 \\ CT & -ST & 0 \\ ST & CT & 0 \end{pmatrix}, \quad [T48] = \begin{bmatrix} 0 \\ -d_{tr} \\ h_{tr} \end{bmatrix}$$

$$\begin{bmatrix} X_{rg} \\ Y_{rg} \\ Z_{rg} \end{bmatrix} = \begin{bmatrix} Z_{tg} \\ CT \cdot X_{tg} - ST \cdot Y_{tg} - d_{tr} \\ ST \cdot X_{tg} + CT \cdot Y_{tg} + h_{tr} \end{bmatrix}$$

Reflector To Turret Transformation:

$$\begin{bmatrix} X_{tg} \\ Y_{tg} \\ Z_{tg} \end{bmatrix} = [R84] \begin{bmatrix} X_{rg} \\ Y_{rg} \\ Z_{rg} \end{bmatrix} + [T84], \quad [T84] = [R84](-1)[T48]$$

$$[R84] = \begin{pmatrix} 0 & CT & ST \\ 0 & -ST & CT \\ 1 & 0 & 0 \end{pmatrix} \quad [T84] = \begin{bmatrix} CT \cdot d_{tr} - ST \cdot h_{tr} \\ -ST \cdot d_{tr} - CT \cdot h_{tr} \\ 0 \end{bmatrix}$$

$$\begin{bmatrix} X_{tg} \\ Y_{tg} \\ Z_{tg} \end{bmatrix} = \begin{bmatrix} CT \cdot Y_{rg} + ST \cdot Z_{rg} + CT \cdot d_{tr} - ST \cdot h_{tr} \\ -ST \cdot Y_{rg} + CT \cdot Z_{rg} - ST \cdot d_{tr} - CT \cdot h_{tr} \\ X_{rg} \end{bmatrix}$$

Turret To Base Transformation:

$$\begin{bmatrix} X \\ Y \\ Z \end{bmatrix} = [R18] \begin{bmatrix} X_{tg} \\ Y_{tg} \\ Z_{tg} \end{bmatrix} + [T18] \quad , \qquad \begin{aligned} &[R18] = [R14][R48] \\ &[T18] = [T14] + [R14][T48] \end{aligned}$$

Using $SET = \sin(ELant + \alpha - \beta)$

$CET = \cos(ELant + \alpha - \beta)$,

$$[R18] = \begin{pmatrix} -CA & SA \cdot SE & SA \cdot CE \\ -SA & -CA \cdot SE & -CA \cdot CE \\ 0 & -CE & SE \end{pmatrix} \cdot \begin{pmatrix} 0 & 0 & 1 \\ CT & -ST & 0 \\ ST & CT & 0 \end{pmatrix} = \begin{pmatrix} SA \cdot SET & SA \cdot CET & -CA \\ -CA \cdot SET & CA \cdot CET & -SA \\ -CET & SET & 0 \end{pmatrix}$$

$$[T18] = \begin{bmatrix} -SA \cdot SE \cdot d_{tr} + SA \cdot CE \cdot h_{tr} - SA \cdot SE \cdot d_{re} + SA \cdot CE \cdot h_{re} \\ CA \cdot SE \cdot d_{tr} - CA \cdot CE \cdot h_{tr} + CA \cdot SE \cdot d_{re} - CA \cdot CE \cdot h_{re} \\ CE \cdot d_{tr} + SE \cdot h_{tr} + CE \cdot d_{re} + SE \cdot h_{re} + h_e \end{bmatrix} = \begin{bmatrix} -SA \cdot SE \cdot d_{te} + SA \cdot CE \cdot h_{te} \\ CA \cdot SE \cdot d_{te} - CA \cdot CE \cdot h_{te} \\ CE \cdot d_{te} + SE \cdot h_{te} + h_e \end{bmatrix}$$

$$\begin{bmatrix} X \\ Y \\ Z \end{bmatrix} = \begin{bmatrix} -CA \cdot X_{tg} + SA \cdot SE \cdot Y_{tg} + SA \cdot CE \cdot Z_{tg} - SA \cdot SE \cdot d_{te} + SA \cdot CE \cdot h_{te} \\ -SA \cdot X_{tg} - CA \cdot SE \cdot Y_{tg} - CA \cdot CE \cdot Z_{tg} + CA \cdot SE \cdot d_{te} - CA \cdot CE \cdot h_{te} \\ -CE \cdot Y_{tg} + SE \cdot Z_{tg} + CE \cdot d_{te} + SE \cdot h_{te} + h_e \end{bmatrix}$$

Turret Frame Origin:

$$\begin{pmatrix} X(Tg) \\ Y(Tg) \\ Z(Tg) \end{pmatrix} = \begin{bmatrix} -SA \cdot SE \cdot d_{te} + SA \cdot CE \cdot h_{te} \\ CA \cdot SE \cdot d_{te} - CA \cdot CE \cdot h_{te} \\ CE \cdot d_{te} + SE \cdot h_{te} + h_e \end{bmatrix} \qquad (= [T18])$$

Base To Turret Transformation:

$$\begin{bmatrix} X_{tg} \\ Y_{tg} \\ Z_{tg} \end{bmatrix} = [R81] \begin{bmatrix} X \\ Y \\ Z \end{bmatrix} + [T81] \quad , \quad [T81] = [R81](-1)[T18]$$

$$[R81] = \begin{pmatrix} SA \cdot SET & -CA \cdot SET & -CET \\ SA \cdot CET & CA \cdot CET & SET \\ -CA & -SA & 0 \end{pmatrix}$$

$$[T81] = \begin{pmatrix} SA \cdot SET & -CA \cdot SET & -CET \\ SA \cdot CET & CA \cdot CET & SET \\ -CA & -SA & 0 \end{pmatrix} \cdot \begin{bmatrix} SA \cdot SE \cdot d_{te} - SA \cdot CE \cdot h_{te} \\ -CA \cdot SE \cdot d_{te} + CA \cdot CE \cdot h_{te} \\ -CE \cdot d_{te} - SE \cdot h_{te} - h_e \end{bmatrix}$$

$$[T81] = \begin{bmatrix} SA^2 \cdot SET \cdot SE \cdot d_{te} - SA^2 \cdot SET \cdot CE \cdot h_{te} + CA^2 \cdot SET \cdot SE \cdot d_{te} - CA^2 \cdot SET \cdot CE \cdot h_{te} + CET \cdot CE \cdot d_{te} + CET \cdot SE \cdot h_{te} + CET \cdot h_e \\ SA^2 \cdot CET \cdot SE \cdot d_{te} - SA^2 \cdot CET \cdot CE \cdot h_{te} - CA^2 \cdot CET \cdot SE \cdot d_{te} + CA^2 \cdot CET \cdot CE \cdot h_{te} - SET \cdot CE \cdot d_{te} - SET \cdot SE \cdot h_{te} - SET \cdot h_e \\ 0 \end{bmatrix}$$

$$[T81] = \begin{bmatrix} SET \cdot SE \cdot d_{te} - SET \cdot CE \cdot h_{te} + CET \cdot CE \cdot d_{te} + CET \cdot SE \cdot h_{te} + CET \cdot h_e \\ -C_{2A} \cdot CET \cdot SE \cdot d_{te} + C_{2A} \cdot CET \cdot CE \cdot h_{te} - SET \cdot CE \cdot d_{te} - SET \cdot SE \cdot h_{te} - SET \cdot h_e \\ 0 \end{bmatrix}$$

$$\begin{bmatrix} X_{sg} \\ Y_{sg} \\ Z_{sg} \end{bmatrix} = \begin{bmatrix} SA \cdot SET \cdot X - CA \cdot SET \cdot Y - CET \cdot Z + SET \cdot SE \cdot (d_{te} + h_{te}) + CET \cdot CE \cdot (d_{te} - h_{te}) + CET \cdot h_e \\ SA \cdot CET \cdot X + CA \cdot CET \cdot Y + SET \cdot Z + C_{2A} \cdot CET \cdot (CE \cdot h_{te} - SE \cdot d_{te}) - SET \cdot CE \cdot d_{te} - SET \cdot SE \cdot h_{te} - SET \cdot h_e \\ -CA \cdot X - SA \cdot Y \end{bmatrix}$$

Appendix II. List Of Symbols.

Reference Optical Telescope

α	Offset angle from the ellipsoid major axis, of the mid ray from gregorian focus to the subreflector.
β	Angle between the paraboloid and ellipsoid axes.
γ	Angle $F_0\, I_1\, F_1$
Θ_H	Half-angle of tangential plane ray fan from the gregorian focus to the subreflector. from the prime focus to subreflector.
Θ_0	Offset angle, from the paraboloid axis, of the tangential fan's mid ray from the prime focus to the main reflector.
a	Semimajor axis of the ellipsoid.
b	Semiminor axis of the ellipsoid.
e	Eccentricity of the ellipsoid.
f_e	Distance from ellipsoid focus point to ellipsoid center point.
f_p	Design focal length of the paraboloid.
d_{sp}	Length of $\perp$ from I_1 to paraboloid axis.
h_{sp}	Projected length of ray $F_0\, I_1$ along paraboloid axis.
d_{mp}	Length of $\perp$ from F_1 to paraboloid axis.
h_{mp}	Projected length of ray $F_0\, F_1$ along paraboloid axis.
r_1	Length of ray $F_1\, I_1$
r_2	Length of ray $F_0\, I_1$
F_0	Prime focus point of reference optical telescope.
F_1	Gregorian focus point of reference optical telescope.
I_1	Intersection point of tangent fan mid ray with subreflector ellipsoid.
V_0	Vertex point of the paraboloid.

Design Telescope

A_d	Origin point of the alidade frame of the design telescope.
$B_d \ (= B)$	Origin point of the base frame.
E_d	Origin point of the elevation frame of the design telescope.
P_d	Focal point of the parent paraboloid.
R_d	Origin point of the reflector frame of the design telescope.
S_d	Origin point of the subreflector frame of the design telescope.
M_d	Gregorian focus point of the parent ellipsoid.
T_d	Origin point of the design turret frame.

$\widehat{X}_{ad}$, $\widehat{Y}_{ad}$, $\widehat{Z}_{ad}$	Basis vectors of the alidade frame of the design telescope.
$\widehat{X}_{ed}$, $\widehat{Y}_{ed}$, $\widehat{Z}_{ed}$	Basis vectors of the elevation frame of the design telescope.
$\widehat{X}_{rd}$, $\widehat{Y}_{rd}$, $\widehat{Z}_{rd}$	Basis vectors of the reflector frame of the design telescope.
$\widehat{X}_{sd}$, $\widehat{Y}_{sd}$, $\widehat{Z}_{sd}$	Basis vectors of the subreflector frame of the design telescope.
$\widehat{X}_{td}$, $\widehat{Y}_{td}$, $\widehat{Z}_{td}$	Basis vectors of the turret frame of the design telescope.

S_{pfE}	$\sin(EL_{ant} + 45.5 \text{ degrees})$
C_{pfE}	$\cos(EL_{ant} + 45.5 \text{ degrees})$
S_{sE}	$\sin(EL_{ant} + 36.7 \text{degrees})$
C_{sE}	$\cos(EL_{ant} + 36.7 \text{degrees})$
ST	$\sin(\alpha - \beta)$
CT	$\cos(\alpha - \beta)$
SET	$\sin(EL_{ant} + \alpha - \beta) = \sin(EL_{ant} + 12.329 \text{ degrees})$
CET	$\cos(EL_{ant} + \alpha - \beta) = \cos(EL_{ant} + 12.329 \text{ degrees})$

Tilted Geometric Telescope

A_g	Origin point of alidade frame of the geometric telescope.
B	Origin point of the base frame.
E_g	Origin point of elevation frame of the geometric telescope.
P_g	Prime focus point of the geometric telescope.
Q	An arbitrary point.
R_g	Origin point of reflector frame of the geometric telescope.
S_g	Origin point of subreflector frame of the geometric telescope.
M_g	Gregorian focus point of the geometric telescope.
T_g	Origin point of turret frame of the geometric telescope.
CE_g	Origin point of ellipsoid frame of the geometric telescope.
H_g	Origin point of receiver house frame of the geometric telescope.
N_i	Origin point of the i'th receiver flange frame.
h_e	Distance from B to E_g.
d_{tm}	Distance from T_g to M_g.
AZ_{ant}	Alidade azimuth angle of the geometric telescope.
EL_{ant}	Elevation angle of the geometric telescope tipping structure.
SA	$\sin(AZ_{ant})$
CA	$\cos(AZ_{ant})$
SE	$\sin(EL_{ant})$
CE	$\cos(EL_{ant})$
$\widehat{X}$, $\widehat{Y}$, $\widehat{Z}$	Basis vectors of the base frame.
$\widehat{X}_{ag}$, $\widehat{Y}_{ag}$, $\widehat{Z}_{ag}$	Basis vectors of alidade frame of the geometric telescope.
$\widehat{X}_{eg}$, $\widehat{Y}_{eg}$, $\widehat{Z}_{eg}$	Basis vectors of elevation frame of the geometric telescope.
$\widehat{X}_{rg}$, $\widehat{Y}_{rg}$, $\widehat{Z}_{rg}$	Basis vectors of reflector frame of the geometric telescope.
$\widehat{X}_{pg}$, $\widehat{Y}_{pg}$, $\widehat{Z}_{pg}$	Basis vectors of prime focus frame of the geometric telescope.
$\widehat{X}_{sg}$, $\widehat{Y}_{sg}$, $\widehat{Z}_{sg}$	Basis vectors of subreflector frame of the geometric telescope.

$\widehat{X}_{tg}$, $\widehat{Y}_{tg}$, $\widehat{Z}_{tg}$	Basis vectors of turret frame of the geometric telescope.
$\widehat{X}_{hg}$, $\widehat{Y}_{hg}$, $\widehat{Z}_{hg}$	Basis vectors of receiver house frame.
$\widehat{X}_{ni}$, $\widehat{Y}_{ni}$, $\widehat{Z}_{ni}$	Basis vectors of i'th receiver flange.
$X(Q)$, $Y(Q)$, $Z(Q)$	Base frame coordinates of (arbitrary) point Q.
$X_{eg}(Q)$, $Y_{eg}(Q)$, $Z_{eg}(Q)$	Geometric elevation frame coordinates of point Q.
$X_{ed}(Q)$, $Y_{ed}(Q)$, $Z_{ed}(Q)$	Design elevation frame coordinates of point Q.
$X_{ag}(Q)$, $Y_{ag}(Q)$, $Z_{ag}(Q)$	Geometric alidade frame coordinates of point Q.
$X_{ad}(Q)$, $Y_{ad}(Q)$, $Z_{ad}(Q)$	Design alidade frame coordinates of point Q.
$X_{rg}(Q)$, $Y_{rg}(Q)$, $Z_{rg}(Q)$	Geometric reflector frame coordinates of point Q.
$[R_{12}]$	Rotation matrix of the coordinate transformation from geometric alidade frame to base frame.
$[T_{12}]$	Translation matrix of the coordinate transformation from geometric alidade frame to base frame.
$[R_{21}]$	Rotation matrix of the coordinate transformation from base frame to geometric alidade frame.
$[T_{21}]$	Translation matrix of the coordinate transformation from base frame to geometric alidade frame.
$[R_{jk}]$	Rotation matrix of the coordinate transformation from frame k to frame j. (Note order of subscripts).
$[T_{jk}]$	Translation matrix of the coordinate transformation from frame k to frame j.
	The matrices $[R_{jk}]$, $[T_{jk}]$ are given explicitly in Appendix I.

Tilted Deformed Telescope

$[D_i]$	Geometric telescope displacement vector from structural node $\mathfrak{N}_i$ to fiducial reference point $\mathfrak{F}_i$.
$\xi_i,\ \eta_i,\ \zeta_i$	$[D_i] = \xi_i \widehat{X}_{eg} + \eta_i \widehat{Y}_{eg} + \zeta_i \widehat{Z}_{eg}$
$[\Delta(EL_{ant})]_{\mathfrak{N}_i} = [\Delta]_{\mathfrak{N}_i}$	Gravity-load-produced displacement of node $\mathfrak{N}_i$ .from its geometric telescope position, expressed in terms of the geometric elevation frame basis vectors.
EL_{surf_rig}	Surface rigging (setting) elevation angle.
EL_{arm_access}	Elevation for upper feed arm at vertical.
EL_{access}	Alternative surface rigging elevation.
$\mathfrak{F}$	A fiducial reference point on the telescope.
$\mathfrak{F}_j$	Fiducial reference point number j.
$\mathfrak{L}$	Laser platform fiducial point near $\mathfrak{N}_i$.
$\mathfrak{N}_i$	Telescope structure node point, number i.
$[\sigma]_{\mathfrak{N}_i}$	Finite-element-analysis-generated displacement coefficient matrix associated with structure node $\mathfrak{N}_i$.
$[\tau]_{\mathfrak{N}_i}$	Finite-element-analysis-generated joint rotation coefficient matrix associated with structure node $\mathfrak{N}_i$.
$\mathbf{t}_{\mathfrak{N}_i} = [Rot(EL_{ant})]_{\mathfrak{N}_i}$	Rotation vector of the structural joint at node $\mathfrak{N}_i$, due to gravity loading.
t	$t = \lvert\mathbf{t}_{\mathfrak{N}_i}\rvert$
$t_x,\ t_y,\ t_z$	$\mathbf{t}_{\mathfrak{N}_i} = t_x \widehat{X}_{eg} + t_y \widehat{Y}_{eg} + t_z \widehat{Z}_{eg}$
$[\delta Rot(\mathbf{t}_{\mathfrak{N}_i})]\,[D_i]$	Additional displacement of $\mathfrak{F}_j$ due to joint rotation at $\mathfrak{N}_i$.

S	Laser station scan mirror center fiducial point.
T	Laser station scan target fiducial point.
A_T	Laser scan mirror azimuth angle of target point T.
E_T	Laser scan mirror elevation angle of target point T.
R, Θ, Φ	Spherical polar scan coordinates of target point T.
$\widetilde{x_T}$, $\widetilde{y_T}$, $\widetilde{z_T}$	Laser station platform local cartesian coordinates of target point T.
$X_e(\mathfrak{F}_i)$, $Y_e(\mathfrak{F}_i)$, $Z_e(\mathfrak{F}_i)$	Geometric elevation frame coordinates of $\mathfrak{F}_i$ after gravity-load displacement.
$X_e(\mathfrak{N}_i)$, $Y_e(\mathfrak{N}_i)$, $Z_e(\mathfrak{N}_i)$	Geometric elevation frame coordinates of $\mathfrak{N}_i$ after gravity-load displacement.
$\widehat{X}_e(\mathfrak{N}_i)$, $\widehat{Z}_e(\mathfrak{N}_i)$, $\widehat{Z}_e(\mathfrak{N}_i)$	Orthogonal triple of unit vectors generated by rotating the geometric elevation frame basis vectors by $[\delta Rot(\mathbf{t}_{\mathfrak{N}_i})]$.
$\mathbf{X}_{eg}(Q)$	Displacement vector of an arbitrary point, Q, from E_g, expressed in terms of geometric elevation frame basis vectors
$[A]_{\mathfrak{N}_i}$	Laser platform orientation matrix. Elements are projections of platform frame basis vectors onto geometric elevation frame basis vectors.
$\mathbf{D}_{eg}(\mathfrak{L})$	Displacement vector of laser platform fiducial point $\mathfrak{L}$ from its associated structural node point, $\mathfrak{N}_i$, expressed in terms of geometric elevation frame basis vectors.

$\mathfrak{N}$	A structure node point of the telescope.
$\mathfrak{N}_T$	Structure node point associated with laser scan target fiducial reference point T.
$\mathbf{D}_{eg}\,(T, l_T)$	Displacement vector of T from $\mathfrak{N}_T$ when actuator extension is equal to l_T.
$\mathbf{D}^0_{eg}\,(T)$	$\mathbf{D}_{eg}\,(T, l_T = 0)$
$\xi_0(T)$, $\eta_0(T)$, $\zeta_0(T)$	Geometric elevation frame components of $\mathbf{D}^0_{eg}\,(T)$.
$\mathbf{D}^1_{eg}\,(T)$	$\mathrm{d}\mathbf{D}_{eg}\,(T, l_T) \,/\, \mathrm{d}l_T$
$\xi_1(T)$, $\eta_1(T)$, $\zeta_1(T)$	Geometric elevation frame components of $\mathbf{D}^1_{eg}\,(T)$.
$\mathbf{D}_{ST}$	Displacement vector of scan target point T from scan mirror center fiducial point S.
$\mathbf{D}(S)$	Displacement vector of S from structure node point $\mathfrak{N}_i$ associated with the scan mirror station platform.
$\mathbf{D}_i \quad (=\mathbf{D}_{eg}(\mathfrak{L}))$	Displacement vector of laser scan platform fiducial reference point $\mathfrak{L}$ from its associated structural node point $\mathfrak{N}_i$.
$\widetilde{X}$, $\widetilde{Y}$, $\widetilde{Z}$	Basis vectors of local laser scan platform frame, of scan station located near structure node point $\mathfrak{N}_i$. The origin point of this frame is at fiducial reference point $\mathfrak{L}$. The scan axis is assumed parallel to $\widetilde{Z}$.

Alidade Structure Corrections

d_{off}	Offset distance between non-intersecting azimuth and elevation axes.
$\mathbf{D}$	An arbitrary displacement vector.
E_g	Origin point of the geometric elevation frame.
$\mathcal{F}$	Arbitrary fiducial reference point embedded in the telescope's tipping structure.
$\mathbf{X}_{eg}(\mathcal{F})$	Displacement vector from geometric elevation frame origin point E_g to $\mathcal{F}$.
$O_G^{(1)}$	Origin point of ground frame of tilted telescope with offset and misalignment of azimuth and elevation axes.
$\vartheta_\perp$	Angle of deviation from perpendicularity, of telescope azimuth and elevation axes.
$C_\perp$	$\cos\vartheta_\perp$
$S_\perp$	$\sin\vartheta_\perp$
$X_{eg}(\mathcal{F})$, $Y_{eg}(\mathcal{F})$, $Z_{eg}(\mathcal{F})$	Geometric elevation frame coordinates of fiducial point $\mathcal{F}$.
$X_G^{(2)}(\mathcal{F})$, $Y_G^{(2)}(\mathcal{F})$, $Z_G^{(2)}(\mathcal{F})$	Ground frame coordinates of fiducial point $\mathcal{F}$, for telescope with shaft offset and misalignment.

Determination Of Azimuth AndElevation

AZ	$AZ = \pi - AZ_{ant}$ Supplement of antenna azimuth.
AZ_{shaft}, EL_{shaft}	Telescope azimuth, elevation shaft orientation angles.
$AZ_{encoder}$, $EL_{encoder}$	Azimuth, elevation shaft angle encoder readout angles.
$AZ_{command}$, $EL_{command}$	Servo setpoint values for azimuth and elevation shaft optical encoder angle readout signals.
$AZ^{(i)}$, $EL^{(i)}$	Traditional pointing model correction term.
AZ_{true}, EL_{true}	True horizon system azimuth, elevation of an observed pointlike astronomical radio source. These angles are properties of the radio source, not the telescope.
$a_{pq}^{(EL)}$, $b_{pq}^{(EL)}$, $c_{pq}^{(EL)}$, $d_{pq}^{(EL)}$	Elevation Fourier coefficients in Condon pointing model.
$a_{pq}^{(AZ)}$, $b_{pq}^{(AZ)}$, $c_{pq}^{(AZ)}$, $d_{pq}^{(AZ)}$	Azimuth Fourier coefficients in Condon pointing model. [Note that the azimuth Fourier term sum is multiplied by $\sec EL$ to give proper behavior approaching zenith].
$AZ_{apparent}$, $EL_{apparent}$	Apparent horizon system azimuth, elevation of an observed radio source, including the deviation of arrival direction due to atmospheric refraction.
$\Delta_{EL}^{(bfp)}$	Pointing model correction for elevation shift to account for orientation of the GBT's main reflector paraboloid axis, when reflector is reconfigured to the optimal shape for a given shaft elevation (best fit paraboloid).
$LAST$	Local Apparent Sidereal Time of observation of source. [$LAST = GMST - \lambda \cdot (1^h/15°) + \Delta\lambda \cos\varepsilon$, where $GMST$ is Greenwich Mean Sidereal Time, λ is geographical longitude, $\Delta\lambda$ is nutation in longitude, ε is obliquity of the ecliptic].

Appendix III. Finite Element Analysis Node Data Files.

We include here a portion of the Node File for the Green Bank Telescope Finite Element Analysis, as a sample of the data file produced by this analysis.

The file is a listing of tipping structure nodes, their geometric elevation coordinates and the coefficients of the displacement matrix and the joint rotation matrix associated with each node. We give a sample of the file's output on the next page. The output variables, in the notation of this Memo, are listed below.

Variable Listed	Variable in Memo
Node ID	Index, i, of node $\mathfrak{N}_i$.
NodeX	$X_{eg}(\mathfrak{N}_i)$
NodeY	$Y_{eg}(\mathfrak{N}_i)$
NodeZ	$h_e + Z_{eg}(\mathfrak{N}_i)$
ZDeltaX	$\sigma_{x,-z}(\mathfrak{N}_i)$
ZDeltaY	$\sigma_{y,-z}(\mathfrak{N}_i)$
ZDeltaZ	$\sigma_{z,-z}(\mathfrak{N}_i)$
ZTiltX	$\tau_{x,-z}(\mathfrak{N}_i)$
ZTiltY	$\tau_{y,-z}(\mathfrak{N}_i)$
ZTiltZ	$\tau_{z,-z}(\mathfrak{N}_i)$
HDeltaX	$\sigma_{x,y}(\mathfrak{N}_i)$
HDeltaY	$\sigma_{y,y}(\mathfrak{N}_i)$
HDeltaZ	$\sigma_{z,y}(\mathfrak{N}_i)$
HTiltX	$\tau_{x,y}(\mathfrak{N}_i)$
HTiltY	$\tau_{y,y}(\mathfrak{N}_i)$
HTiltZ	$\tau_{z,y}(\mathfrak{N}_i)$

Distances are given in inches.

Node File for GBT Finite Element Analysis

Node ID	NodeX	NodeY	NodeZ	ZDeltaX	ZDeltaY	ZDeltaZ	ZTiltX	ZTiltY	ZTiltZ	HDeltaX	HDeltaY	HDeltaZ	HTiltX	HTiltY	HTiltZ
40982	65.86	-2524.97	4181.96	-0.033	-4.0744	-3.9002	0.00157	-0.00001	-0.00008	-0.0295	8.577	1.8984	-0.00418	0.00018	-0.00054
41020	0	-2520.11	4434.21	0	-4.4404	-3.9024	0.00141	0	0	0	9.6744	1.8567	-0.00432	0	0
41040	106.07	-2520.11	4434.21	-0.0029	-4.4373	-3.8982	0.00157	0.00012	0.00001	0.0096	9.6488	1.8423	-0.0044	0.00005	-0.00016
41060	122.94	-2780.56	4377.18	-0.0086	-4.354	-4.2824	0.00146	0.00022	0.00003	-0.0209	9.4376	2.9201	-0.00426	0.00053	-0.00001
41080	0	-2787.53	4434.21	0	-4.4396	-4.2746	0.00145	0	0	0	9.6814	2.9937	-0.00424	0	0
41082	0	-2590.76	4434.21	0	-4.44	-3.9935	0.00135	0	0	0	9.6742	2.1656	-0.0043	0	0
50000	0	-2159.02	4459.06	0	-4.4914	-3.457	0.00037	0	0	0	9.7803	0.3821	-0.00332	0	0
50001	0	-2176.99	4475	0	-4.4973	-3.4636	0.00037	0	0	0	9.8332	0.4418	-0.00332	0	0
50002	0	-2194.96	4490.91	0	-4.5032	-3.4702	0.00038	0	0	0	9.8861	0.5016	-0.00333	0	0
50004	0	-2351.53	4640.36	0	-4.7122	-3.8472	0.00066	0	0	0	10.5945	1.0481	-0.00445	0	0
50005	0	-2327.96	4608.71	0	-4.6923	-3.828	0.00065	0	0	0	10.4457	0.9416	-0.00454	0	0
50010	0	-2329.08	4706	0	-4.758	-3.8288	0.00071	0	0	0	10.8871	0.9467	-0.00451	0	0
50020	0	-2408.99	4667	0	-4.729	-3.8802	0.00061	0	0	0	10.7095	1.3066	-0.00449	0	0
50030	0	-2409.74	4672.47	0	-4.7328	-3.878	0.00059	0	0	0	10.7396	1.3129	-0.00421	0	0
50040	51.12	-2408.99	4667	0.0002	-4.7285	-3.8784	0.00061	-0.00005	0.00002	-0.0012	10.7076	1.3069	-0.00449	-0.00001	-0.00006
50110	0	-2427.14	4707.78	0	-4.7568	-3.8911	0.00084	0	0	0	10.8926	1.3919	-0.00461	0	0
50120	0	-2412.48	4692.43	0	-4.7442	-3.8796	0.00073	0	0	0	10.8215	1.324	-0.00462	0	0
50140	14	-2412.48	4692.43	0.0001	-4.7442	-3.8796	0.00073	-0.00002	-0.00003	0	10.8215	1.324	-0.00462	0	-0.00001
50150	0	-2443.41	4672.58	0	-4.7263	-3.9061	0.00071	0	0	0	10.7331	1.4612	-0.00455	0	0
50220	0	-2556.36	4600.07	0	-4.6841	-3.9687	0.00118	0	0	0	10.3904	1.997	-0.00448	0	0
50240	51.12	-2556.36	4600.07	0.0002	-4.6841	-3.9671	0.00118	-0.00005	-0.00004	0.0018	10.3888	1.997	-0.00448	-0.00005	-0.00003

Bibliography.

[Buz-1]
G. Buzanoski. *GBT Finite Element Analysis Macros in Quattro Pro.* GBT Memo 130. May 30, 1955.

[Con-1]
J.J. Condon. *GBT Pointing Equation.* GBT Memo 75. 1992.

[Fisher-1]
R. Fisher, D.E.Hogg, L. Macknik. *Division of Concerns in the GBT Pointing Correction System.* GBT Memo 103. April 23, 1993.

[Ghi-1]
F. Ghigo. *Pointing Calibration of the ESSCO 45-Ft Antenna at Green Bank.* NRAO Electronics Division (GB) Internal Report No. 288. June 1990.

[Gor-1]
M.A. Gordon, S. Huang, O. Cate, K.I. Kellerman, B. Vance. *On-Line Pointing Correction of the 140-Ft Telescope.* NRAO Telescope Operations Division Report No. 11. June 15, 1973.

[Greve-1]
A. Greve and C. Thum. *The Pointing of the IRAM 30-m Telescope.* Tech. Bericht 78, pp 44-47, Max-Planck-Institut für Radioastronomie. Workshop on Pointing and Pointing Models. March 7 & 8, 1996. ISSN 0939-3153.

[Gol-1]
M.A. Goldman. *GBT Dish Laser Range Measurement Corrections.* GBT Memo 154. June 25, 1996.

[Hoe-1]
S. von Hoerner. *Astronomical Pointing Parameters.*
GBT Memo 110. November 17, 1993.

[Hoe-2]
S. von Hoerner. *Focal Length Adjustment of the 140-Ft.*
NRAO (GB) Electronics Division Internal Report No. 160.
May 1975.

[Hoe-3]
S. von Hoerner. *140-Ft Pointing Errors and Possible Corrections.*
NRAO (GB) Electronics Division Internal Report No. 164.
December 1975.

[Hoe-4]
S. von Hoerner. *Refraction Correction for the 140 Ft-Pointing.*
NRAO (GB) Electronics Division Internal Report No. 101.
May 1976.

[Hoe-5]
S. von Hoerner. *140-Ft, Pointing Program, and Thermal*
Shielding *of Shaft and Yoke.*
NRAO (GB) Electronics Division Internal Report No. 102.
November 1976.

[Hoe-6]
S. von Hoerner. *140-Ft Pointing Errors After Thermal Shielding.*
NRAO (GB) Electronics Division Internal Report No. 107.
November 1977.

[Hogg-1]
D.E. Hogg and J.R. Fisher.
A Revised Description of the GBT Pointing System.
GBT Memo 122. February 7, 1995.

[King-1]
L King. NRAO GBT Drawing C35102M081-1, Rev. B.

[Madd–1]
R.J. Maddalena. *Proposed Changes to the Pointing Model for the 140-ft Telescope.*
Limited distribution memo. August 24, 1992.

[Meeks–1]
M.L. Meeks, J.A. Ball and A.B. Hull.
The Pointing Calibration of the Haystack Antenna.
IEEE Trans. AP-16(6), 746-751 (1968).

[Nor-1]
R. Norrod and S. Srikanth. *A Summary of the GBT Optics Design.*
GBT Memo 155. March 1996.

[Pau-1]
I. Pauliny-Toth. *Pointing Corrections for the 140-Ft Under Computer Control.*
Limited distribution memo. May 7, 1969.

[Par-1]
D.H. Parker. *A Status Report on the GBT Laser Demonstration at the 140 Foot Telescope.*
GBT Memo 157. August 28, 1996.

[Par-2]
D.H. Parker. Subject: FEA Model.
Limited distribution memo. January 5, 1995.

[Par-3]
D.H. Parker. *Notes on Surface / Pointing Meetings 11 / 29 - 12 / 5.*
Memo for record. December 8, 1994.

[Payne-1]
J.M. Payne, D. Parker and R.F. Bradley.
Rangefinder with Fast Multiple Range Capability.
Rev. Sci. Instr. 63 (6), 3311-3316 (1992).

[Payne-2]
J.M. Payne. *Pointing the GBT .*
GBT Memo 84. September 16, 1992.

[RSI-1]
Radiation Systems, Inc.. 1501 Moran Road, Sterling, VA 20166.
The Green Bank Telescope.
3rd Design Review. October 20-22, 1992.

[Schr-1]
J. Schraml. *Pointing and Focus Calibration of the 36-Foot Telescope.*
NRAO Internal Report. September, 1969.

[Schwab-1]
F. Schwab. *Laser Rangefinder Locations and Orientations.*
Limited distribution memorandum. March 6, 1996.

[Ulich-1]
B.L. Ulich. *Pointing Characteristics of the 36-Foot Telescope.*
NRAO Engineering Division Internal Report No. 105.
February, 1976.

[Wells-1]
D. Wells and L. King. *The GBT Tipping-Structure Model in C.*
GBT Memo 124. March 21, 1995.

[Wells-2]
D.C. Wells. *The GBT Precision Pointing System.*
GBT Memo 85. September 25, 1992.

[Wells-3]
D. Wells and L. King. *GBT Best-Fitting-Paraboloid [BFP] in C.*
GBT Memo 131. June 20, 1995.